uOttawa

L'Université canadienne
Canada's university

FACULTÉ DES ÉTUDES SUPÉRIEURES ET POSTOCTORALES

uOttawa

L'Université canadienne
Canada's university

FACULTY OF GRADUATE AND POSDOCTORAL STUDIES

Shili Lu

AUTEUR DE LA THÈSE / AUTHOR OF THESIS

M.Sc. (Systems Science)

GRADE / DEGREE

Systems Science

FACULTÉ, ÉCOLE, DÉPARTEMENT / FACULTY, SCHOOL, DEPARTMENT

Stochastic Power Control for Wireless Networks : Probabilistic QoS Measures

TITRE DE LA THÈSE / TITLE OF THESIS

C.D. Charalambous

DIRECTEUR (DIRECTRICE) DE LA THÈSE / THESIS SUPERVISOR

CO-DIRECTEUR (CO-DIRECTRICE) DE LA THÈSE / THESIS CO-SUPERVISOR

EXAMINATEURS (EXAMINATRICES) DE LA THÈSE / THESIS EXAMINERS

Nasiruddin Ahmed

Tet Yeap

Gary W. Slater

LE DOYEN DE LA FACULTÉ DES ÉTUDES SUPÉRIEURES ET POSTDOCTORALES /
DEAN OF THE FACULTY OF GRADUATE AND POSTDOCORAL STUDIES

Stochastic Power Control for Wireless Networks: Probabilistic QoS Measures

Shili Lu

Department of Systems Science
University of Ottawa
Ottawa, Canada

April 2005

A thesis submitted to the Faculty of Graduate and Postdoctoral Studies
in partial fulfillment of the requirements for the degree of
Master of Science

Under the supervision of Professor Charalambos D. Charalambous

Your file Votre référence
ISBN: 0-494-11334-0
Our file Notre référence
ISBN: 0-494-11334-0

Acknowledge

I would like to express my sincere gratitude to my supervisor, Professor Charalambos D. Charalambous for his careful guidance and valuable suggestions for completing this thesis.

I am grateful to Professor Jean-Michel Thizy, who was the Director of Systems Science Program, for his support and help in the department.

I would like to thank Dr. Nickie Menemenlis, who had completed her research at McGill University for the Ph. D. degree under the supervision of Professor Charalambos D. Charalambous. Her thesis, and many papers pointed out by her gave me a great help in my study. I would also like to take the opportunity to thank Stojan Denic, Lingling Wang, Xin Li, Jun Zhan, Yingxia Yuan, Yixin Wang, Farzad Rezaei, Mohammad Pour, and other colleagues in the Broadband Wireless and Internetworking Research Laboratory for lots of technical suggestions and their friendship.

I am greatly indebted to my wife, my daughter, and my whole family for their love and support throughout my graduate study.

A very special thanks goes out to Dr. Tet Hin Yeap and Dr. Nasir Uddin Ahmed as my thesis defence examiners to read my thesis and give me great comments.

I recognize that this research would not have been possible without the financial assistance of the University of Ottawa (Admission Scholarships, Teaching Assistantships and other financial aid). I express my gratitude to those agencies.

Abstract

For wireless network systems, iterative power control algorithms have been proposed to minimize the transmission power, while maintaining reliable communication between mobiles and base stations. However, since the measurements are random, the channel characteristics always are described by Stochastic Differential Equations (SDE). Based on the stochastic approximation methods, and using time-varying step size sequences, we can get an approximation algorithm to reach an optimal power allocation.

After the study of optimal power allocation, the probabilistic Quality of Service (QoS) measures are introduced to evaluate the performance of any control strategy. It provides tight bounds that relate to the probability of failure in achieving the desired QoS requirements.

This thesis addresses mobile systems consisting of M transmitters and M receivers, which are subject to motion, and their power is described by SDE. The optimal power control problem is formulated, and the outage probability corresponding to a desired QoS requirements is computed using Moment Generating Function (MGF).

Numerical results show that each user needs only to know its own channel gain and its own output assigned by the base station to update the transmitter power in order to maintain a desired Signal to Interference Ratio (SIR) and QoS requirement at the receiver.

Contents

List of Figures

Chapter 1

Introduction

1.1 Introduction of Wireless Networks

A wireless network provides a wireless connection to the Public Switched Telephone Network (PSTN) for any user located within the given radio range of a system. The basic wireless network system consists of mobile stations, base stations, and a Mobile Switching Center (MSC)[2]. Figure 1.1.1 gives an illustration of a wireless network system. The mobile station contains a transceiver, an antenna, and control circuitry. The mobiles usually are used as a portable hand held unit, or are set in a vehicle. The base stations consist of several transmitters and receivers, which simultaneously handle full duplex communications, and have towers to support several transmitting and receiving antennas. The base station serves as a bridge between all mobile users in the cell and connects the simultaneous mobile calls to the MSC. The MSC coordinates the activities of all of the base stations and connects the entire cellular system to the PSTN.

Each base station is allocated a group of radio channels to be used within a small geographic area called a cell. Neighbouring base stations are assigned different groups of channels so that the interference between base stations and mobiles is minimized. The design process of selecting and allocating channel groups for all of the base stations within the system is called frequency reuse [1], [2]. Figure 1.1.2 illustrates the concept of frequency reuse. Cells

with the same label use the same group of channels.

Frequency reuse implies that in a given coverage area there are several cells that use the same set of frequencies called co-channel cells. The interference between signals from these cells is called co-channel interference. Interference is the major limiting factor in the performance of the wireless network system [1], [2]. In practical wireless network systems, the power transmitted by every mobile is under constant control by the serving base station. It ensures that each mobile transmits the smallest power necessary to reduce the interference and maintains a good quality link on the reverse channel. Power control not only helps prolong battery life for the mobile, but also reduces the reverse channel SIR in the system [2], [4], [18]. In the CDMA (Code Division Multiple Access) system, each mobile controls its transmitter power level, then its signal arrives at the base station with the minimum required SIR. As a result, the system can reach a maximum capacity. Figure 1.1.3 illustrates the distribution of mobile users over the coverage area in adjacent cells.

1.2 Power Control in CDMA

To minimize the average SIR for each mobile user, it requires each user to provide the same power level at the base station receiver. Since the signal and the interference are continually varying, power control updates are sent by the base station every 1.25msec [2]. Power control commands are sent to each mobile user on the forward control sub channel, which instructs the mobile to raise or lower its transmitted power in 1dB step [2]. If the received signal is low, the base station instructs the mobile station to increase the mean output power level. If the mobile's power is high, the base station transmits a command to let the mobile station decrease its power level.

Because the transmitting paths are varying for different propagation environments, there exists a power path loss that needs to be compensated in the base station. Estimating the power path loss in wireless communication systems over long distance is very important because it is the major cause for signal attenuation, generally known as shadowing. In doing the estimation, in order to reach a required SIR (Signal-to-Interference Ratio), the power control problem is usually formulated as an optimization problem, which minimizes the sum of powers of all the transmitters subject to the desired minimum SIR [5], [6], [14], [15], [19].

Most power control works have been done on the CDMA (Code-Division Multiple Access) systems assuming that the power control system is deterministic. However, because the stochastic natures of the link gain, the attenuation, the received power, and the SIR are all random processes in time, stochastic optimal power control scheme is very important and useful [4], [5], [8], [9], [20], [21]. We introduce some special random processes to describe the character of the channels. Then the scheme can be used to implement in practice to update the power level effectively.

The signal attenuation coefficient is proportional to the square root of the received power; it represents how much the received signal magnitude is attenuated at a distance d, with respect to the magnitude of the transmitted signal [1], [2], [7], [8], [9], [11]. It is defined by the equation:

$$r(d) \equiv \sqrt{P_r(d)/P_t}, \tag{1.2.1}$$

where $P_r(d)$ is the received power at distance d and P_t is the transmitter power. The average power path loss $\overline{PL}(d)$ for a given path is the difference between P_t and $P_r(d)$, describing the power path loss in dBs, it is defined as:

$$\overline{PL}(d) = 10 \log P_t - 10 \log P_r(d). \tag{1.2.2}$$

In real measurements, the power path loss $PL(d)$ at distance d is described by adding a zero-mean Gaussian distributed random variable $\tilde{X}$. That is

$$PL(d)[dB] = \overline{PL}(d)[dB] + \tilde{X}, \tag{1.2.3}$$

in which case, we can get $r(d)$=$e^{(kPL(d)[dB])}$, where k is a constant. It means that the attenuation has an exponential relationship with the power path loss for a given path or distance. By using the Stochastic Differential Equations (SDE), we can get the relationship of the power path loss and the signal attenuation with different distance and varying time [7], [8], [11]. We consider the signal attenuation as the channel gain, so the power control problem can be specified as an optimization problem for the total transmitted power while the SIR for each transmitter-receiver pair is greater than the target SIR. This needs the linear programming approach to solve the problem [5], [6], [12], [30].

1.3 Linear Programming Approach

Considering the variation of both time t and distance d, which models the time-space propagation characteristic of the attenuation and using SDE, we denote the signal attenuation $r(d)$ as $S_{ij}(t,d)$ and the power path loss $PL(d)$ as $X_{ij}(t,d)$ for time-space propagation environments, where i,j refer to the transmitters and the receivers. Then we can compute the power path loss $X_{ij}(t,d)$ and the signal attenuation $S_{ij}(t,d)$ at any location along the propagation path as a function of time. Then for some different locations such as M transmitters (MS-Mobile Station) and M receivers (BS-Base Station), we consider the signal attenuation S_{ij} as the channel gain between BSi and MSj denoted by $G_{ij}(t,d)$, where $G_{ij}(t,d) = [g_{ij}(t,d)]_{M\times M}$, $S_{ij}(t,d) = [s_{ij}(t,d)]_{M\times M}$. We define the relationship of signal attenuation S_{ij} and channel gain G_{ij} by $s_{ij} = \sqrt{g_{ij}}$.

In wireless communication systems, the channel link quality is usually measured by the Signal to Interference Ratio (SIR). We use the theory of power control and the linear programming approach to solve the problem, and compute the optimal power allocation from the following formulation. Let Γ_i denotes the SIR of user i, the power control problem can be stated as:

$$\begin{aligned} &\min \sum_{i=1}^{M} p_i \\ &\text{s. t. } \Gamma_i \equiv \frac{p_i g_{ii}}{\sum_{j \neq i}^{M} p_j g_{ij} + \eta_i} \geq \bar{\gamma}_i, \end{aligned} \tag{1.3.4}$$

where $p_i \geq 0$ is the transmitter power of the ith MS, g_{ij} is the channel gain of the transmitter j to the receiver assigned to transmitter i, $\eta_i \geq 0$ is the noise power level at ith receiver, and $\bar{\gamma}_i \geq 0$ is the required SIR for BSi (receiver i). We define $\gamma_i = \frac{\bar{\gamma}_i}{1+\bar{\gamma}_i}$, then $0 \leq \gamma_i \leq 1$. Then we will use an approximation algorithm that can converge with the solution of the above linear programming problem for equality case. The algorithm comes from the stochastic approximation theory [5], [10], [24].

1.4 Probabilistic QoS Measures

In order to design an optimal system in wireless communication network, we try to optimize the transmission power and the capacity of the system with respect to the number of transmitters M, thus linking power control and admission control problems. We introduce QoS measures, which can be used to evaluate any control algorithm. They also can be used as measures for blocking new transmitters into the network or for dropping existing ones [5]. The method is based on Chernoff bounds theory [1], [12], [28]. It computes the probability of failure in achieving the QoS requirement for each mobile user, and finds the optimal power sets in order to make the bound as small as possible [5]. Considering the signal attenuation

as different stochastic distribution, we define:

$$I^n(p) = \sum_{j=1}^{M} p_j g_{nj} + \eta_n - \frac{1}{\gamma_n} p_n g_{nn} \tag{1.4.5}$$

The probability of the failure is $P(I^n(p) \geq 0)$, which is called the outage probability of the nth transmitter-receiver pair. By the Chernoff bounds, we have [5], [12], [14], [15]:

$$P(I^n(p) \geq 0) \leq E[exp(s_n I^n(p))], s_n > 0. \tag{1.4.6}$$

By the definition in (1.4.5), $I^n(p)$ is a random process because we take the signal attenuation $s_{nj} = \sqrt{g_{ij}}$ as Rayleigh distribution, Rice distribution, and Nakagami-m distribution, also η_n as Additive White Gaussian Noise (AWGN) with $N(0, \sigma^2)$, where σ^2 is variance of random variable. Because it is difficult to compute the expected value of the complex random process $I^n(p)$ in this thesis, we derive the Moment Generating Function (MGF) expression for different channels and analyze the outage probability. After analyzing the related parameters, we can show that there exists an optimal power set $\{p_i^*\}$ to satisfy the above bound.

1.5 Thesis Organization

This thesis focuses on using SDE to get the optimal power allocation, and completing the probability QoS measures to find the optimal bound satisfaction for the desired communication requirements SIR by using MGF.

It is organized as follows:

In Chapter 2, we introduce the concepts of wireless network systems, including the wireless channel characteristics and multipath propagation channel models.

In Chapter 3, we derive the expression of the power path loss and the signal attenuation

with distance d and time t by using SDE for different propagation environments of dynamical models of log-normal shadowing.

(1) For fixed observation time t, the model describes the dependence of attenuation $S(t,d)$ on distance d, which represents the attenuation characteristic of the propagation environment for distance d. The model also describes the power path loss $X(t,d)$ as an Ornstein-Uhlenbeck random process, which is a function of d.

(2) For fixed transmitter-receiver distance d, we have a model for describing the dependence of $S(t,d)$ on t in order to capture the random attenuation coefficient variations with varying time. The power path loss $X(t,d)$ is still described as the Ornstein-Uhlenbeck random process as a function of time t corresponding to a given observation distance d.

(3) For both t and d varying, we wish to know the time-space propagation characteristics of the signal attenuation $S(t,d)$ in respect to the relative movement of the transmitter and the receiver to each other. For the distance $d = v_c\tau$, v_c is the speed of light given in meter/second, and τ represents the channel multipath delay for a fixed value of t. So in this thesis, the distance d and the delay τ will be used interchangeably, though mostly we use time delay τ. Therefore we will use $S(t,\tau)$ replace $r(t,d)$, and $X(t,\tau)$ replace $PL(t,d)$.

In Chapter 4, we describe the formulation of the power control optimization problem using linear programming to find the optimal power allocation in order to satisfy the QoS requirements, then we do the simulation to analyze it.

In Chapter 5, we propose the probabilistic QoS measure method to find tight bounds for the probability of failure to achieve the desired QoS requirements. Because it is difficult to compute the expected value of the random variables, we use the Moment Generating Function (MGF) to derive upper bounds. Three different propagation channels, namely Rayleigh distribution, Rice distribution, and Nakagami-m distribution are compared with their different

Chernoff bounds. Simulations and analysis are also given in this chapter.

In Chapter 6, we give the summary of this thesis and present some future topics in this field.

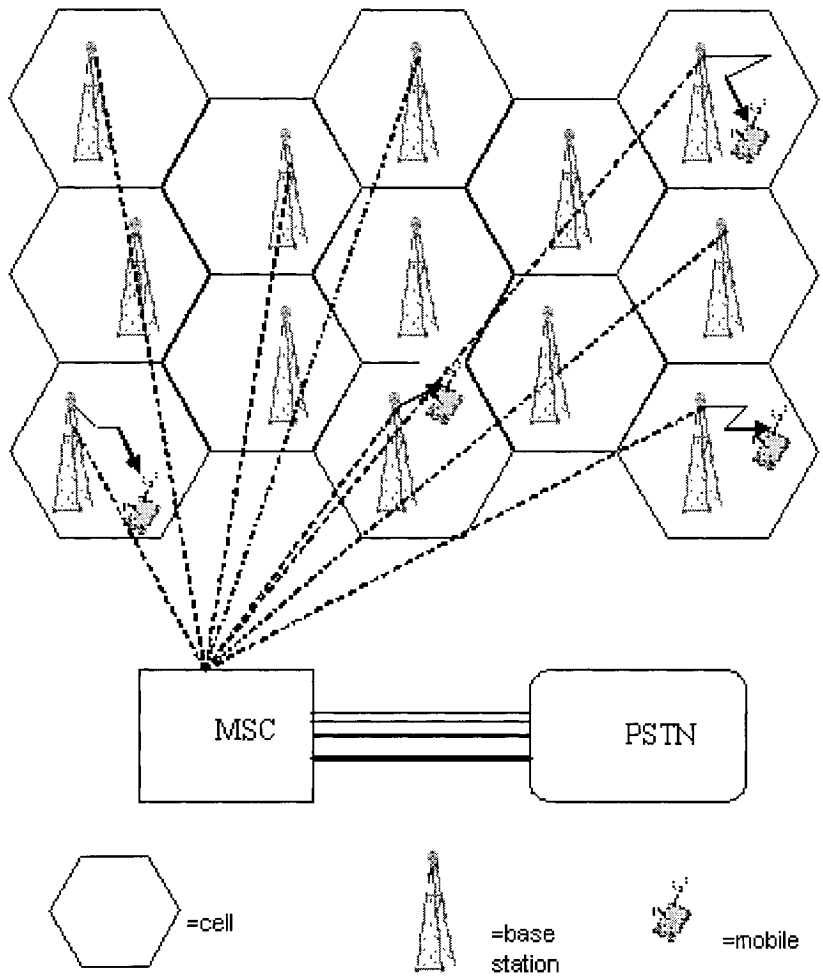

Figure 1.1.1: An illustration of the wireless network system. The towers represent base stations that provide radio access between mobile users and the mobile switching center (MSC).

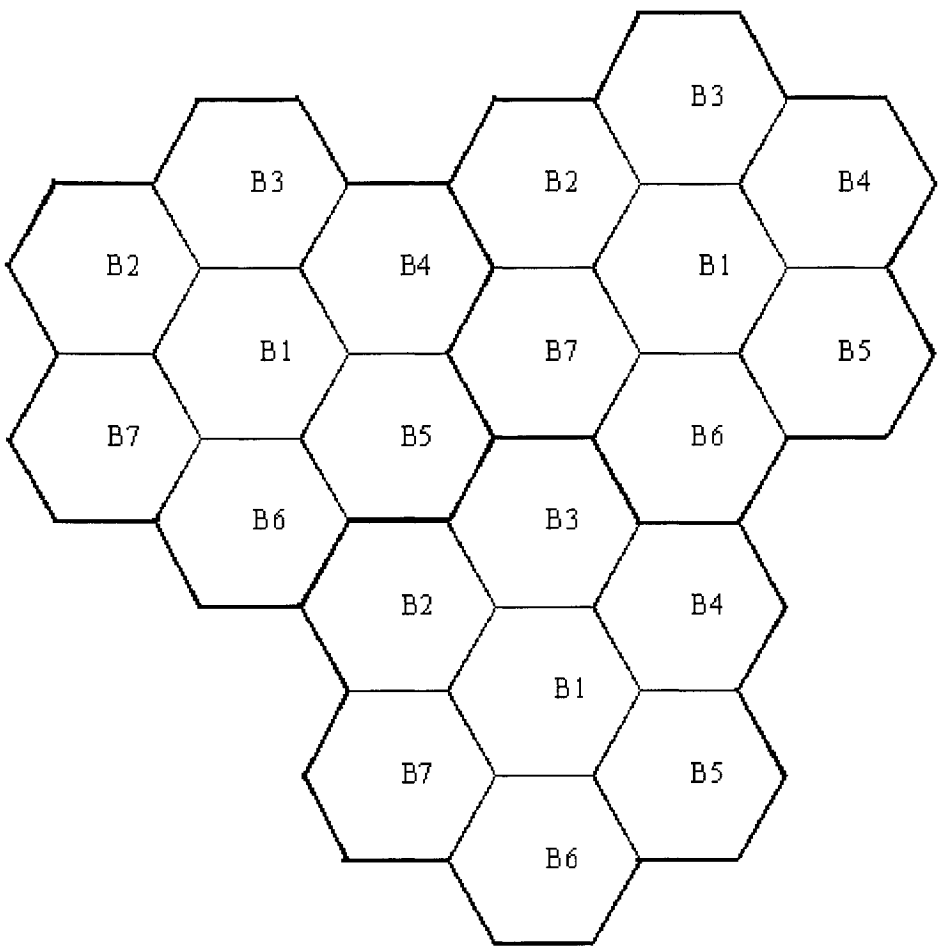

Figure 1.1.2: An illustration of the cellular frequency reuse. Cells with the same label use the same set of frequencies.

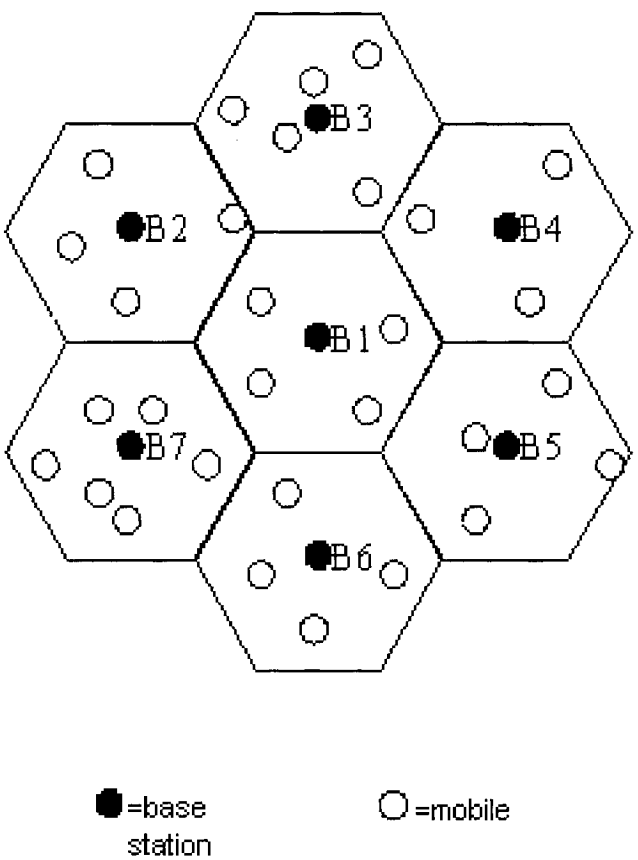

Figure 1.1.3: An illustration of the distribution of mobile users over the coverage area in adjacent cells.

Chapter 2

Channel Modelling

The mobile radio channel places a fundamental role on the performance of wireless communication systems. The transmitting path between the transmitter and the receiver can vary from simple Line-of-Sight (LOS) to one that is severely obstructed by buildings, mountains and foliage [2]. Wireless radio channels are extremely random and therefore do not offer easy analysis. So modelling the radio channel has been one of the most difficult parts of the mobile radio system design.

The wireless channel characteristics play an important role in many stages of the design such as deciding the power of the transmitted signal, the nature of the decoding techniques, the modulation schemes, and the signal coding. Furthermore, interference by other users and ambient noise causes additional uncertainties, which must be accounted for in the design. If the receivers know the channel characteristics of the other users and some information about their signals, one could subtract it from the received signal and thus alleviate and improve the performance of the decoder. The better characterization of the channel may also lead to the better interference minimization from other users [1], [2]. In fact, a wireless communication system is a dynamic system for tracking and computing the signal attenuation in order to arrange and constitute the channel for the whole system.

In wireless communications, the various transmitter and receiver components are typically designed and optimized in absence of exact and complete knowledge about the channel characteristics due to its inherent random and time varying nature.

The modelling of wireless channels has been and continues to be one of the most important components in the design of wireless communication systems. This is due to the variety of ways electromagnetic energy injected into the channel that interacts with the environment of propagations, diffractions, and scattering [1], [2]. Then there are the continuously and arbitrarily changing characteristics of the propagation environment between the transmitter and the receiver.

The result of this complex propagation mechanism is the presence of a random number of signal components that are originating from a single emitted signal, which arrives at the receiver from different directions and travels via different paths, thus having undergone different attenuations, phase shifts, and time delays [2]. These signal components add vectorially at the receiver, thus giving rise to signal fluctuations, called fading. The signal fluctuations are responsible for the degradation of the communication system performance. Fading is customarily classified into large-scale fading and small-scale fading giving rise to log-normal and short-term Multipath Fading Channels (MFC) respectively [2]. Short-term fading corresponds to severe signal envelope fluctuations, which occur in densely built-up areas and are mainly due to scattering. Log-normal shadowing corresponds to the less severe mean signal envelope fluctuations, which occur in much larger areas, such as less populated or suburban areas, and is mainly due to reflections and power path loss due to distance. The different channel models are obtained by characterizing the statistical properties of the received signal in different environments [2].

Following, we firstly explain two basic concepts in wireless channel modelling design.

Frequency reuse

Frequency reuse in mobile cellular systems means that each cell has a frequency that is far enough away from the frequency in the bordering cell that it does not provide interference problems [1], [2]. The same frequency is used at least two cells apart from each other. A cellular system separates each cell that shares the same channel set. This minimizes the interference while letting the same frequencies be used in another part of the system.
The design process of selecting and allocating channel groups for all of the base stations within the system is called frequency reuse. Figure 1.1.2 illustrates the concept of frequency reuse.

Interference

In the wireless communication systems, the fundamental consideration is that communication channel performance is interference-limited rather than noise-limited. The cellular networks are generally designed in a way that the additive noise is low enough and the performance of the receiver is usually limited by the level of interference from other signals. In general, interference can be described as co-channel interference (CCI), adjacent cell interference (also referred to as crosstalk), and multipath or intersymbol interference (ISI) [1], [2], [4].

As we describe before, the emphasis of the channel models is to predict the average received signal strength at a given distance from the transmitter, as well as the variability of the signal characters during a particular observation period. So the distance between the transmitter and the receiver is the major factor in the channel models [1], [2], [7], [8], [9], [11]. As the fact that there are short or long distances for observations, there are two fundamental propagations namely small-scale fading and large-scale path-loss. The detailed properties of them are introduced in the next two subsections. We also explain some of the important characteristics of these two channels.

2.1 Small-Scale Fading and Multipath Propagation Channel

Definition 2.1.1 Small-Scale Propagation Model

Propagation models that characterize the rapid fluctuations of the received signal strength over very short travel distance (a few wavelengths) are called small-scale propagation models.

Small-scale fading is produced by interferences between two or more versions of the transmitted signal that arrives at the receiver at very short times. There are four main factors in the propagation channel that influence small-scale fading. They are: (1) multipath propagation, (2) speed of the mobile, (3) speed of surrounding objects, and (4) the transmission bandwidth of the signal [1], [2].

Doppler Shift

Temporal changes in a propagation medium are both dynamic and random while the relative motion between transmitter and receiver gives rise to frequency shift in the original signal. This phenomenon is called Doppler shift.

Fading

Fading is an essential property of any wireless communication channel. It is described as the rapid changes in the signal amplitude at the receiver due to the vectorial addition of various signal components, which arrives from different paths due to reflections, diffractions, and scattering [2].

Fading is an essential characteristic of a multipath fading channel. In general, two classes of fading exist: long-term fading and short-term fading. Based on multipath time delay spread, there are two types of small-scale fading: flat fading and frequency selective fading.

Flat Fading:

When the bandwidth of the transmitted signal is less than the bandwidth of the channel

or when the channel impulse response time (also referred to as multipath delay spread) is less than the duration of transmitted signal, then the multipath fading channel experiences flat fading. In flat fading, the frequency domain (spectral) characteristics of the transmitted signal are preserved at the receiver.

Frequency Selective Fading:

When the bandwidth of the transmitted signal is more than the bandwidth of the channel or when the multipath delay spread is larger than the duration of the transmitted signal, the multipath channel undergoes frequency selective fading. The spectral characteristics of the transmitted signal are not preserved at the receiver because various signal frequency components of the transmitted signal arrive at the receiver from different paths, and thus the characteristics are subject to different levels of signal attenuations. Frequency selective fading introduces intersymbol interference (ISI) into the system, which can be resolved using different types of adaptive equalizers. Based on Doppler spread, there are two types of fading:

Fast Fading:

If the duration of the transmitted signal is greater than the channel coherence time, then the rate of fading is described as fast. In fast fading, the channel varies faster than the time required to complete one period of received signal.

Slow Fading:

Slow fading occurs when the signal duration is less than the coherence channel time. In slow fading, the channel changes slowly than the time needed to receive one complete period of signal, thus the optimization and demodulation of the received signal is easier to perform.

The short-term fading models suggest various distributions for the received signal (Rayleigh distribution, Rice distribution, and Nakagami-m distribution). They also provide information on the frequency response of the channel described by the Doppler power spectral

density. On the other hand, the log-normal shadowing model is described by the average power path loss due to distance and reflection of signals from surfaces. When measured in dB, it gives rise to the normal distribution which implies that the power path loss coefficient is log-normally distributed [2], [7], [8], [11].

The various parameters of the channel are measured using both narrow band and wide band signals. Models are subsequently constructed using the measured parameters. A widely used approach to construct a fading channel is to pass white noise through a shaping filter that represents the Doppler power spectral density. A specular component may be added and may represent the line-of-sight (LOS); therefore the simulation can represent a channel. A common methodology to simulate the various components of the multipath channel is to use the tapped delay line where each tap represents one path.

The small-scale propagation models characterize the rapid fluctuations of the received signal for short transmitter-receiver separation distances or short time durations. These models are more suited for representing urban or heavily populated areas. The main propagation mechanism for this type of environment is scattering. Signals are scattered at the neighbourhood of the receiver. Many copies of the transmitted signal arrive at the receiver via a number of different paths at slightly different times. At the receiver, plane waves add vectorially giving rise to rapid and severe signal fluctuations. This gives rise to the short-term fading channel model, where the term fading refers to the rapid and severe received signal fluctuations due to scattering in this type of environment [2], [5], [9].

Contrast to the short observation distance, the large-scale propagation model is useful to estimate the radio coverage area of the transmitters. Next part, we discuss the concepts of the large-scale propagation.

2.2 Large-Scale Path-Loss Propagation Channel

Definition 2.2.1 Large-Scale Propagation Model

Propagation models that predict the mean signal strength for an arbitrary transmitter-receiver separation distance that is very large (several hundreds or thousands of meters) are called large-scale propagation models.

Reflection:

Reflection occurs when an electromagnetic wave impinges on a surface that has dimensions larger than the wavelength of the propagating wave.

Diffraction:

Diffraction is due to the initiation and propagation of secondary wavelets from the main wave front because of an obstacle. The secondary wavelets combine to form a new front allowing the main wave to propagate in the shadowed region or behind the obstructions.

Scattering:

Scattering occurs when an electromagnetic wave impinges on a surface that is with dimensions smaller than the wavelength of the propagating wave.

These three basic propagation mechanisms impact propagation environments in a mobile communication system by different methods [2]. For example, reflections occur from the surface of the earth and from buildings and walls, diffraction depends on the geometry shape of the objects at high frequency channels, and scattering is produced by rough surfaces, small objects or by other irregularities in the channel.

In theory and application, propagation models indicate that the average received signal power decreases logarithmically with distance. The average large-scale path loss for an arbitrary transmitter-receiver separation is expressed as a function of distance by using a path loss exponent α, $\overline{PL}(d) \propto (\frac{d}{d_0})^{\alpha}$ or $\overline{PL}(d)[dB] = \overline{PL}(d_0)[dB] + 10\alpha \log \frac{d}{d_0}$, where α is the

path loss exponent that indicates the rate at which the path loss increases with distance d, d_0 is the close-in reference distance that is determined from measurements close to the transmitter, and d is the transmitter-receiver separation distance.

Propagation measurements in a mobile radio channel show that the average received signal strength at any point decays as a power law of the distance of separation between the transmitter and the receiver. The average received power P_r at a distance d from the transmitter is approximated by [1], [2], [7], [8], [11]:

$$\overline{PL}(d)[dB] = \overline{PL}(d_0)[dB] + 10\alpha \log \frac{d}{d_0}, \tag{2.2.1}$$

where $\overline{PL}(d_0)[dB]$ is the average power received at a close-in reference point in the far field region of the transmitter at a small distance d_0 from the transmitter, and α is the path loss exponent.

Each base station constantly monitors the signal strengths of all its reverse voice channels to determine the relative location of each mobile user with respect to the base station. Every mobile station measures the received power from surrounding base stations and continually reports the results of the measurements to the serving base station.

Interference is the major limiting factor in the performance of cellular radio systems. Interference is more severe in urban areas due to the greater radio frequency noise floor and the large number of base stations and mobiles.

In practical cellular radio and personal communication systems, the power levels transmitted by every mobile user are under constant control by the serving base stations. This is done to ensure that each mobile transmits the smallest power necessary to maintain a good quality link on the reverse channel. Power control not only helps prolong battery life for the mobile, but also reduces the reverse channel SIR in the system. Power control is especially important for emerging CDMA spread spectrum systems that allow every user in every cell to share the same radio channel [2], [3], [4], [5].

Most cellular radio systems operate in urban areas where there is no direct LOS path between the transmitter and the receiver. Due to multiple reflections from various objects, the signal travels along paths of varying lengths. The interaction between these signals causes multipath fading at a specific location and the strengths of the signals decrease as the distance between the transmitter and the receiver increases.

The path loss that represents signal attenuation as a positive quantity measured in dB is defined as the difference (in dB) between the effective transmitted power and the received power. By using power path loss model to estimate the received signal level as a function of distance, it becomes possible to predict the SIR for a mobile communication system.
The large-scale propagation models characterize the received signals when the transmitter-receiver separation distances are very large. These models are suited for representing sub-urban environments, or the not-heavily populated areas. The main propagation mechanism of electromagnetic waves in this type of environment is reflection. Attenuation of the signal strength is due to power path loss along the distance traveled by the signal and due to reflections occurring along the path when the parts of the transmitted power are absorbed by the reflected surface and the parts are carried beyond reflections. This gives rise to the log-normal shadowing channel model, where the term shadowing refers to the received signal attenuation in this type of environment and log-normal refers to the distribution of the power path loss observed by measurements at each instant of time [2], [8], [11]. The characteristics of the received signal traveled through this type of environment are fluctuations around a slowly varying mean.
The model in (2.2.1) does not consider the fact that the surrounding environment may be very different at two different locations, which have the same transmitter-receiver separation. So it leads to that the actual measured signals are much more different than the average val-

ues predicted by (2.2.1). The power path loss $PL(d)$ at a particular location is random and log-normal distributed in dB about the mean distance-dependent value. It can be expressed as [2], [8], [11]:

$$PL(d)[dB] = \overline{PL}(d) + \tilde{X} = \overline{PL}(d_0)[dB] + 10\alpha \log \frac{d}{d_0} + \tilde{X}, \tag{2.2.2}$$

then the received power is

$$P_r(d)[dB] = P_t(d)[dB] - PL(d)[dB], \tag{2.2.3}$$

where $\tilde{X}$ is Additive White Gaussian Noise (AWGN) with $N(m, \sigma^2)$.

Log-normal shadowing implies that measured signal levels at a specific transmitter-receiver separation have a Gaussian distribution about the distance-dependent mean of (2.2.1) [1], [2], [11]. The close-in reference distance d_0, the power path loss exponent α, and the standard deviation σ^2 statistically describe the power path loss model for an arbitrary transmitter-receiver location. This model can be used in computer simulation to provide received power levels for random locations in wireless network system design and analysis.

In practice, the value of α and σ^2 are computed from measured data using linear regression method. By estimating the good value of α and σ^2, we also can reach the minimized difference between the measured and estimated power path loss.

Chapter 3

Stochastic Differential Equations in Log-Normal Shadowing

3.1 Introduction

When the transmitter-receiver separation distance is large (always several times of the wavelength) and the propagation environment is not heavily populated, estimating the power path loss in wireless communication over long distance is very important because it is the main cause for signal attenuation, generally known as shadowing, which needs to compensate in the receiver [7], [8], [11].

Large-scale channel models attempt to predict the reflection and the power path loss for long distance. The multipath propagation of large-scale channel model is shown in Figure 3.1.1. There are various possible paths between the transmitter and the receiver. Traditional models do not take into consideration of the relative motion between the transmitter and the receiver; they treat the power path loss as static. Also they do not consider the correlation properties of the power path loss in space and at different observation times. In reality, these properties exist and one way to model them is through stochastic processes. So the stochastic differential equations are introduced to estimate the dynamic power path loss for the space-time propagation environment [7], [11].

In an arbitrary time-varying environment, computations of the power path loss and the signal attenuation are complex and uncertain because of the random processes of the received

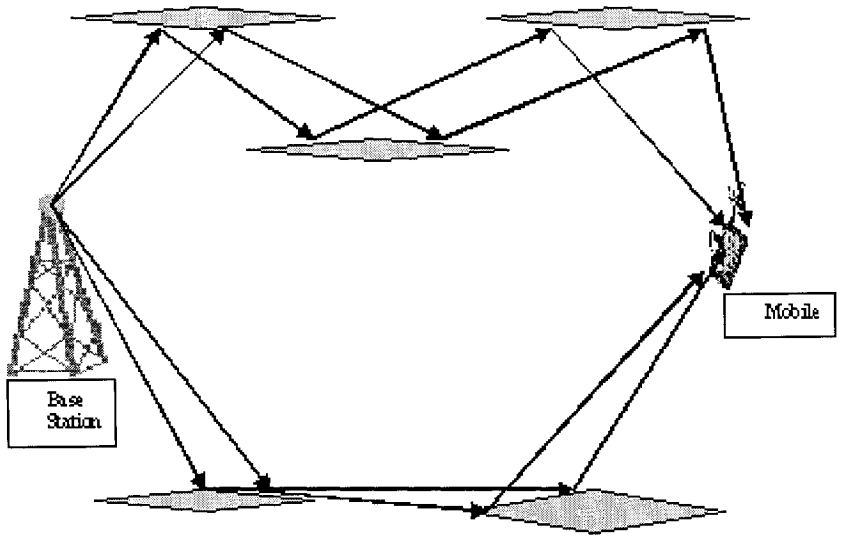

Figure 3.1.1: An illustration of multipath propagation of large scale channel model

signals. In this chapter we develop some dynamic models related to traditional lognormal shadowing models.

There are three models:

1. For fixed observation time t, we consider the model describing the dependence of the attenuation coefficients $S_{ij}(t, d)$ with respect to distance d, capturing the spatial characteristics of the propagation environment.

2. For fixed observation location d, we present the model describing the dependence of the attenuation coefficients $S_{ij}(t, d)$ with respect to time t, capturing the temporal variations of the propagation environment.

3. Space-time model captures the dynamic characteristics of the channel, where both the transmitter and the receiver move relatively to each other at a variable speed with a varying observation time. So the attenuation coefficients $S_{ij}(t, d)$ are described by distance d and time t.

Received Average Power

The received average power of a signal for an arbitrary transmitter-receiver separation distance d is given by [1], [2], [7], [11]:

$$P_r(d) = P_r(d_0)\left(\frac{d_0}{d}\right)^{\alpha}, \quad d \geq d_0 \tag{3.1.1}$$

where $P_r(d)$ is called the received average power of the signal, $P_r(d_0)$ is the received signal power at a reference distance d_0 from the transmitter, and α is the path-loss exponent. Usually we select d_0=2m for close-in distance within 1km or d_0=100m for large distance over 10km, and the path-loss exponent α depends on the propagation medium. The value of α is typically chosen between 2 and 5. In general, the denser the urban environment is, the greater the path loss exponent α. For the free space propagation environment or for a line of sight path, α=2; for modelling urban cellular systems, α=4.

Average Power Path-loss

The average power path loss for a given path is defined by the difference between the decibel power of the transmitted signal P_t, and the average decibel power of the received signal $P_r(d)$, and it is expressed by [11]:

$$\begin{aligned} \overline{PL}(d)[dB] &= 10\log\frac{P_t}{P_r(d)} = 10\log P_t - 10\log P_r(d) && (3.1.2) \\ &= \overline{PL}(d_0)[dB] + 10\alpha\log\frac{d}{d_0} && (3.1.3) \end{aligned}$$

where $d > d_0$, $\overline{PL}(d_0) = 10\log P_t - 10\log P_r(d_0)$ is the power path loss in dB's at a reference distance d_0.

The average power path loss given in (3.1.2) represents the ensemble average of all possible

power path loss values for a path of a given length. This averaging is need since the static channel models capture power path loss values that may be different from one observation instant to the next instant because of the variations of the propagation environment. From (3.1.3), we can see that the power path loss in dB's increases with the logarithm of distance with a slope equal to the power path loss exponent α.

In real measurements, this relationship is best described by adding to the equation (3.1.3) a zero-mean Gaussian distributed random variable $\tilde{X}$ with $N(0, \sigma^2)$. So we have:

$$PL(d)[dB] = \overline{PL}(d)[dB] + \tilde{X}, \quad d \geq d_0. \tag{3.1.4}$$

The random variable $\tilde{X}$ can be interpreted as representing the variability of power path loss due to numerous reflections occurring along the path from one observation instant to the next instant. An increased number of reflections can lead to increase the average power path loss.

Signal Attenuation Coefficient

The signal attenuation coefficient is proportional to the square root of the power of the received signal and represents how much the received signal magnitude is attenuated at a distance d with respect to the magnitude of the transmitted signal [1], [2], [11]. It is given by:

$$r(d) \equiv \sqrt{P_r(d)/P_t}, \tag{3.1.5}$$

where $P_r(d)$ represents the received power at distance d including the variability of power path loss due to the reflections and other uncertainties of the propagation environments, and P_t is the transmitted power.

Combining (3.1.2) and (3.1.4), we have

$$\overline{PL}(d)[dB] + \tilde{X} = 10 \log \frac{P_t}{P_r(d)}, \tag{3.1.6}$$

$$\frac{\overline{PL}(d)[dB] + \tilde{X}}{10} = \frac{\ln (P_t/P_r(d))}{\ln 10}. \tag{3.1.7}$$

Let $c = \frac{\ln 10}{10}$, then

$$c(\overline{PL}(d)[dB] + \tilde{X}) = \ln \frac{P_t}{P_r(d)}, \tag{3.1.8}$$

$$\frac{P_t}{P_r(d)} = e^{c(\overline{PL}(d)[dB]+\tilde{X})}, \tag{3.1.9}$$

that is

$$\frac{P_r(d)}{P_t} = e^{-c(\overline{PL}(d)[dB]+\tilde{X})}. \tag{3.1.10}$$

Substitute it to (3.1.5), we have

$$r(d) = e^{-\frac{c}{2}(\overline{PL}(d)[dB]+\tilde{X})} = e^{-\frac{c}{2}(PL(d)[dB])}. \tag{3.1.11}$$

Since $\tilde{X}$ is a normal distributed random variable, the above equation indicates that the attenuation coefficient $r(d)$ is log-normal distribution, hence we call this kind of channel as log-normal shadowing. Considering the varying observation time t, we can see that the attenuation coefficient $r(t,\tau)$, equivalently $S(t,\tau)$ also becomes a random process with respect to the observation time t and spatial location d or equivalently the time-delay τ.

Since the received signal amplitude is proportional to the attenuation coefficient, it is clear that the received signal amplitude decreases as distance increases. Further, for a given distance the received signal amplitude decreases as α increases.

For $\tilde{X}$ is normal distributed, from equation (3.1.11), it is clear that the attenuation coefficient, $r(d)$, is log-normal distributed, whereby the nomenclature of log-normal shadowing effects which gives rise to the nomenclature of log-normal channel [2], [7], [8], [11]. In other words, in view of the Center Limit Theory (CLT), the multiplication of random variables gives rise to a log-normal distribution for the same reason that the addition of random variables gives rise to normal distributed random variables. That is, over large areas, the attenuation coefficient is modeled by the following log-normal density function:

$$f(r) = \frac{1}{\sqrt{2\pi}\sigma_X r} e^{\left(-\frac{\left(\ln r - m\right)^2}{2\sigma_X^2}\right)}, \quad r \geq 0, \quad E[r] = e^{\left(m+\frac{\sigma_X^2}{2}\right)}, \tag{3.1.12}$$

e.g., $r = e^{kX}$, which implies that the overall power path loss in decibels is normal distributed $X \sim N(m; \sigma_X^2)$. Here $X \triangleq \overline{PL}(d)[dB]$ represents the total power path loss for a given propagation distance d, along which the signal travels including the power path loss due to reflections. The statistics (m, σ_X^2) of this distribution are often obtained by matching them to the observed data, i.e. by subtracting the real data from theoretical computations and computing the distribution of the difference which turns out to be normal distributed. In particular, the mean of the random variable X will depend on the length of the path plus the average power path loss due to an average number of reflections while its variance will depend on the variations of the propagation environment, e.g. variations in the number and nature of obstacles from one observation instant to the next instant.

Following is three types of dynamic models of log-normal shadowing.

(1) For fixed observation time t, the model describes the dependence of attenuation $S(t, \tau)$ on τ, which represents the attenuation characteristics of the propagation environment for distance $d = v_c\tau$ as well as the power path loss $X(t, \tau)$ is described by Ornstein-Uhlenbeck random process as a function of τ.

(2) For fixed transmitter-receiver distance $d = v_c\tau$, we have a model for describing the dependence of attenuation $S(t, \tau)$ on t in order to capture the random attenuation coefficient variations with varying time. The power path loss $X(t, \tau)$ is also described by Ornstein-Uhlenbeck random process as a function of time t corresponding to a given observation distance d.

(3) For both t and τ varying, we wish to know the time-space propagation characteristics of the attenuation coefficient $S(t, \tau)$ respect to the transmitter and the receiver moving continuously relative to each other.

All three models are using stochastic differential equations (SDE). After simulation, we can see that the power path loss and attenuation trajectories are log-normal distributed. It is

in agreement with the attenuation describing the log-normal shadowing effects of each path traveling through different propagation environments [7], [8], [9], [11].

The following three subsections give the detailed description of each model respectively.

3.2 Spatial Log-Normal Dynamical Model

This section gives the derivation of the model which describes the dynamic behavior of the attenuation coefficients $\{S(t,\tau)\}$. The model where time t is fixed is captured via a SDE as a function of time-delay τ, or distance $d = v_c\tau$, from the transmitter. By fixed observation time, we interpret this situation like taking a snapshot at the propagation environment and examining its attenuation properties as a function of distance. The statistical properties (first and second moments) and probability distributions of the model are computed in special cases.

3.2.1 Some Definitions and Results in SDE

Definition 3.2.1 Standard Brownian Motion

A scalar standard Brownian motion or standard Wiener process over [0,T] is a random variable $W(t)$ that depends continuously on $t \in [0,T]$ and satisfies the following three conditions [1], [2], [26], [29].

1. $W(0) = 0, P-a.s.;$

2. *For* $0 \leq s < t \leq T, \{W(t)\}_{t\geq 0}$ *has stationary independent increments, and the increments* $W(t)-W(s)$ *are normal distributed with* $E\big[W(t)-W(s)\big] = 0, \quad Var\big(W(t)-W(s)\big) = t-s;$

3. *For* $0 \leq s < t < u < v \leq T$, *the increments* $W(t)-W(s)$ *and* $W(v)-W(u)$ *are independent.*

For computational purposes, it is useful to consider discrete Brownian motion, where $W(t)$ is specified at discrete t values. In our computing, we let $\delta t = \frac{T}{N}$ for given positive integer N and $W(t_j)$ with $t_j = j\delta t$. Then the three conditions respect to $W(0) = 0$ and $W(t_j) = W(t_{j-1}) + dW(t_j), j = 1, ..., N$. Each $dW(t_j)$ is an independent random variable of the form $\sqrt{\delta t}N(0,1)$.

Definition 3.2.2 Itô stochastic integral and Itô formula

Let $W(t)$ be a standard Wiener process defined on the probability space $(\Omega, \mathcal{A}, P)$ and $\{\mathcal{A}(t) : t \in [a,b]\}$ be a class of sub-σ-algebra of $\mathcal{A}$ satisfying the following conditions:

1. *$\mathcal{A}(t_1) \subseteq \mathcal{A}(t_2)$ if $t_1 < t_2$.*
2. *$W(t)$ is $\mathcal{A}(t)$-measurable.*
3. *For $s > 0, W(t+s) - W(t)$ is independent of $\mathcal{A}(t)$.*

Let $\mathcal{L}_s$ represents the class of random function f which satisfies the following conditions:

1. *f is measurable on $[a,b] \times \Omega$.*
2. *$f(t)$ is $\mathcal{A}(t)$-measurable for almost all $t \in [a,b]$.*
3. *$\int_a^b |f(t)|dt < \infty$ with probability 1.*

If f and g are random functions with $f \in \mathcal{L}_s$ and $g \in \mathcal{L}_s$, then the form of stochastic integral $\int_a^b g(t)dW(t)$ is called **Itô stochastic integral** *[10], [26], [27], [28] as it satisfies:*

$$E\int_a^b g(t)dW(t) = 0, \tag{3.2.13}$$

$$E\Big|\int_a^b g(t)dW(t)\Big|^2 = \int_a^b E|g(t)|^2 dt, \tag{3.2.14}$$

then the equation

$$X(t) = X(a) + \int_a^t f(s)ds + \int_a^t g(s)dW(s), \quad a \le t \le b \tag{3.2.15}$$

defines a stochastic process with continuous sample paths with probability 1. The first integral in (3.2.15) is an ordinary integral and the second integral is the Ito stochastic integral. In this case, the process $X(t)$ is said to possess the stochastic differential:

$$dX(t) = f(t)dt + g(t)dW(t). \tag{3.2.16}$$

Equation (3.2.16) is called **Ito stochastic differential equation**, *the increments $X(t) - X(s)$ for $t > s$ are given by:*

$$X(t) - X(s) = \int_s^t f(u)du + \int_s^t g(u)dW(u). \tag{3.2.17}$$

Definition 3.2.3 Ornstein-Uhlenbeck process

For the Langevin equation

$\dot{X}(t) = -\gamma X(t) + \delta W(t)$,

where $W(t)$ is a white noise process, the corresponding stochastic differential equation

$dX(t) = -\gamma X(t)dt + \delta dW(t)$

has the following solution by the previous result of Ito fornula

$$X(t) = e^{-\gamma t}\Big(X(0) + \delta \int_0^t e^{\gamma s} dW(s)\Big). \tag{3.2.18}$$

The process $X(t)$ given by the above equation is known as the **Ornstein-Uhlenbeck process** *[1], [2], [11], [27], [28].*

3.2.2 Spatial Log-Normal Dynamic Model

This model captures the dynamics of the attenuation coefficient $S(t, \tau)$ in the τ dimension, or equivalently as a function of distance d, where $d = v_c\tau$, in the case where t is fixed. A SDE is derived for $S(t, \tau)$ as a function of τ for t fixed. Considering the transmission of a continuous signal arriving at the receiver via the path of total length d_n, under the assumption, the signal undergoes many reflections along the way. Let t be fixed and $0 < d_1 < d_2 < d_3 < ... < d_M$ denote the observation distances from the transmitter with corresponding delays $0 < \tau_1 <$

$\tau_2 < \tau_3 < ... < \tau_M$, where d_M is the total path length d, and τ_M is the total time-delay τ, for the signal to travel a distance d. Let $S(t,\tau_j)$ denote the attenuation coefficient associated with the jth observation instance, corresponding to delay τ_j, and a corresponding distance $d_j = v_c\tau_j$, $1 \leq j \leq M$, along that paths as shown in Figure(3.1.1). Here $S(t,\tau_j)$ is the analog to $r(\tau_j) = \{e^{-c\overline{PL}_d(d_j)[dB]}(1/P^j_{\ell r})\}^{1/2}$ in (3.1.11) indexed by j, where $P^j_{\ell r} = \Pi_{m=1}^{M_j} P_{\ell r_m}$, M_j is the number of reflections up to time delay τ_j or distance d_j, and $\sqrt{1/P_{\ell r_m}}$ is the attenuation coefficient corresponding to the mth reflection along path d up to the time delay τ_j. Suppose that the propagation environment from the transmitter to the receiver is such that a subset of the attenuation coefficients, i.e. $\sqrt{1/P_{\ell r_m}}$, associated with $S(t,\tau_j)$, corresponding to those of $S(t,\tau_{j-1})$, $1 \leq j \leq M_j$. Then (to a first-order approximation) the percent changes

$$\frac{S(t,\tau_2) - S(t,\tau_1)}{S(t,\tau_1)}, ..., \frac{S(t,\tau_{M_j}) - S(t,\tau_{M_{j-1}})}{S(t,\tau_{M_{j-1}})} \tag{3.2.19}$$

are independent random variables. Moreover, these attenuation coefficients are non-negative and usually exhibit oscillatory behavior. These properties (i.e. independent ratios) support the Brownian motion for the attenuation coefficients $\{S(t,\tau_j)\}$. Therefore, we can let $S(t,\tau) = e^{kX(t,\tau)}$, where $k = -c/2$ and $\{X(t,\tau)\}_{\tau \geq 0}$ is a Brownian motion with non-zero drift. $X(t,\tau)$ is the analog to $\overline{PL}(d)[dB]$ in (3.1.4) indexed by τ, i.e. the power path loss as a function of distance for $\tau = d/v_c$ at a fixed time t. It represents how much the signal power has lost at various locations, where the different users may be located at particular instants of time t. It is described by the Itô differential equation:

$$dX(t,\tau) = \gamma(t,\tau)d\tau + \delta(t,\tau)dW(\tau), \quad X(t,\tau_0) = \overline{PL}(d_0)[dB], \quad \tau \geq \tau_0, \ \ \tau_0 = d_0/v_c, \tag{3.2.20}$$

where $\{W(\tau)\}_{\tau \geq 0}$ is a standard Brownian motion which is assumed to be independent of $X(t,\tau_0)$. It is also assumed that $\theta(t,\tau) \triangleq \{\gamma(t,\tau), \delta(t,\tau)\}$ are random parameters for fixed t, which are independent of the Brownian motion and $X(t,\tau_0)$. The dependence of θ on t implies that the set of parameters $\theta(t,\tau)$ are associated with a given observation time t.

A different observation time t is captured by a different set $\theta(t,\tau)$. Clearly the random parameters $\{\gamma(t,\tau),\delta(t,\tau)\}$ can be used to model the propagation environment of a given path. Following is the two special examples for discussing.

1. Fixed t, $\theta(t,\tau)$ independent of τ: $\theta(t)$

For fixed t and in the case where $\theta(t,\tau)$ is independent of τ, we define $\theta(t) \triangleq \theta(t,\tau)$ and thus $\theta(t) \triangleq (\gamma(t),\delta(t))$, i.e. constant for each observation instant t. In the remaining of this section, since t is fixed, we use the notation $X(\tau) \triangleq X(t,\tau)$ and (3.2.20) is rewritten as

$$dX(\tau) = \gamma(t)d\tau + \delta(t)dW(\tau), \quad X(\tau_0) = \overline{PL}(d_0)[dB], \quad \tau \geq \tau_0, \ \ \tau_0 = d_0/v_c, \tag{3.2.21}$$

which has a unique solution for every $X(\tau_0)$ if $\gamma(t)$ and $\delta(t)$ for $t \in (t_0,T)$ are measurable and bounded constants. The solution of (3.2.21) is given by

$$X(\tau) = X(\tau_0) + \int_{\tau_0}^{\tau} \gamma(t)ds + \int_{\tau_0}^{\tau} \delta(t)dW(s), \tag{3.2.22}$$

$$X(\tau) = X(\tau_0) + \gamma(t)(\tau - \tau_0) + \delta(t)(W(\tau) - W(\tau_0)). \tag{3.2.23}$$

In this case, for a given $\theta(t)$ and $X(\tau_0)$ is Gaussian or constant, the distribution of $X(\tau)$ evolves like a Brownian motion with non-zero drift coefficient and in particular with mean $X(\tau_0) + \gamma(t)(\tau - \tau_0)$ and variance $\delta(t)^2\tau$. An application of the stochastic Itô differential rule to $S(\tau) = e^{kX(\tau)}$ yields the Itô stochastic differential equation (SDE):

$$dS(\tau) = S(\tau)\Big[\Big(k\gamma(t) + \frac{(k\delta(t))^2}{2}\Big)d\tau + k\delta(t)dW(\tau)\Big], \quad S(\tau_0) = e^{kX(\tau_0)}. \tag{3.2.24}$$

From (3.2.24), we also write

$$\frac{dS(t,\tau)}{S(t,\tau)} = (k\gamma(t) + \frac{(k\delta(t))^2}{2})d\tau + k\delta(t)dW(\tau). \tag{3.2.25}$$

The parameter $(k\gamma(t) + \frac{(k\delta(t))^2}{2})$ is the instantaneous conditional expected percentage change of the signal attenuation per unit delay, $(k\delta(t))^2$ is the instantaneous conditional variance

per unit delay, and $S(\tau_0)$ is the attenuation at observation distance d_0. The equation (3.2.25) can be solved to yield a unique solution given an initial value $S(\tau_0)$

$$S(\tau) = S(\tau_0)\exp\Big(k\gamma(t)\tau + k\delta(t)W(\tau)\Big), \quad S(\tau_0) = e^{kX(\tau_0)}. \tag{3.2.26}$$

From (3.2.21), we deduce that for a given $\theta(t)$ and $X(\tau_0)$, $\{X(\tau)\}_{\tau\geq\tau_0}$ is a special case of an Ornstein-Uhlenbeck process and thus $\{S(\tau)\}_{\tau\geq\tau_0}$ is a log-normal random process, that is, it has a log-normal probability distribution. Model (3.2.24) generates the signal attenuation factor $S(\tau)$ as a function of τ or distance $d = v_c\tau$ of a path corresponding to a fixed observation time t and has the measured characteristics (i.e. the log-normal distribution). When the parameters $(\gamma(t), \delta(t))$ are zero, then $S(\tau_0) = e^{kX(\tau_0)}$, $\forall\tau$, $\tau \in [\tau_0, \infty)$ and $S(\tau)$ will be a log-normal random variable, provided $X(\tau_0)$ is a normal distributed random variable. That is to say we arrive at the traditional lognormal model. Figures 3.2.2 to 3.2.7 give the relation of the power path loss $X(t,\tau)$ and the signal attenuation $S(t,\tau)$ with different distances as well as the different initial reference distances d_0.

2. Fixed t, $\theta(t,\tau) \triangleq \{\gamma(t,\tau), \delta(t)\}$

Considering the next particular case where for a fixed t, $\gamma(t,\tau) = \frac{10\alpha}{\tau\ln 10}$ and $\delta(t,\tau) = \delta(t)$. The solution of (3.2.21) is given by (3.2.22) and can be computed from:

$$X(t,\tau) = X(t,\tau_0) + 10\alpha\log v_c\tau - 10\alpha\log v_c\tau_0 + \delta(t)[W(\tau) - W(\tau_0)], \tag{3.2.27}$$

where for a given $\delta(t)$ and if $X(t,\tau_0)$ is Gaussian or constant, the distribution of $X(t,\tau)$ evolves like a Brownian motion with non-zero drift coefficient. Clearly, with $d = v_c\tau$, it is noticed that the power path loss given by (3.2.27) varies logarithmically with distance and it corresponds exactly to the power path loss given by (3.1.4) with $\overline{PL}(d_0) \triangleq X(t,\tau_0)$ and $\tilde{X} \triangleq \delta(t)[W(\tau) - W(\tau_0)]$. The mean of (3.2.27) is $\overline{PL}(d_0) + 10\alpha\log v_c\tau - 10\alpha\log v_c\tau_0$ and

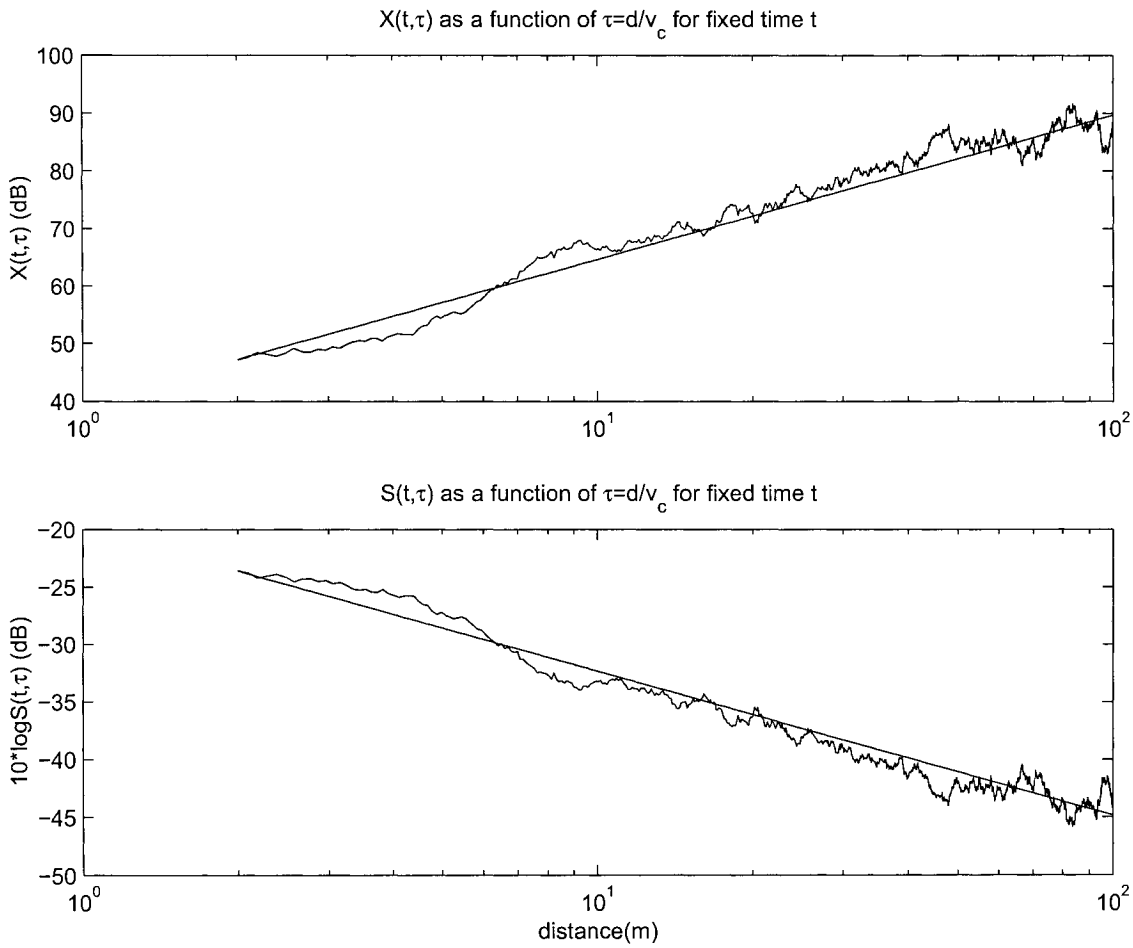

Figure 3.2.2: An illustration of power path loss and attenuation with distance 100m for a given observation time and d_0=2m.

the variance is $\delta(t)^2(\tau - \tau_0)$. It follows that the SDE for $S(t,\tau)$ is given by:

$$\frac{dS(t,\tau)}{S(t,\tau)} = \Big(\frac{10k\alpha}{\tau} + \frac{(k\delta(t))^2}{2}\Big)d\tau + k\delta(t)dW(\tau), \quad S(t,\tau_0) = e^{kX(t,\tau_0)}. \tag{3.2.28}$$

The parameter $(\frac{10k\alpha}{\tau} + \frac{(k\delta(t))^2}{2})$ is the local conditional expected percentage change of the signal attenuation per unit delay, $(k\delta(t))^2$ is the local conditional variance per unit delay, and $S(t,\tau_0)$ is the attenuation at observation distance $d_0 = v_c\tau_0$. The solution of (3.2.28) can be obtained directly from (3.2.27) and it yields

$$S(t,\tau) = e^{k\left(\overline{PL}(d_0)+10\alpha\log d\right)} e^{\delta(t)[W(\tau)-W(\tau_0)]}. \tag{3.2.29}$$

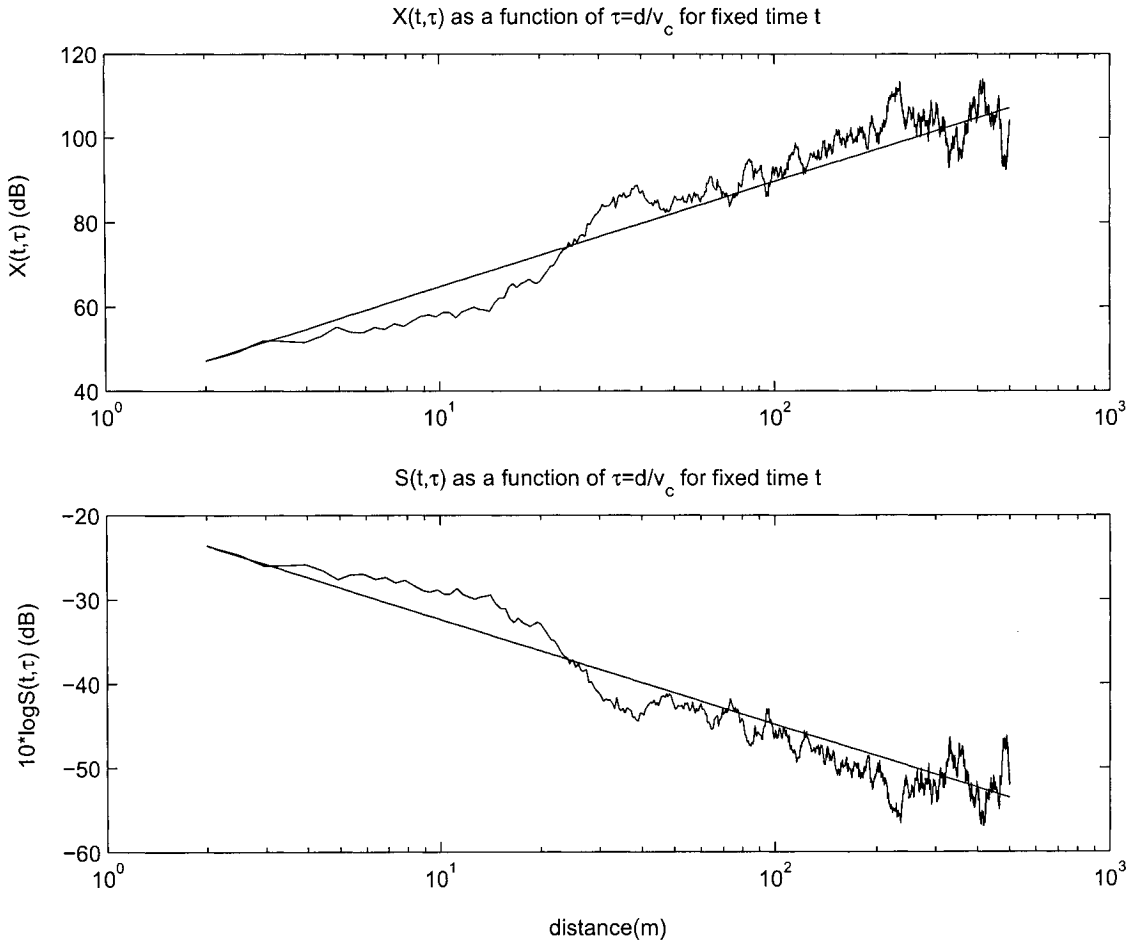

Figure 3.2.3: An illustration of power path loss and attenuation with distance 500m for a given observation time and d_0=2m.

Since for a given $\delta(t)$ and if $X(t,\tau_0)$, is Gaussian or constant, $X(t,\tau)$ in (3.2.27) evolves like a Brownian motion for all $\tau \geq \tau_0$, then $\{S(t,\tau)\}_{\tau\geq\tau_0}$ is a log-normal random process, that is, it has a log-normal probability distribution. When the parameters $\{\gamma(t,\tau),\delta(t,\tau)\}$ are zero, then $S(t,\tau) = S(t,\tau_0) = e^{kX(t,\tau_0)}$, $\forall\tau_0 \in [\tau_0,\infty)$ and $S(t,\tau)$ will be a log-normal random variable, provided $X(t,\tau_0)$ is a normally distributed random variable.

Figure 3.2.2 to 3.2.7 illustrates the power path loss and signal attenuation as a function of distance for different fixed observation time t. These figures demonstrate, as expected, that the mean of the process $X(t,\tau)$ increases logarithmically with distance and therefore that

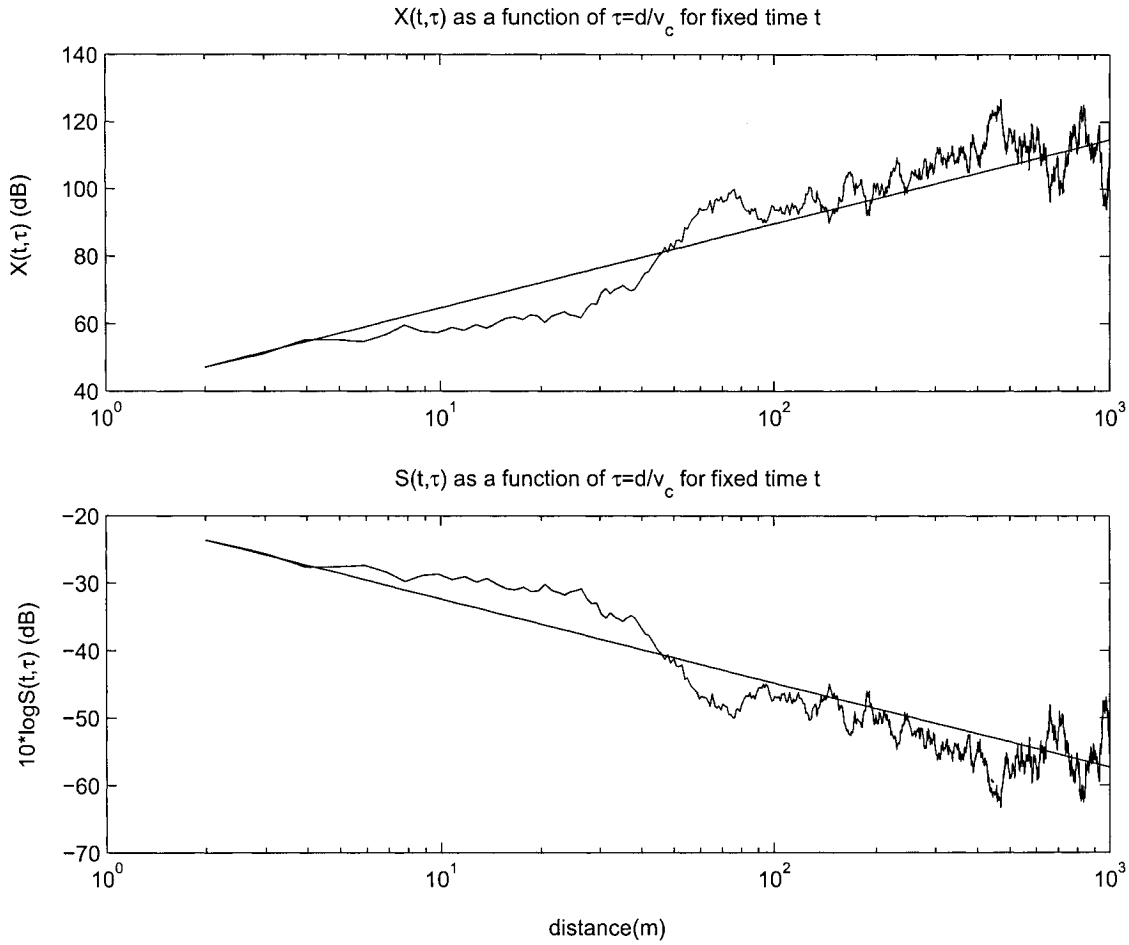

Figure 3.2.4: An illustration of power path loss and attenuation with distance 1000m for a given observation time and d_0=2m.

$S(t,\tau)$ decreases logarithmically with distance, for the particular set of parameters chosen $\gamma(t,\tau) = \frac{10\alpha}{\tau \ln 10}$ and $\delta(t,\tau) = \delta(t)$. These figures also illustrate that the variance of the process $X(t,\tau)$ increases as the realization increases. In order to bound this increase one would have to choose the parameter $\theta(t,\tau)$ appropriately, i.e. random or as a function of τ.

3. Fixed t, $\theta(t,\tau) \triangleq \{\gamma(t,\tau), \delta(t,\tau)\}$

For a particular set of parameters $(\gamma(t), \delta(t))$, $X(\tau)$ should be increasing linearly with the logarithm of distance, as indicated in (3.1.3), with a rate of increase the power path loss

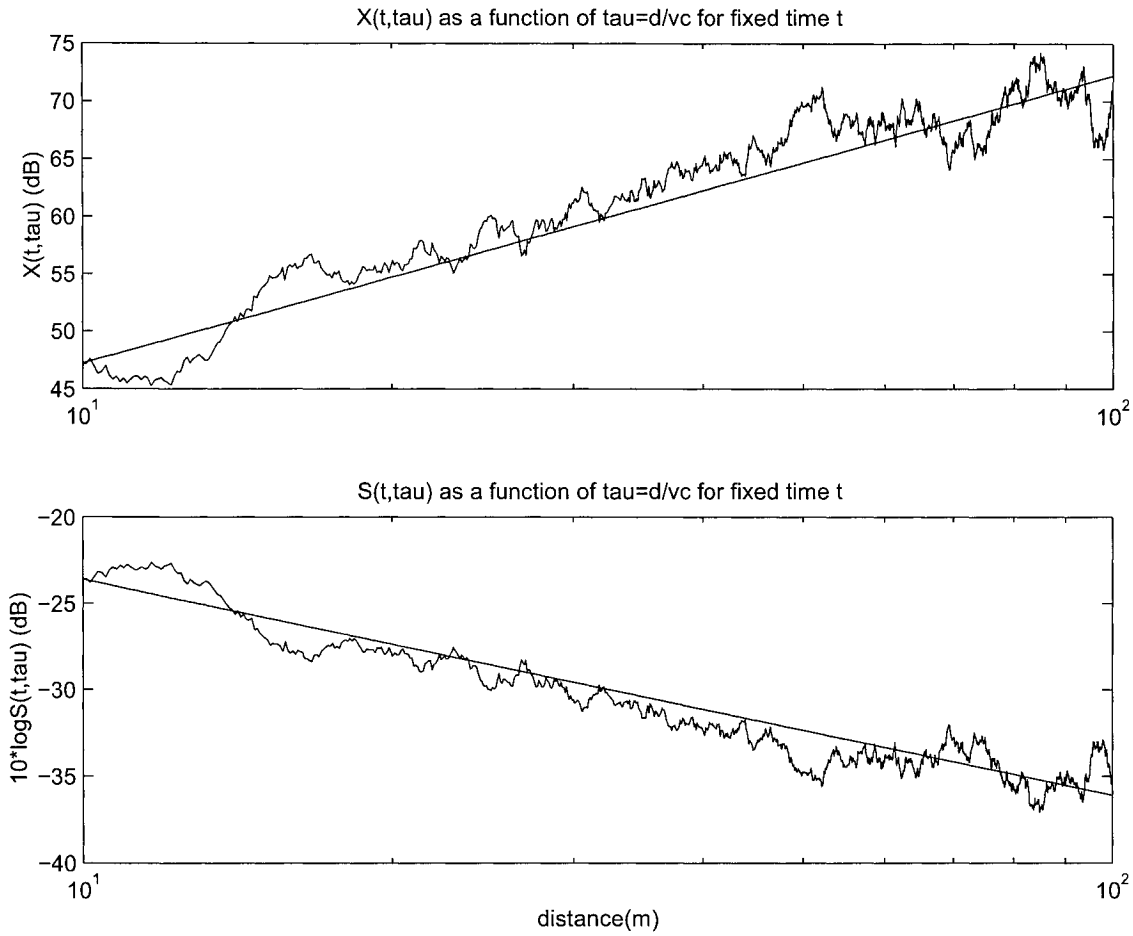

Figure 3.2.5: An illustration of power path loss and attenuation with distance 100m for a given observation time and d_0=10m.

exponent α. The mean of the process $X(\tau)$ should correspond to the average power path loss, i.e. $\overline{PL}(d)[dB] = \overline{PL}(d_0) + 10\alpha \log(\frac{v_c\tau}{v_c\tau_0})$ of (3.1.3), which captures the propagation environment characteristics and which increases logarithmically with distance. It is shown in previous section that a generalization of $\gamma(t)$ to a function of τ, i.e. $\gamma(t,\tau)$, enables the model to reproduce the observed rate of increase of power path loss (or equivalently decrease of attenuation) logarithmically with distance. This is done by a generalization of the Brownian motion model to one which has random process parameters $\theta(t,\tau) \stackrel{\Delta}{=} \{\gamma(t,\tau), \delta(t,\tau)\}_{\tau \geq \tau_0}$, adapted to an underlying filtration $\{\mathcal{A}_\tau\}_{\tau \geq \tau_0}$ associated with the probability basis $(\Omega, \mathcal{A}, P)$

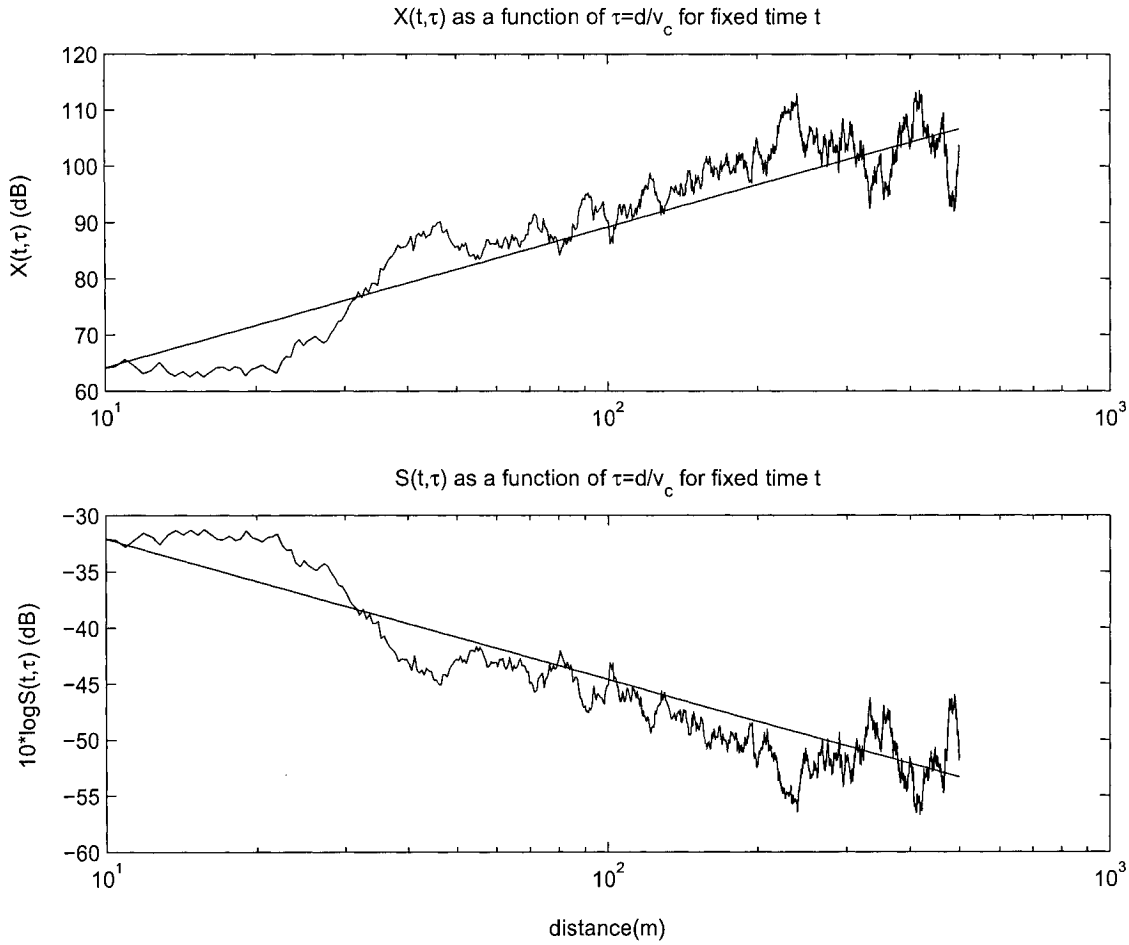

Figure 3.2.6: An illustration of power path loss and attenuation with distance 500m for a given observation time and d_0=10m.

on which the power path loss and signal attenuation evolves continuously with respect to τ. This part explains the general formula of parameter set $\theta(t,\tau)$, for fixed t, $X(t,\tau)$ is given by:

$$dX(t,\tau) = \gamma(t,\tau)d\tau + \delta(t,\tau)dW(\tau), \quad X(t,\tau_0) = \overline{PL}(d_0)[dB] \text{ at time } t, \quad \tau \geq \tau_0, \ \tau_0 = d_0/v_c, \tag{3.2.30}$$

where $\{W(\tau)\}_{\tau \geq \tau_0}$ is a standard Brownian motion which is assumed to be independent of $X(t,\tau_0)$. So the equation (3.2.30) has a unique solution for every $X(t,\tau_0)$ if $\{\gamma(t,\tau), \delta(t,\tau)\}$

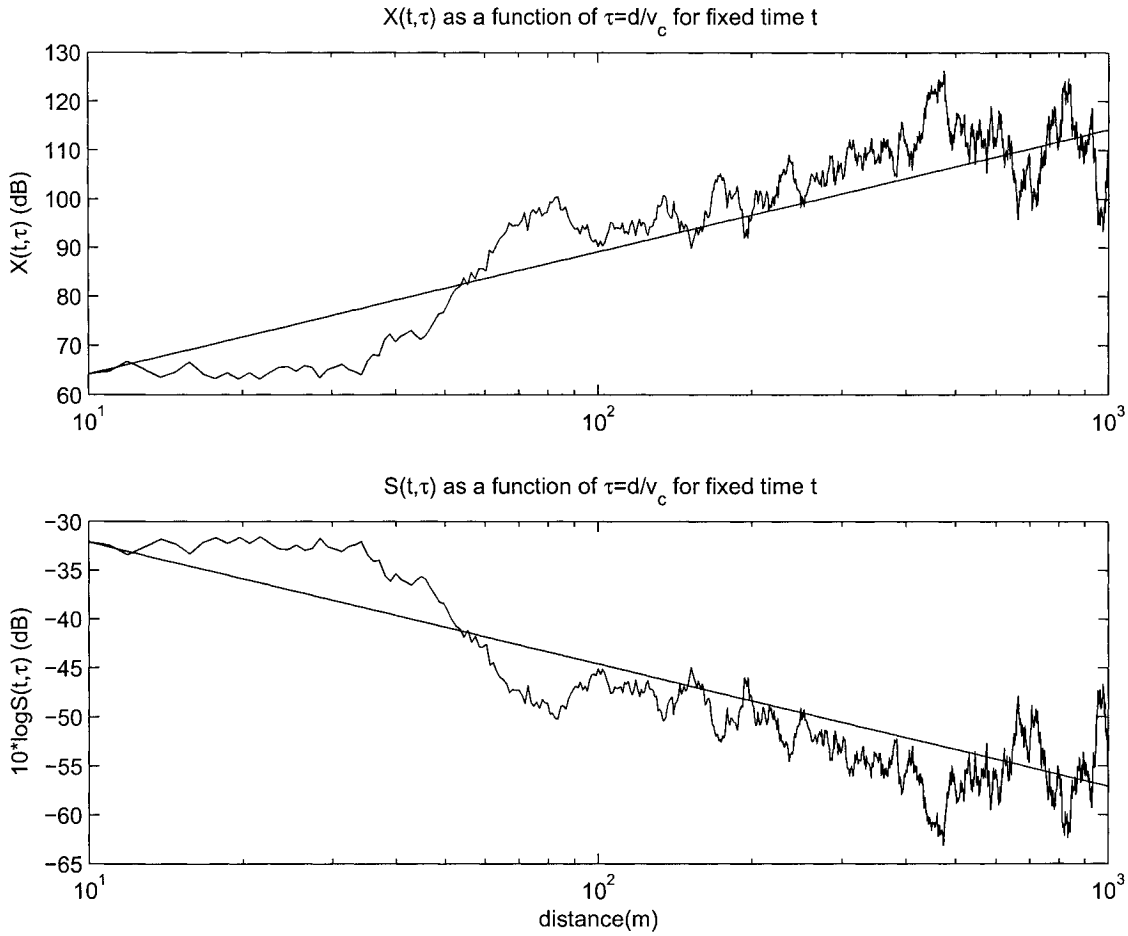

Figure 3.2.7: An illustration of power path loss and attenuation with distance 1000m for a given observation time and d_0=10m.

with $t \in (t_0, T), \tau \geq \tau_0$ are measurable and bounded, and it is given by:

$$X(t,\tau) = X(t,\tau_0) + \int_{\tau_0}^{\tau} \gamma(t,s)ds + \int_{\tau_0}^{\tau} \delta(t,s)dW(s). \tag{3.2.31}$$

An application of the Itô's stochastic differential rule to $S(t,\tau) = e^{kX(t,\tau)}$ yields the Itô stochastic differential equation (SDE):

$$\begin{aligned} dS(t,\tau) &= S(t,\tau)\Big[\Big(k\gamma(t,\tau) + \frac{(k\delta(t,\tau))^2}{2}\Big)d\tau + k\delta(t,\tau)dW(\tau)\Big] \\ &\triangleq S(t,\tau)\Big[\alpha(t,\tau)d\tau + \beta(t,\tau)dW(\tau)\Big], \qquad S(t,\tau_0) = e^{kX(t,\tau_0)}. \end{aligned} \tag{3.2.32}$$

This model is very general, it does not satisfy any of the properties of the Brownian motion process, and it becomes more general in capturing properties of the power path loss process. For fixed t, $S(t,\tau)$ generated with $\theta(t,\tau) = \theta(\gamma(t,\tau), \delta(t,\tau))$ and a given $X(t,\tau_0)$, would have the same properties as those for $S(\tau)$ in (3.2.21).

1. $\{S(t,\tau)\}_{\tau\geq\tau_0}$ has continuous trajectories and $\{\ln S(t,\tau)\}_{\tau\geq\tau_0}$ has stationary independent increments, that is, $\Big(S(t,\tau) - S(t,\sigma)\Big)/S(t,\sigma), \tau > \sigma$ is independent of the past history of the signal $\{S(t,\tau); 0 \leq \tau \leq \sigma\}$, and $\Big(S(t,\tau) - S(t,\sigma)\Big)/S(t,\sigma)$ is identical distributed to $\Big(S(t,\tau-\sigma) - S(t,\tau_0)\Big)/S(t,\tau_0)$.

2. $\{S(t,\tau)\}_{\tau\geq\tau_0}$ is log-normal distributed random process. In particular, $kX(t,\tau) = \ln S(t,\tau)$ has increments $X(t,\tau) - X(t,\sigma)$ which are normal distributed with mean $\int_\sigma^\tau \gamma(t,u)du$ and variance $\delta(t)^2(\tau-\sigma)$, which are independent over disjoint intervals, $X(t,\tau_4) - X(t,\tau_3)$, $X(t,\tau_2) - X(t,\tau_1)$, $\tau_4 > \tau_3 \geq \tau_2 > \tau_1 \geq \tau_0$. Thus, the increments of $\{X(t,\tau)\}_{\tau\geq\tau_0}$ are independent, stationary, and identical distributed.

3. The local variance of the signal $\{S(t,\tau)\}_{\tau\geq\tau_0}$ increases when its realization increases, i.e. distance increases, and the volatility parameter $\delta(t)$ increases.

3.3 Temporal Log-Normal Dynamic Model

The second model captures the dynamics of the attenuation coefficient $S(t,\tau)$ as a function of time t for a particular location $d = v_c\tau$ from the transmitter. A SDE is derived for $S(t,\tau)$ as a function of t for fixed τ. A similar argument, as the one used for the Brownian motion in Section 3.2 is used to demonstrate the independence of the ratios of the attenuation coefficients $S(t,\tau)$, with respect to the variable t. In this case, for fixed τ, corresponding to given distance, the attenuation coefficients are examined at time instants, $0 < t_1 < t_2, \ldots, < t_m$ as illustrated in Figure 3.3.8. Similar with the discussion in Section 3.2, the ratios

$$\frac{S(t_2,\tau)}{S(t_1,\tau)}, \ldots, \frac{S(t_m,\tau)}{S(t_{m-1},\tau)}$$

are independent random variables and thus the attenuation coefficients $\{S(t_j,\tau)\}$ satisfy the properties of Brownian motion. As in the case of the Brownian motion, the signal attenuation is defined by $S(t,\tau) = e^{kX(t,\tau)}$, where the power path loss process $X(t,\tau)$ is examined as a function of time t. $X(t,\tau)$ is the analog to $\overline{PL}(d)[dB]$ in (3.1.2) for fixed $d = v_c\tau$ as a function of time t. It represents how much power the signal has lost at a particular location as a function of time t. It is generated by a mean-reverting version of a general linear SDE given by:

$$dX(t,\tau) = \beta(t,\tau)\Big(\gamma(t,\tau) - X(t,\tau)\Big)dt + \delta(t,\tau)dW(t), \qquad (3.3.33)$$
$$X(t_0,\tau) = \overline{PL}_d(d)[dB].$$

The initial condition $X(t_0,\tau)$ can be obtained from the Brownian motion model (3.2.20) which calculates $X(t_0,\tau)$ for fixed $t = t_0$ as a function of τ. Here the random processes $\theta(t,\tau) \triangleq \{\beta(t,\tau),\gamma(t,\tau),\delta(t,\tau)\}_{t\geq 0}$ are adapted to an underlying filtration $\mathcal{A}_{t\geq 0}$ (or measurable to the σ-algebra) generated by the σ-algebra, $\sigma\{W(s);0 \leq s \leq t\}$ and $\{W(t)\}_{t\geq 0}$ is a standard Brownian motion process which is independent of $X(t_0,\tau)$. If the random processes $\{\theta(t,\tau)\}_{t\geq 0}$ are measurable and bounded, (3.3.33) has a unique solution for every $X(t_0,\tau)$ given by

$$X(t,\tau) = e^{-\beta([t,t_0],\tau)}\Big(X(t_0,\tau) + \int_{t_0}^{t} e^{\beta([u,t_0],\tau)}\Big[\beta(u,\tau)\gamma(u,\tau)du + \delta(u,\tau)dW(u)\Big]\Big),$$
$$\beta([t,t_0],\tau) \triangleq \int_{t_0}^{t}\beta(u,\tau)du. \qquad (3.3.34)$$

Moreover, using Itô's stochastic differential rule on $S(t,\tau) = e^{kX(t,\tau)}$ with respect to τ we obtain

$$dS(t,\tau) = S(t,\tau)\Big[\Big(k\beta(t,\tau)[\gamma(t,\tau) - X(t,\tau)] + \frac{1}{2}k^2\delta^2(t,\tau)\Big)dt + k\delta(t,\tau)dW(t)\Big],$$
$$S(t_0,\tau) = e^{kX(t_o,\tau)}. \qquad (3.3.35)$$

The dependence of θ on τ implies that the set of parameters $\theta(t,\tau)$ are associated with a given observation location at distance d from the transmitter. Clearly the random parameters θ can

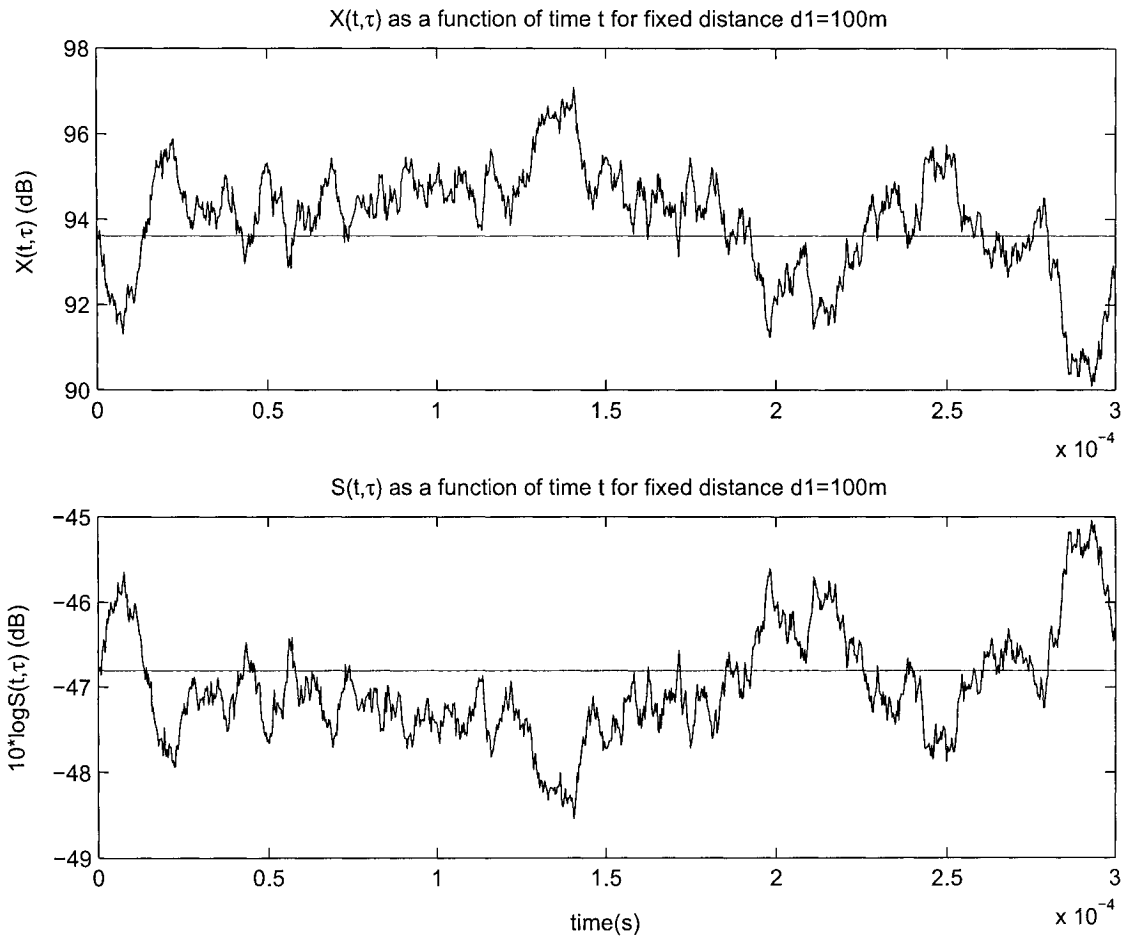

Figure 3.3.8: An illustration of power path loss and attenuation with time varying for given distance where x_0=47.2dB and parameter $\delta = 450$.

be used to model how the attenuation coefficients vary at any location along the propagation path as a function of time t. A different location is characterized by a different set $\theta(t, \tau)$. In particular, $\gamma(t, \tau)$ corresponds to the average power path loss at distance d from the transmitter, namely $\overline{PL}(d)[dB]$, and the model will track and converge to this value as time progresses. Two examples are presented for which it is possible to obtain densities and first and second moments.

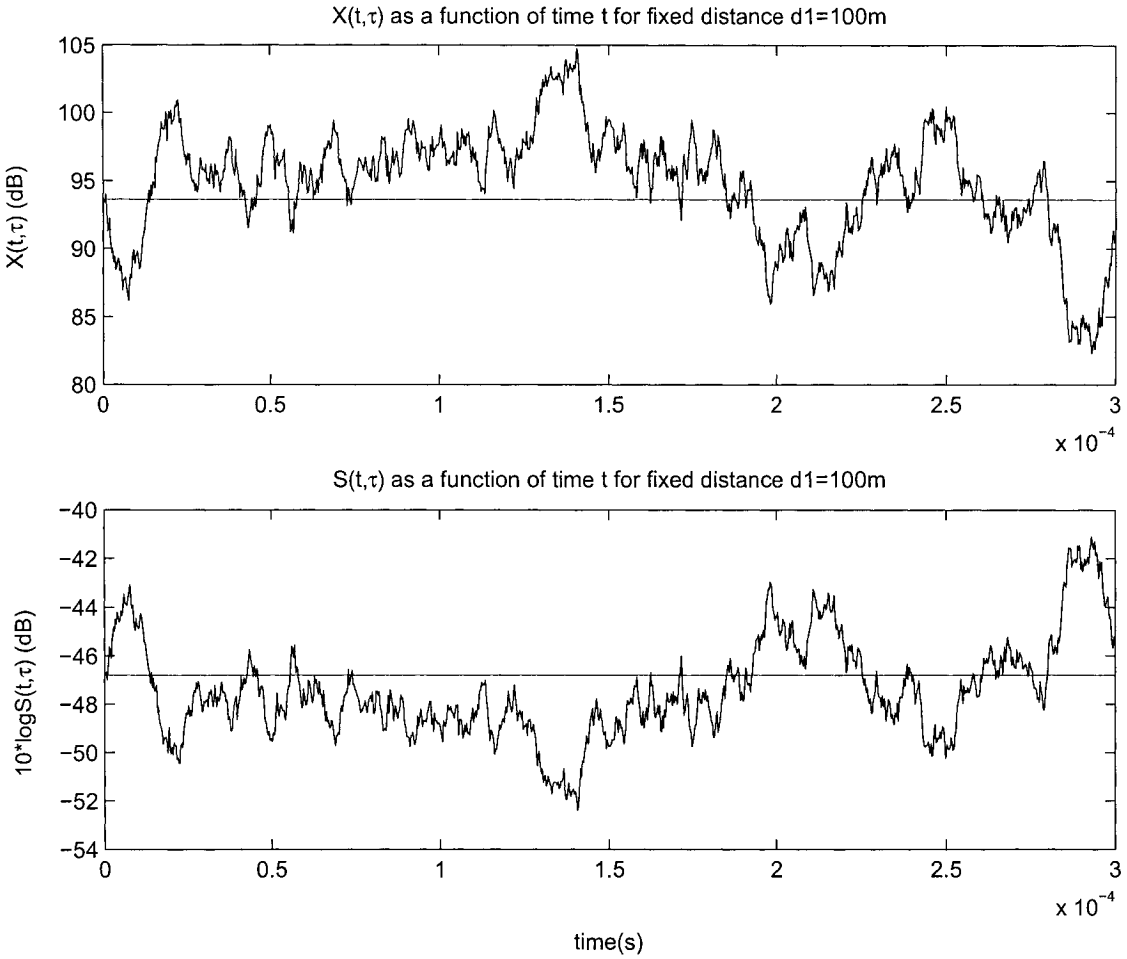

Figure 3.3.9: An illustration of power path loss and attenuation with time varying for given distance where x_0=47.2dB and parameter $\delta = 1450$.

1. Fixed τ, $\theta(t,\tau)$ independent of t: $\theta(\tau) = \{\beta(\tau), \gamma(\tau), \delta(\tau)\}$

For fixed τ and in the special case where $\{\beta(t,\tau), \gamma(t,\tau), \delta(t,\tau)\}_{t\geq 0}$ are independent of t and chosen according to some probability distribution, we define $\theta(\tau) \triangleq \theta(t,\tau)$ and $\theta(\tau) = \{\beta(\tau), \gamma(\tau), \delta(\tau)\}_{\tau\geq 0}$, i.e. constant for a particular location $d = v_c\tau$, thus characterizing the dynamics with respect to time of a particular location with respect to time. In this section we use the notation $X(t) \triangleq X(t,\tau)$ and $\{X(t)\}_{t\geq t_0}$ is being generated by a mean-reverting

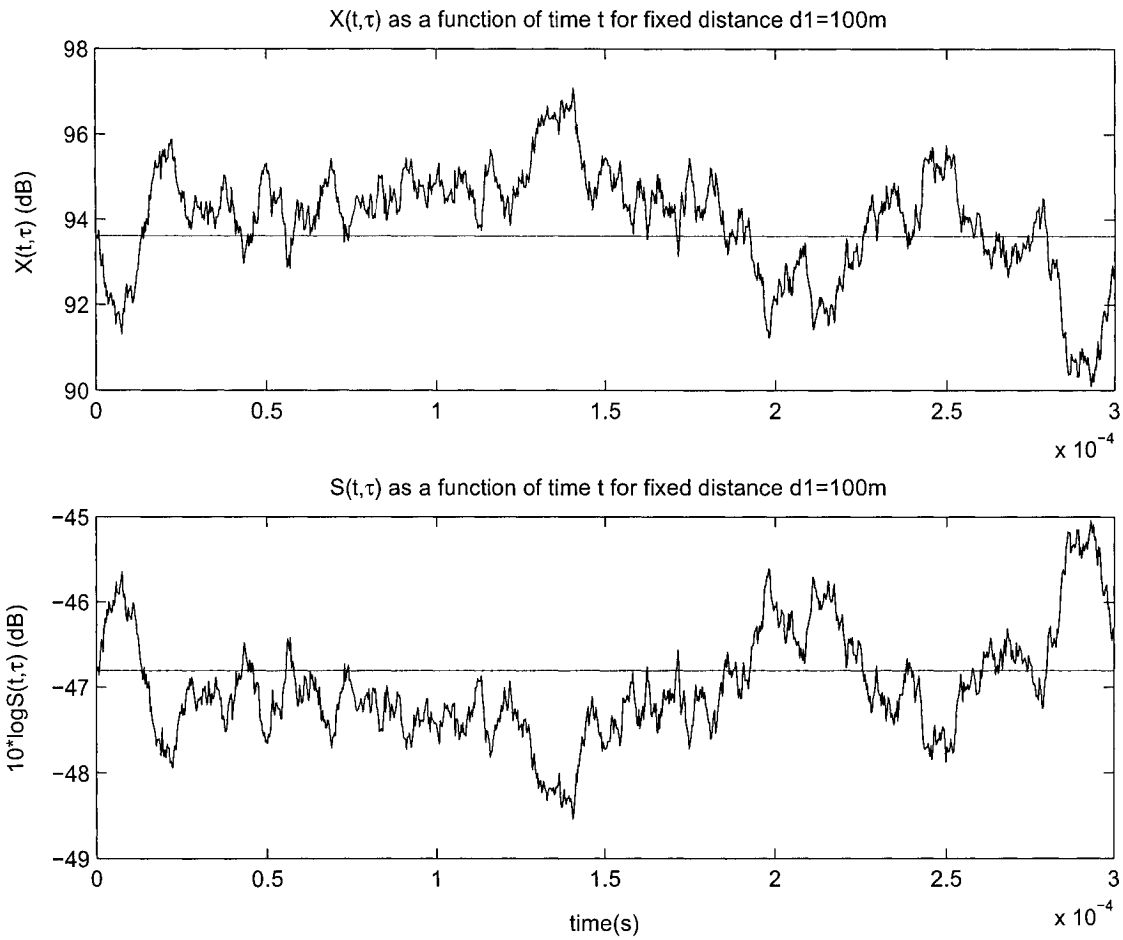

Figure 3.3.10: An illustration of power path loss and attenuation with time varying for given distance where x_0=64.2dB and parameter $\delta = 450$.

version of an Ornstein-Uhlenbeck process given by

$$dX(t) = \beta(\tau)\big(\gamma(\tau) - X(t)\big)dt + \delta(\tau)dW(t), \quad X(t_0) = \overline{PL}(d)[dB],$$
$$d = \tau/v_c, \quad \beta(\tau) > 0, \quad \delta(\tau) > 0, \quad \gamma(\tau) = \overline{PL}_d(d)[dB]. \tag{3.3.36}$$

Here $\{W(t)\}_{t\geq 0}$ is a standard Brownian motion process which is independent of $X(t_0)$ and the random parameter $\theta(\tau)$. Clearly, if $S(t) = e^{kX(t)}$, and (3.3.36) is assumed, then $\{\beta(\tau), \gamma(\tau), \delta(\tau)\}$ of (3.3.36) are specified explicitly, characterizing the attenuation for a specific location of the propagation environment. It is shown that the first term in (3.3.36)

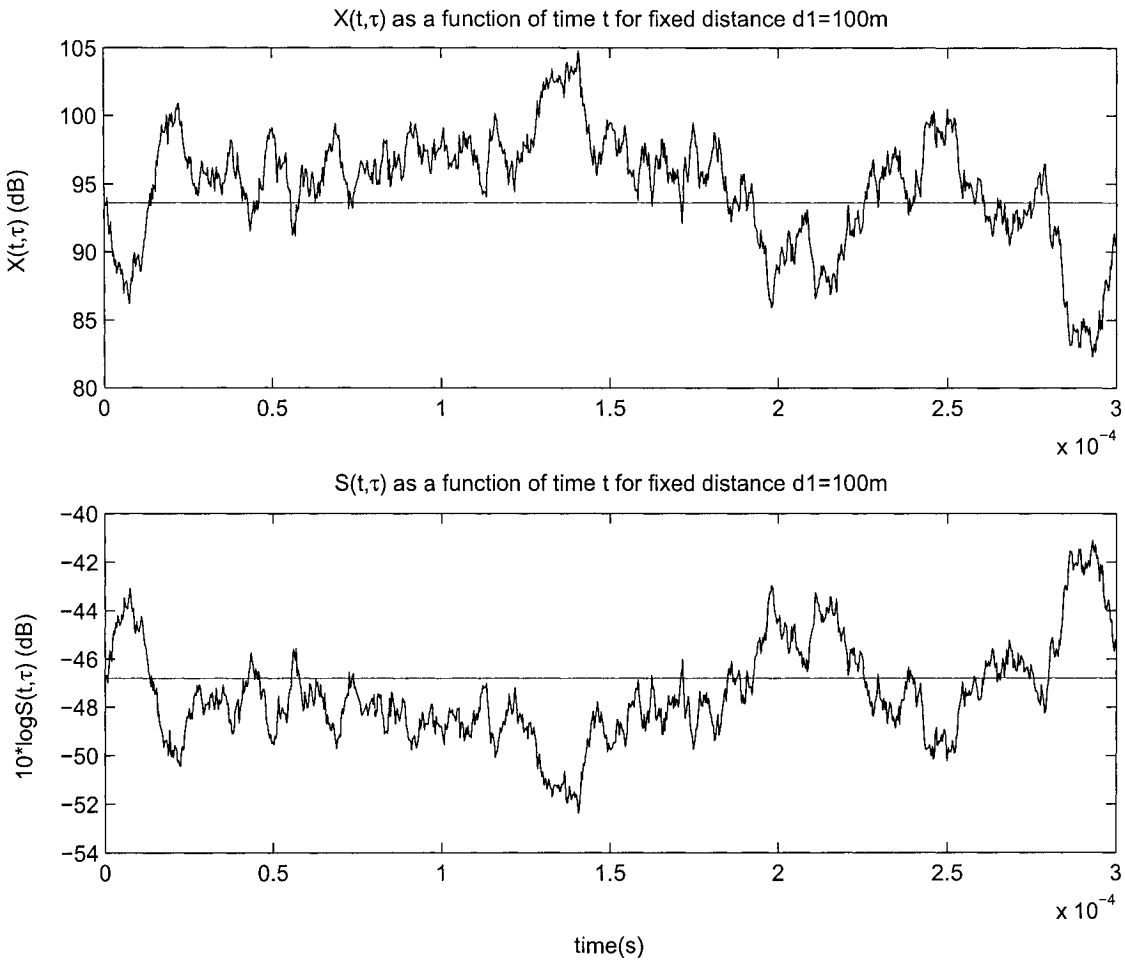

Figure 3.3.11: An illustration of power path loss and attenuation with time varying for given distance where x_0=64.2dB and parameter $\delta = 1450$.

implies an adjustment towards the value $\gamma(\tau)$, where $\beta(\tau)$ is the speed of the adjustment. This implies that every time that $\gamma(\tau)$ changes, the model should track these changes with a speed dictated by $\beta(\tau)$. The parameter $\gamma(\tau)$ models the average power path loss for an arbitrary distance d traveled by the signal as given by (3.1.2). To determine the behavior of $\{S(t)\}_{t\geq 0}$, we first examine the behavior implied by (3.3.36). For a given $\theta(\tau)$, the solution of (3.3.36) starting at $X(s)$ is

$$X(t) = e^{-\beta(\tau)(t-s)}\Big(X_s + \gamma(\tau)(e^{\beta(\tau)(t-s)} - 1) + \delta(\tau)e^{-\beta(\tau)s}\int_s^t e^{\beta(\tau)u}dW(u)\Big). \qquad (3.3.37)$$

Consequently, $\{X(t)\}_{t\geq 0}$ is a Gaussian random process, and the conditional expected value and variance of X at time t conditional on its current value at s for $t > s$ and $\theta(\tau)$ are:

$$E\big[X(t)|X(s),\theta(\tau)\big] = e^{-\beta(\tau)(t-s)}\Big(X_s + \gamma(\tau)(e^{\beta(\tau)(t-s)} - 1)\Big), \tag{3.3.38}$$

$$Var\Big(X(t)|X(s) = X_s,\theta(\tau)\Big) = \delta(\tau)^2\Big(\frac{1 - e^{-2\beta(\tau)(t-s)}}{2\beta(\tau)}\Big). \tag{3.3.39}$$

As the observation instant t becomes large, the random process $\{X(t)\}_{t\geq 0}$ converges in law to a Gaussian random variable with mean $\gamma(\tau) = \overline{PL}_d(d)[dB]$ and variance $\frac{\delta(\tau)^2}{2\beta(\tau)}$. That is,

$$f_\theta(X_\infty,\infty;X_s,s) = \frac{1}{\sqrt{2\pi\frac{\delta(\tau)^2}{2\beta(\tau)}}}\exp\Big(-\frac{(X_\infty - \gamma(\tau))^2}{2(\frac{\delta(\tau)^2}{2\beta(\tau)})}\Big). \tag{3.3.40}$$

The steady-state conditional mean of $\{X(t)\}_{t\geq 0}$ for large t represents the average power path loss for a given location along the propagation under the assumption that the environment is not moving anymore.

From (3.3.37), the dynamics of $S(t,\tau)$ are obtained by the Itô differential rule to yield

$$dS(t) = S(t)\Big(k\beta(\tau)\big[\gamma(\tau) - X(t)\big] + \frac{1}{2}(k\delta(\tau))^2\Big)dt + S(t)k\delta(\tau)dW(t),$$
$$S(t_0) = e^{kX(t_0)}. \tag{3.3.41}$$

Clearly, for a given set $\theta(t,\tau)$ the joint process $\{S(t),X(t)\}_{t\geq 0}$ is a Markov process since $kX(t) = \log S(t)$, the distribution of $S(t)$ is log-normal distribution, and it is straight forward to derive the density and the moments for $S(t)$ similar with the Section 3.2.

2. Fixed τ, $\theta(t,\tau) \triangleq \{\beta(\tau),\gamma(t,\tau),\delta(\tau)\};\gamma(t,\tau)$ as function of t

From the general case (3.3.33), we let $\theta(t,\tau) \triangleq \{\beta(\tau),\gamma(t,\tau),\delta(\tau)\}$, that is to say $\beta(\tau),\delta(\tau)$ are constants and $\gamma(t,\tau)$ is a function of time t. If we consider t_0=0, so the general equation (3.3.33) becomes

$$dX(t,\tau) = \beta(\tau)\Big(\gamma(t,\tau) - X(t,\tau)\Big)dt + \delta(\tau)dW(t), \tag{3.3.42}$$
$$X(t_0 = 0,\tau) = \overline{PL}(d)[dB].$$

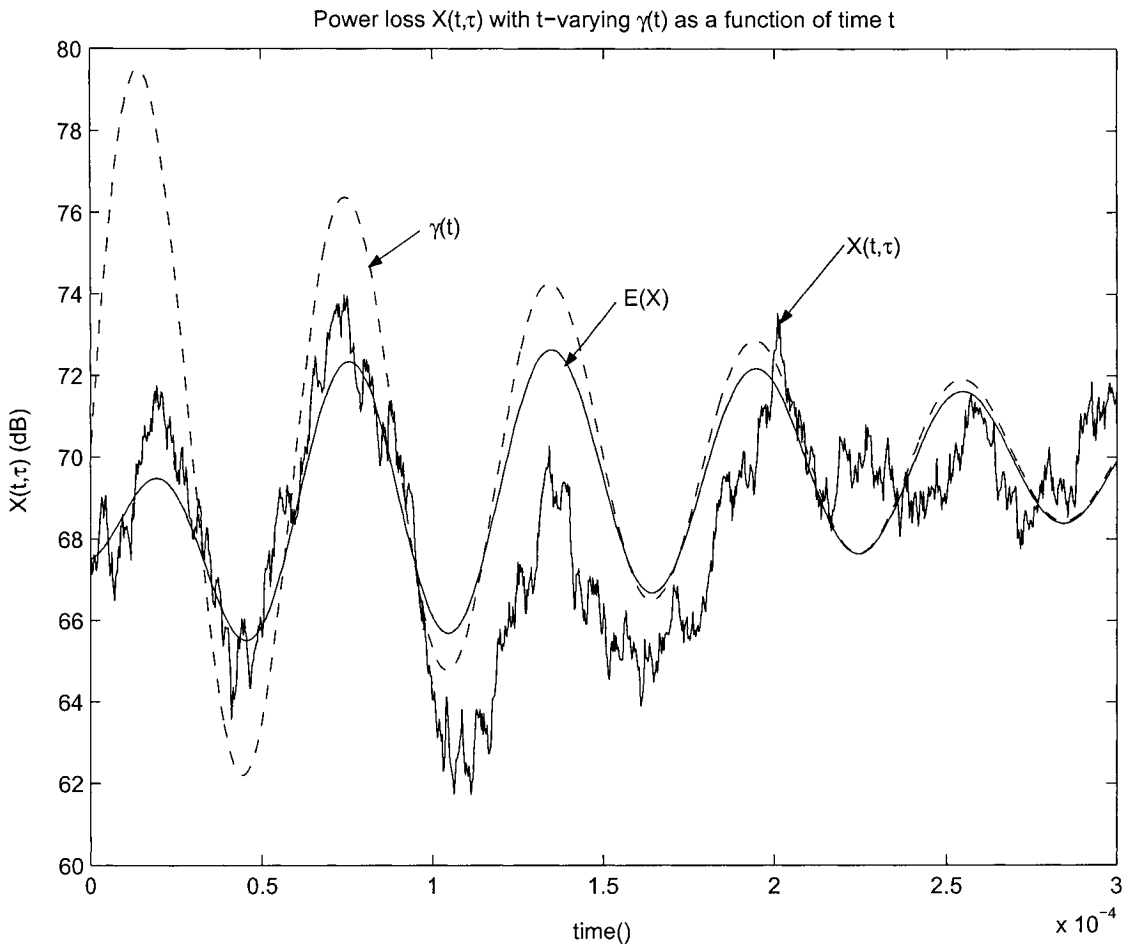

Figure 3.3.12: An illustration of the time-spreading and time variations properties of the channel for lower β=105,000.

The solution is

$$X(t,\tau) = e^{-\beta(\tau)}\Big(X(t_0=0,\tau) + \int_0^t e^{\beta(\tau)}\Big[\beta(\tau)\gamma(u,\tau)du + \delta(\tau)dW(u)\Big]\Big). \qquad (3.3.43)$$

Given a special case $\gamma(t,\tau) = \bar{\gamma} * \left(1 + 0.15e^{(-2t/T)}sin(\frac{10\pi t}{T})\right)$. $\bar{\gamma} = 70dB$ is corresponding to a distance $d = 12m$ for the model of power path loss with distance in (3.2.27). T is the observation interval.

Figure 3.3.12 and 3.3.13 are plotted by giving selected parameters $\delta(\tau) = 1234$, and $\beta(\tau) = 105,000$, $\beta(\tau) = 220,000$ respectively. They illustrate that the power path loss converges

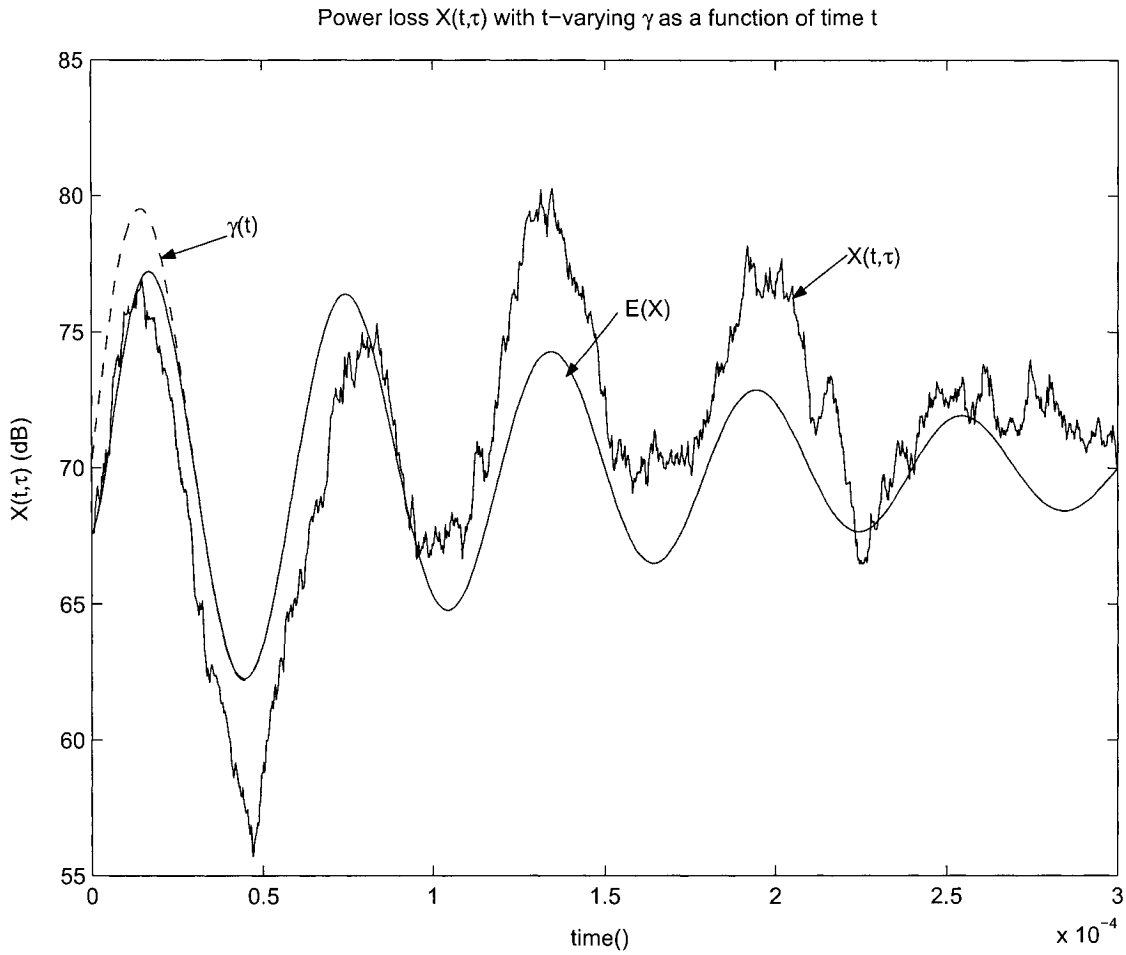

Figure 3.3.13: An illustration of the time-spreading and time variations properties of the channel for higher β=220,000.

to $\gamma(t,\tau)$ which represents the temporal variations of the propagation environments. If we change to different location and select different parameter $\delta(\tau)$ and $\beta(\tau)$, we can have different $\tilde{\gamma}$, then get the corresponding power path loss that still increases logarithmically with distance d.

3. Fixed τ, $\theta(t,\tau) \triangleq \{\beta(t,\tau), \gamma(t,\tau), \delta(t,\tau)\}$

Considering the mean-reverting log-normal model (3.3.33), when we fix the observation location e.g. τ is fixed, then the parameters of $\theta(t,\tau) \triangleq \{\beta(t,\tau), \gamma(t,\tau), \delta(t,\tau)\}$ are time varying

random processes. The solution of the power path loss $X(t,\tau)$ and the signal attenuation $S(t,\tau)$ have the general forms given by (3.3.34) and (3.3.35) respectively. For fixed τ, at each instant of observation time, the power path loss $X(t,\tau)$ is normal distributed and the corresponding attenuation $S(t,\tau)$ is log-normal distributed. As time increases, the lognormal random process approaches a lognormal random variable. So the random parameters $\{\beta(t,\tau),\gamma(t,\tau),\delta(t,\tau)\}$ can be used to model how the attenuation varies at any location with the multipath propagation as a function of time t. That is to say for a different transmitter-receiver pair, it can be characterized by a different set of $\{\beta(t,\tau),\gamma(t,\tau),\delta(t,\tau)\}$.

After using linear SDE in modelling the dynamic behavior in time and space of the log-normal shadowing channel models, we can get the power path loss $X(t,\tau)$ and the signal attenuation coefficient $S(t,\tau)$ respectively for each instant of time and each observation location. From (3.3.38) and (3.3.39), we can get the first and second moments of $X(t,\tau)$. For $S(t,\tau) = e^{kX(t,\tau)}$, we also can get the first and second moments of $S(t,\tau)$ for a different transmitter-receiver pair. It is the basis for next chapter of power control problem since we can take these signal attenuation coefficients as channel gains.

3.4 Space-Time and Multipath Log-Normal Model

3.4.1 Space-Time Log-Normal Channel Model

Considering again the mean-reverting log-normal model with time-varying random processes $\theta(t,\tau)$, i.e. for fixed τ, $\theta(t,\tau)$ varies with time, satisfying the conditions discussed above where the power path loss equation is given by (3.3.33). In the previous section, the model (3.3.33) captures the time variations corresponding to a fixed location d. In particular, we use the time variations of $\gamma(t,\tau)$ to model any arbitrary time variations of the mean, due to variations of the propagation environment between the transmitter and the fixed location d. Here we extend this model to capture space variations, in addition to time variations, using

the fact that $\gamma(t,\tau)$ is both a function of t and τ [7], [8], [9], [11].

Considering that the observation point moves away from location d, with velocity v_m, in an arbitrary direction defined by the angle ϕ, as shown in Figure 3.4.14. At time t, the new distance from the transmitter to the new observation point d', is given by:

$$\begin{aligned} d'(t) &= \sqrt{(d+t\ \ v_m\cos\phi)^2+(t\ \ v_m\sin\phi)^2} \\ &= \sqrt{d^2+(v_m\ \ t)^2+2\ \ d\ \ t\ \ v_m\cos\phi}, \end{aligned} \tag{3.4.44}$$

and according to (3.1.2) the average power path loss at that new location, corresponding mean $\gamma(t,\tau)$ is thus given by:

$$\gamma(t,\tau)=\overline{PL}_d(d(t))[dB]=\overline{PL}(d_0)+10\alpha\log\frac{d'(t)}{d_0}+\xi(t), \tag{3.4.45}$$

where $d(t)$ is given by (3.4.44), and $\xi(t)$ is an arbitrary function of time which presents additional temporal variations in the propagation environment. The receiver is in relative motion with respect to the transmitter and the power path loss is also relative to the transmitted signal.

Similar with previous section about the power path loss $X(t,\tau)$ generated by (3.3.33), we can see that in the space-time environment, the power path loss $X(t,\tau)$ is relative to both distance d and time t.

3.4.2 Multipath Log-Normal Channel Model

In a multipath time-varying environment, all the parameters characterize the channel model, i.e. attenuation coefficients, phase-shift, number of paths and sub paths, and time delays, are characterized as random processes. A multipath structure is depicted in Figure 3.1.1 giving rise to the multipath log-normal channel [2], [9], [11]. The paths are usually identified and possibly ordered according to their arrival times. As a consequence of the different propagation paths, the overall received signal consists of the superposition of copies of the

transmitted signal, which arrive from different directions, therefore undergo different attenuations, phase-shifts, and time delays. The multiple copies of the transmitted signal arriving at the receiver at different delays give rise to the time-spreading characteristics of the channel.

So we can consider that the normal distributed power path loss $X(t,\tau)$ and the log-normal distributed signal attenuation $S(t,\tau)$ in dB can be associated with each path. Assuming there are n possible paths, for each single path of the n paths, it may undergo one or several reflections. In such a multipath environment, the power path loss variations of each path of n from the transmitter to any neighborhood receiver are given by (3.1.4) and can be changed with

$$PL(d_n)[dB] = \overline{PL}(d_n)[dB] + \tilde{X}_n, \tag{3.4.46}$$

where the subscript n is to distinguish the different paths.

In general, a multipath channel model is described by its response that acts like a filter between the transmitter and the receiver. At the receiver, the signal manifests itself as the superposition or vectorial sum of the various signal components that arrive at different time delays.

The statistical temporal multipath channel model is given by the following low-pass equivalent time-varying impulse response,

$$C_\ell(t;\tau) = \sum_{n=1}^{N(t)} r_n(t,\tau) e^{j\Phi_n(t,\tau)} \delta(\tau - \tau_n(t)). \tag{3.4.47}$$

This is more general than the traditional multipath channels because the attenuation coefficients are function of both t and τ. Here $C_\ell(t;\tau)$ denotes the response of the channel at time t, due to an impulse applied at time $t-\tau$. The random processes which characterize this channel are $\{r_n(t,\tau), \Phi_n(t,\tau), \tau_n(t)\}_{t\geq 0}$, which denote the signal attenuation, the phase, and the propagation time delay respectively. The $N(t)$ denotes the number of waves impinging

on the receiver antenna at time t. The attenuation coefficient $r_n(t,\tau)$ corresponds to the path having been subjected to a delay $\tau_n(t)$. The parameter $r_n(t,\tau)$ is both a function of t and τ, where by its dependence on τ it captures the characteristics of different propagating environments, i.e. $r_n(t,\tau_n(t))$ has different statistics than $r_j(t,\tau_j(t))$. The dynamics of the attenuation coefficient $r_n(t,\tau)$, equivalent to $S(t,\tau)$, as a function of time t are computed using the mean reverting log-normal process given by (3.3.35). The phase $\Phi_n(t,\tau)$ is typically a function of the phase of the emitted signal and the phase-shift along the path which depends on the carrier frequency, the movement between the transmitter and the recciver, and the angle of arrival of the plane wave onto the receiver. When the input to the channel is a low-pass signal $S_\ell(t)$, then the low-pass equivalent representation of the received signal is:

$$y_\ell(t) = \int_{-\infty}^{\infty} C_\ell(t;\tau) S_\ell(t-\tau) d\tau = \sum_{n=1}^{N(t)} r_n(t,\tau_n(t)) e^{j\Phi_n(t,\tau_n(t))} S_\ell(t-\tau_n(t)), \qquad (3.4.48)$$

while its band-pass representation is given by:

$$y(t) = Re\Big\{ y_\ell(t) e^{j\omega_c t} \Big\} = Re\Big\{ \Big[\sum_{n=1}^{N(t)} r_n(t,\tau_n(t)) e^{j\Phi_n(t,\tau_n(t))} S_\ell(t-\tau_n(t)) \Big] e^{j\omega_c t} \Big\}. \qquad (3.4.49)$$

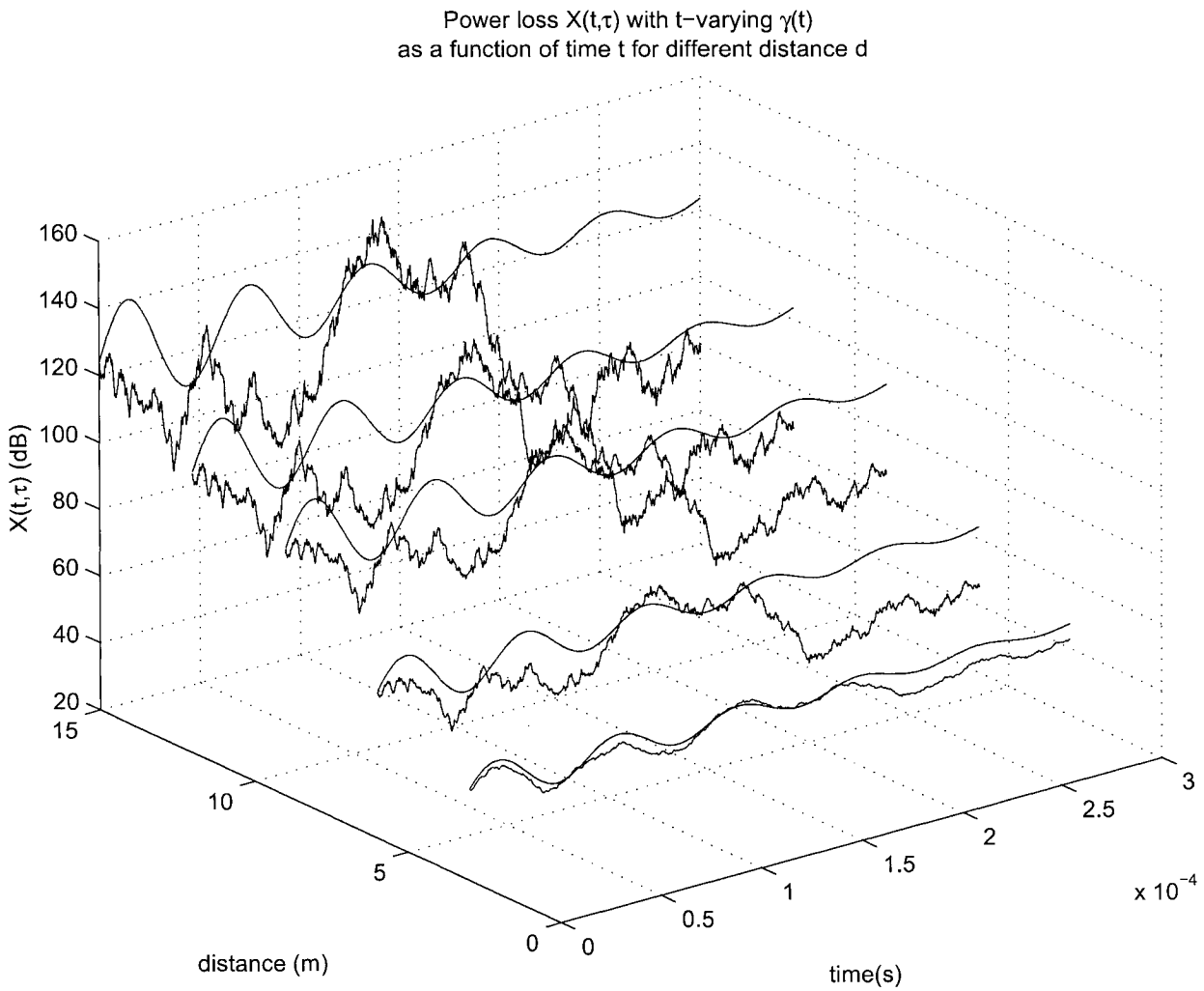

Figure 3.4.14: An illustration of the space-time properties of the channel.

Chapter 4

Optimal Power Allocation Using Linear Programming

4.1 Introduction

In general case, the channel gain G_{ij} can be interpreted in many ways, such as power attenuation, lognormal shadowing, cross correlation between codes, and the antenna direction and size. In our study, from previous chapters, we consider that the signal attenuation can be lognormal shadowing as the channel gain. In this chapter, for power allocation problem, we take the signal attenuation as constant channel gain for a given transmitter-receiver pair. We consider a network with M transmitters which transmit at power level p_1,p_2,...,p_M, and M receivers where ith receiver is assigned to transmitter i. The signal power received at the ith receiver from transmitter j is given by $G_{ij}F_{ij}p_j$, the total interference power is given by $\sum_{j\neq i}^{M} G_{ij}F_{ij}p_j$, and the noise level at the ith receiver is η_i. So the SIR of the ith receiver is given by [4], [5], [14], [15]:

$$\Gamma_i = \frac{G_{ii}F_{ii}p_i}{\sum_{j\neq i}^{M} G_{ij}F_{ij}p_j + \eta_i}, \tag{4.1.1}$$

where the terms F_{ij} model Rayleigh fading and are assumed to be unit mean independent exponential distributed random variables. Then we have $E[G_{ii}F_{ii}p_i] = G_{ii}p_i$ and $E[G_{ij}F_{ij}p_j] = G_{ij}p_j$.

4.1.1 Outage Probability

Definition 4.1.1 Outage Probability

We assume that the reception can occur at the ith receiver provided the SIR Γ_i exceeds a given threshold SIR denoted as $\bar{\gamma}_i$. Then the outage probability of the ith transmitter-receiver pair is given by:

$$\begin{aligned} O_i &= Prob\Big(\Gamma_i \leq \bar{\gamma}_i\Big) \\ &= Prob\Big(G_{ii}F_{ii}p_i \leq \bar{\gamma}_i(\sum_{j\neq i}^{M} G_{ij}F_{ij}p_j + \eta_i)\Big) \\ &= Prob\Big(F_{ii} \leq \frac{\bar{\gamma}_i}{G_{ii}p_i}(\sum_{j\neq i}^{M} G_{ij}F_{ij}p_j + \eta_i)\Big). \end{aligned} \tag{4.1.2}$$

Suppose $z_1, ..., z_n$ are independent exponential distributed random variables with means $E(z_i) = \frac{1}{\lambda_i}$. We know that

$$Prob\Big(z_1 > \sum_{i=2}^{n} z_i\Big) = \prod_{i=2}^{n} \frac{\lambda_i}{\lambda_1 + \lambda_i}. \tag{4.1.3}$$

Then

$$Prob\Big(z_1 \leq \sum_{i=2}^{n} z_i\Big) = 1 - Prob\Big(z_1 > \sum_{i=2}^{n} z_i\Big) = 1 - \prod_{i=2}^{n} \frac{\lambda_i}{\lambda_1 + \lambda_i}. \tag{4.1.4}$$

The derivation of this result is given in Appendix A. So applying this result to the expression of outage probability (4.1.2), the outage probability can be expressed in analytical form as [14], [15]:

$$O_i = 1 - e^{\frac{-\bar{\gamma}_i\eta_i}{G_{ii}p_i}} \prod_{j\neq i}^{M} \frac{1}{1 + \bar{\gamma}_i\frac{G_{ij}p_j}{G_{ii}p_i}}. \tag{4.1.5}$$

We define the worst outage probability over all transmitter-receiver pairs as $O = maxO_i$, it is an important factor for the system and power allocation.

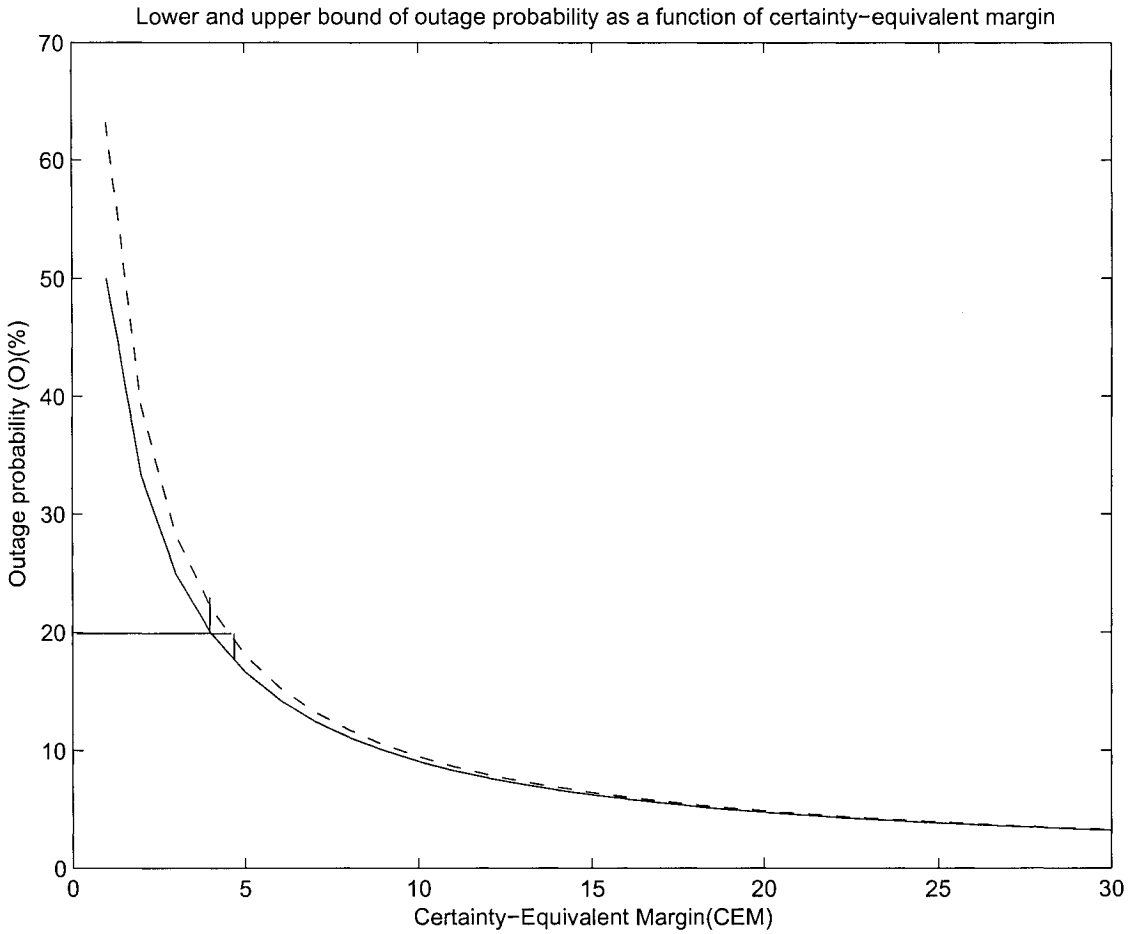

Figure 4.1.1: Exact outage probability as a function of CEM.

4.1.2 Certainty Equivalent Margin

Definition 4.1.2 CEM (Certainty Equivalent Margin)

The CEM (Certainty Equivalent Margin) is the ratio of ith SIR to the reception threshold SIR without noise, as $CEM = \frac{\Gamma_i}{\bar{\gamma}_i}$. *By the definition, both the signal and interference power are replaced by the expected value of these random variables.*

Now we also define the CEM with noise denoted as CEM^{η}*:*

$$CEM^{\eta} = \frac{\Gamma_i}{\bar{\gamma}_i} = \frac{G_{ii}p_i}{\bar{\gamma}_i(\sum_{j\neq i}^{M} G_{ij}p_j + \eta_i)}. \tag{4.1.6}$$

For $z_1, ..., z_n \geq 0$, it can be shown that the inequalities

$$1 + k + \sum_{i=1}^{n} z_i \leq e^k \prod_{i=1}^{n}(1 + z_i) \leq e^{(k+\sum_{i=1}^{n} z_i)} \tag{4.1.7}$$

hold for some given constant k.

Combining with the definition of outage probability, we have

$$O = max\Big(1 - e^{(\frac{-\bar{\gamma}_i \eta_i}{G_{ii} p_i})} \prod_{j \neq i}^{M} \frac{1}{1 + \bar{\gamma}_i \frac{G_{ij} p_j}{G_{ii} p_i}}\Big). \tag{4.1.8}$$

Using the inequality in (4.1.7), it leads to

$$O \leq 1 - \frac{1}{e^{max(\bar{\gamma}_i(\sum_{j \neq i}^{M} G_{ij} p_j + \eta_i))}} = 1 - e^{\frac{-1}{CEM^\eta}}. \tag{4.1.9}$$

In the similar way, we can get

$$\frac{1}{1 + CEM^\eta} \leq O. \tag{4.1.10}$$

In appendix A.2, we give the detailed derivation of (4.1.9) and (4.1.10). Then we have the lower and upper bounds on outage probability as following [14], [15]:

$$\frac{1}{1 + CEM^\eta} \leq O \leq 1 - e^{\frac{-1}{CEM^\eta}}. \tag{4.1.11}$$

Figure 4.1.1 plots the upper and lower bounds of outage probability O as a function of CEM. Also from Figure 4.1.1, we can see that the lower and upper bounds are very close within about 5%.

4.2 Optimal Power Allocation

For the power allocation problem, we want to minimize the total transmit power subject to the constraints that each transmitter-receiver pair can attain a maximum allowed outage

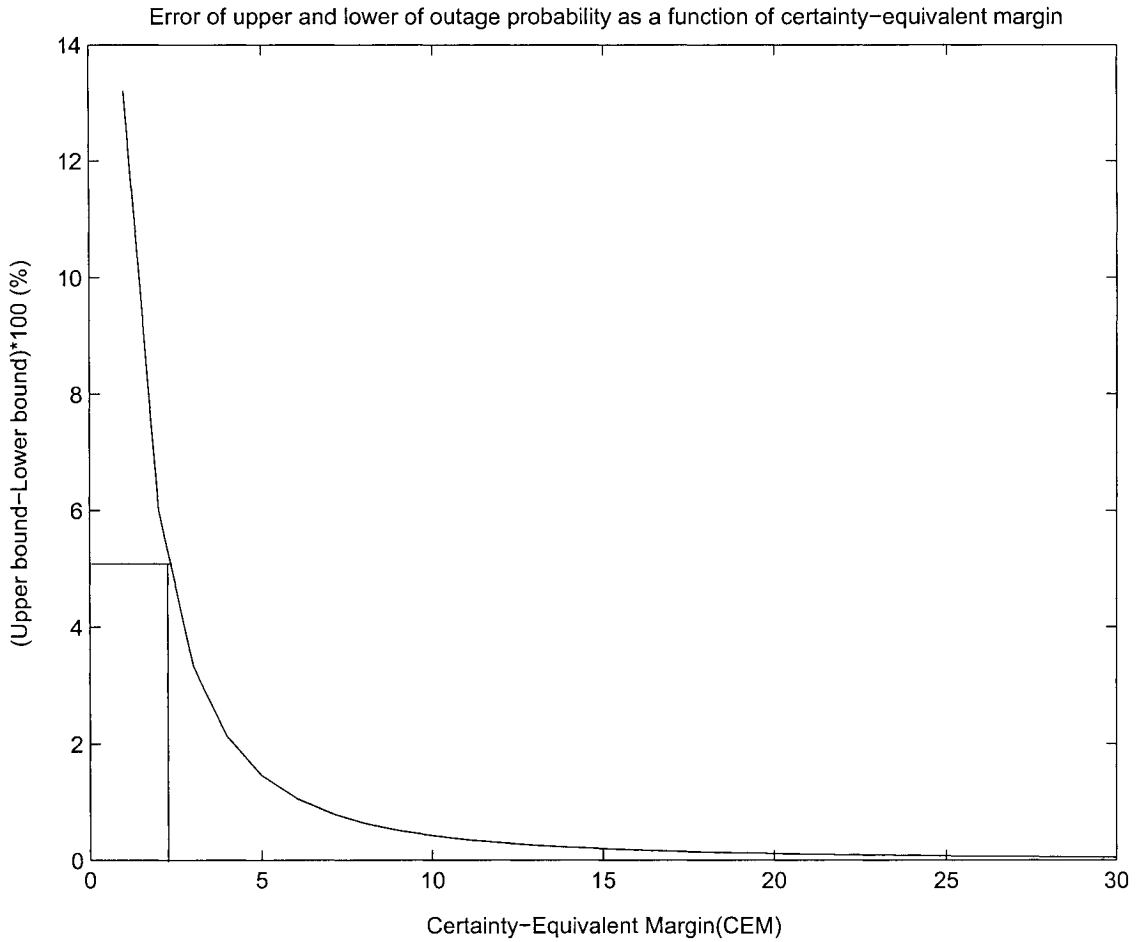

Figure 4.1.2: Error of exact outage probability as a function of CEM.

probability or equivalent to reach a minimum allowed QoS requirement SIR. This is the linear programming problem as the following form [4], [14], [15]:

$$\begin{aligned} &\min \sum_{i=1}^{M} p_i, \\ &\text{s. t. } O_i \leq O_i^{max}, i = 1, 2, ..., M, \end{aligned} \tag{4.2.12}$$

where O_i^{max} is the maximum allowed outage probability for the ith transmitter-receiver pair. This value can be selected as same for each pair, or different for different SIR to be assigned to different users. In our study, we assume this constraint as the same value.

By the definition (4.1.2) of outage probability O_i and combining with (4.1.5), we can express the constraints $O_i \leq O_i^{max}$ as:

$$1 - O_i^{max} \leq e^{(\frac{-\bar{\gamma}_i \eta_i}{G_{ii} p_i})} \prod_{j \neq i}^{M} \frac{1}{1 + \bar{\gamma}_i \frac{G_{ij} p_j}{G_{ii} p_i}}. \tag{4.2.13}$$

Also, we can rewrite it as:

$$(1 - O_i^{max}) e^{(\frac{\bar{\gamma}_i \eta_i}{G_{ii} p_i})} \prod_{j \neq i}^{M} (1 + \bar{\gamma}_i \frac{G_{ij} p_j}{G_{ii} p_i}) \leq 1. \tag{4.2.14}$$

Then our power allocation problem can be stated as:

$$\begin{aligned} &\min \sum_{i=1}^{M} p_i, \\ &\text{s. t. } (1 - O_i^{max}) e^{(\frac{\bar{\gamma}_i \eta_i}{G_{ii} p_i})} \prod_{j \neq i}^{M} (1 + \bar{\gamma}_i \frac{G_{ij} p_j}{G_{ii} p_i}) \leq 1, i = 1, 2, ..., M. \end{aligned} \tag{4.2.15}$$

4.2.1 Simulation of the Power Allocation

The left-hand side of the constraint inequality (4.2.15) is a polynomial function of the powers p_1, ..., p_M. So the above problem is a linear programming problem with the variables p_1, ..., p_M. We can use interior-point methods to solve it. The numerical results are completed by using MATLAB functions *flin* and *fmin* to solve linear programming problem [25], [30]. Follow the Chapter 3, we used the stochastic differential equations to compute the distance dependent power attenuation G_{ij}. Corresponding to the attenuation, we set the threshold SIR varying from 3 to 12. Furthermore, an AWGN noise power $\sigma^2 = 10^{-13}$ was chosen corresponding to approximately a 1MHz bandwidth. In our study, we select different noise power from 0.1 to 0.5 with the above unit σ^2. Also we set outage probability as 5%. Using these parameters to do the simulation, we get each transmitter power for 6 of 10 users in a short period.

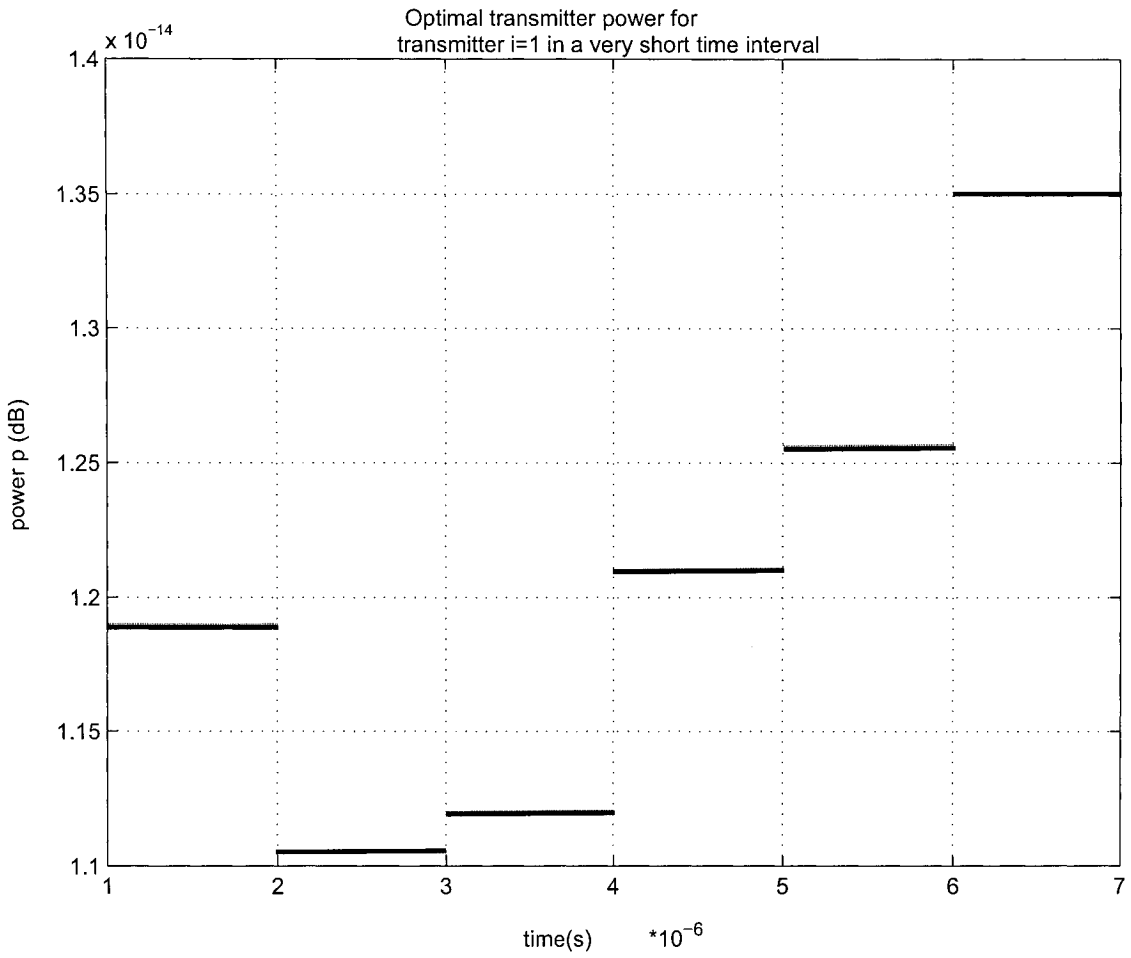

Figure 4.2.3: Power allocation for a small interval example of p_1.

Figure 4.2.3 to 4.2.8 indicate that for each transmitter power p_1, ..., p_6, in the very short period, the power is varying in a very small range.

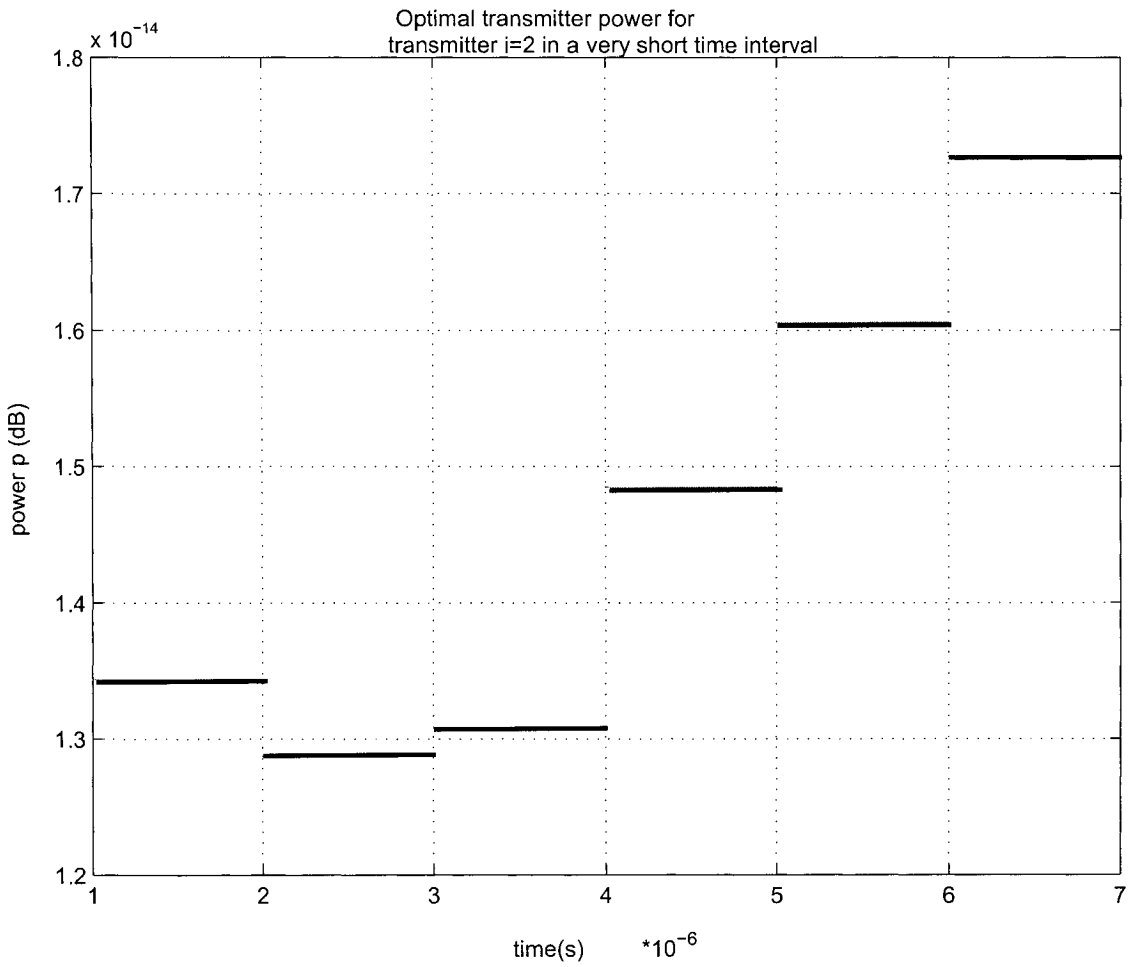

Figure 4.2.4: Power allocation for a small interval example of p_2.

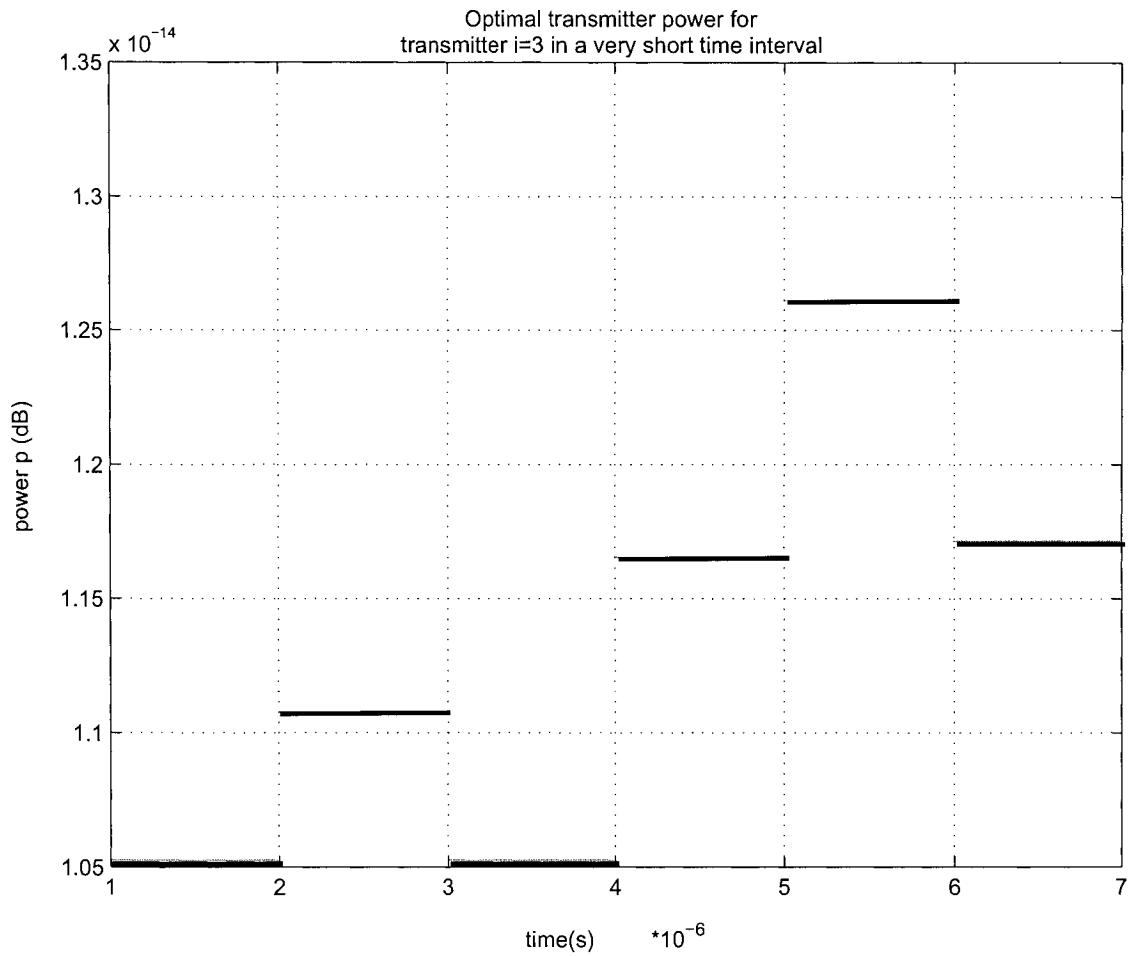

Figure 4.2.5: Power allocation for a small interval example of p_3.

4.3 Power Control Algorithm

In this section, we describe the iterative algorithm to solve the optimization problem (4.2.15). From the constraint, we can rewrite it as:

$$e^{(\frac{\bar{\gamma}_i \eta_i}{G_{ii} p_i})} \prod_{j \neq i}^{M} (1 + \bar{\gamma}_i \frac{G_{ij} p_j}{G_{ii} p_i}) \leq \frac{1}{(1 - O_i^{max})}. \tag{4.3.16}$$

Taking the logarithm of it, we have:

$$\frac{\bar{\gamma}_i \eta_i}{G_{ii} p_i} + \sum_{j \neq i}^{M} \log(1 + \bar{\gamma}_i \frac{G_{ij} p_j}{G_{ii} p_i}) \leq \log \frac{1}{(1 - O_i^{max})}. \tag{4.3.17}$$

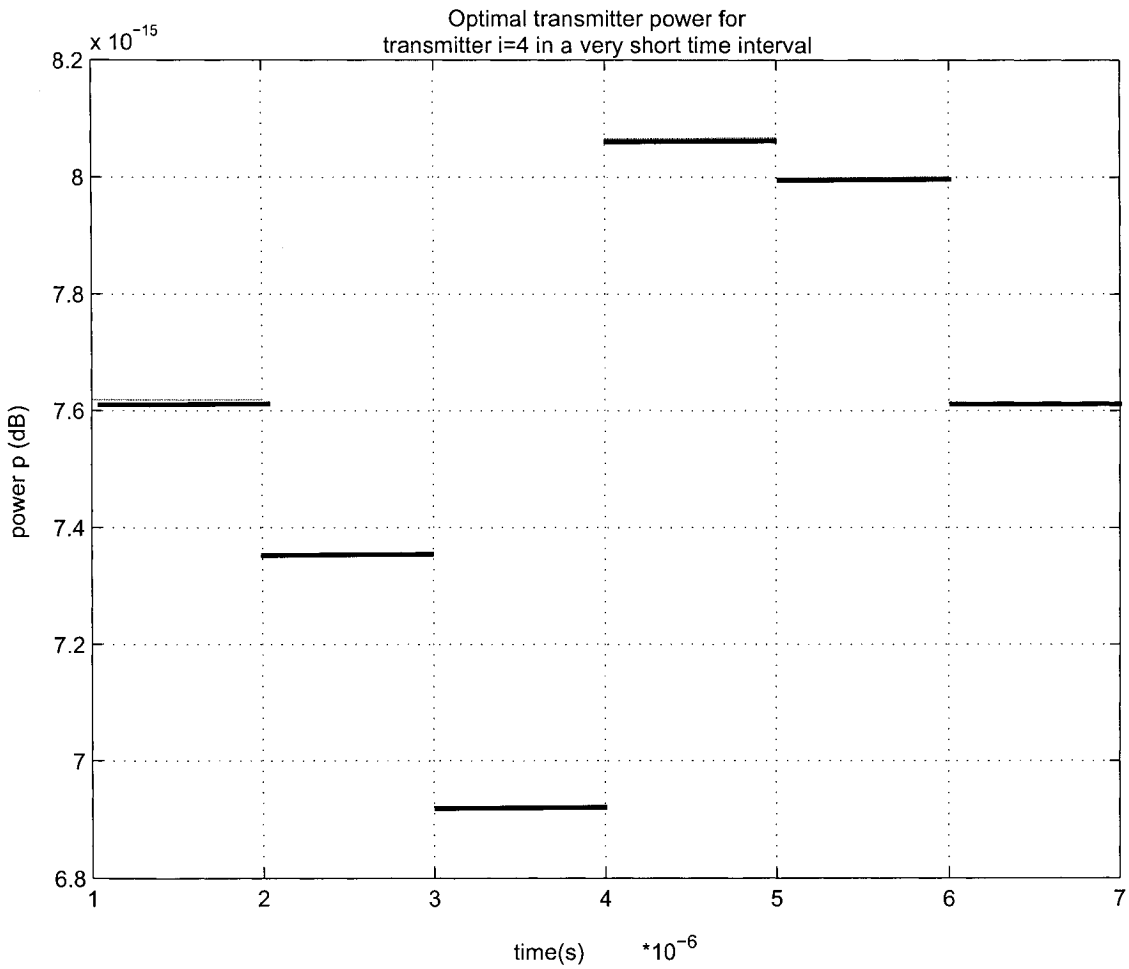

Figure 4.2.6: Power allocation for a small interval example of p_4.

We can express the above inequality as follows:

$$\frac{\frac{\bar{\gamma}_i \eta_i}{G_{ii}} + p_i \sum_{j \neq i}^{M} \log(1 + \bar{\gamma}_i \frac{G_{ij} p_j}{G_{ii} p_i})}{\log \frac{1}{(1 - O_i^{max})}} \leq p_i. \tag{4.3.18}$$

Now we define

$$I_i(P) = \frac{\frac{\bar{\gamma}_i \eta_i}{G_{ii}} + p_i \sum_{j \neq i}^{M} \log(1 + \bar{\gamma}_i \frac{G_{ij} p_j}{G_{ii} p_i})}{\log \frac{1}{(1 - O_i^{max})}};$$
$$T_i(P) = \min_p I_i(P). \tag{4.3.19}$$

Furthermore, we propose a new power control algorithm given by:

$$P(n+1) = T(P(n)), \tag{4.3.20}$$

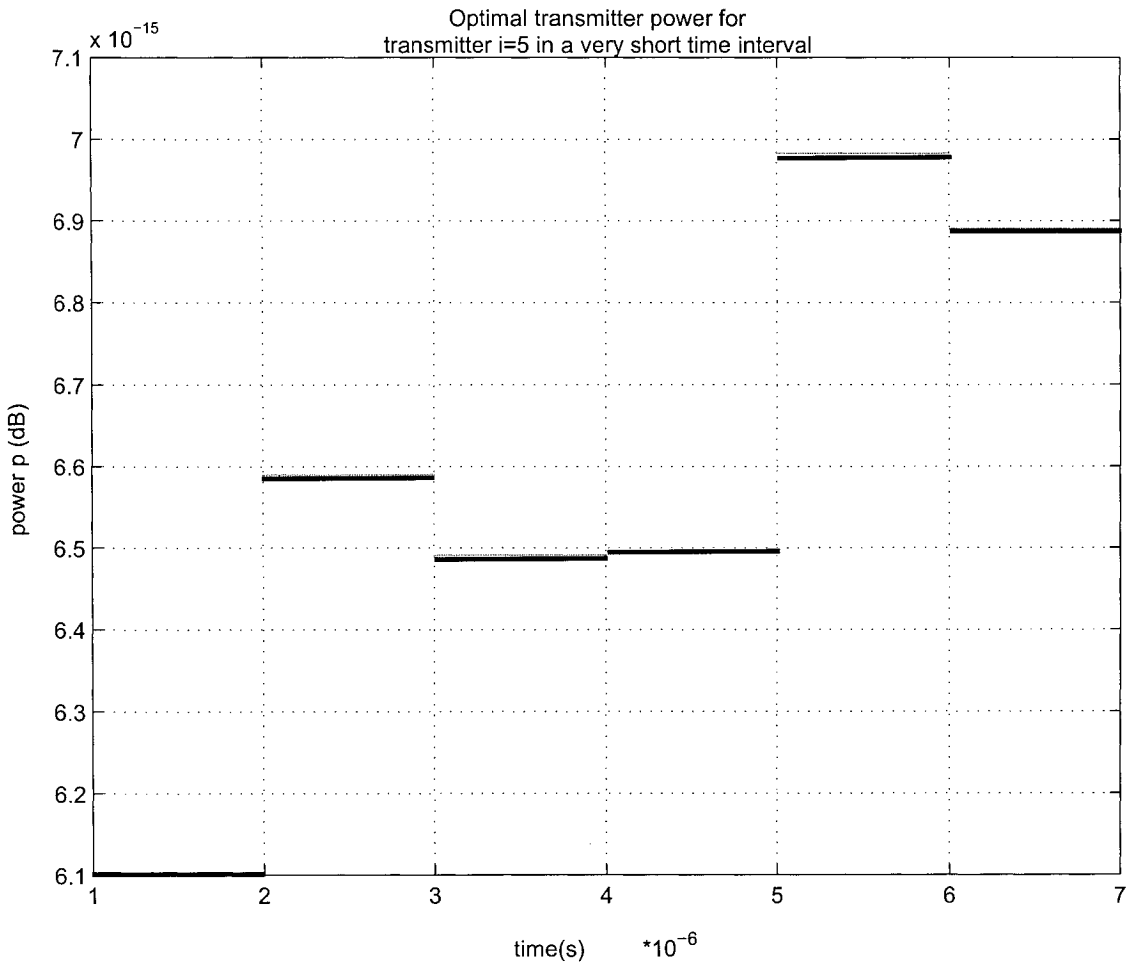

Figure 4.2.7: Power allocation for a small interval example of p_5.

where $P = \{p_1, p_2, ..., p_M\}$, $T(P) = [T_1(P), ..., T_M(P)]^T$ and it is initialized with power set $\{p_i\}$ to the receiver noise level η_0 for each i.

We call $T_i(P)$ as the standard interference function [10], [15], [17]. It has the following properties:

1. Positivity $T_i(P) > 0$.

2. Monotonicity if $P \geq P^1$, then $T_i(P) \geq T_i(P^1)$.

3. Scalability for all $\alpha > 1$, $\alpha T_i(P) > T_i(\alpha P)$.

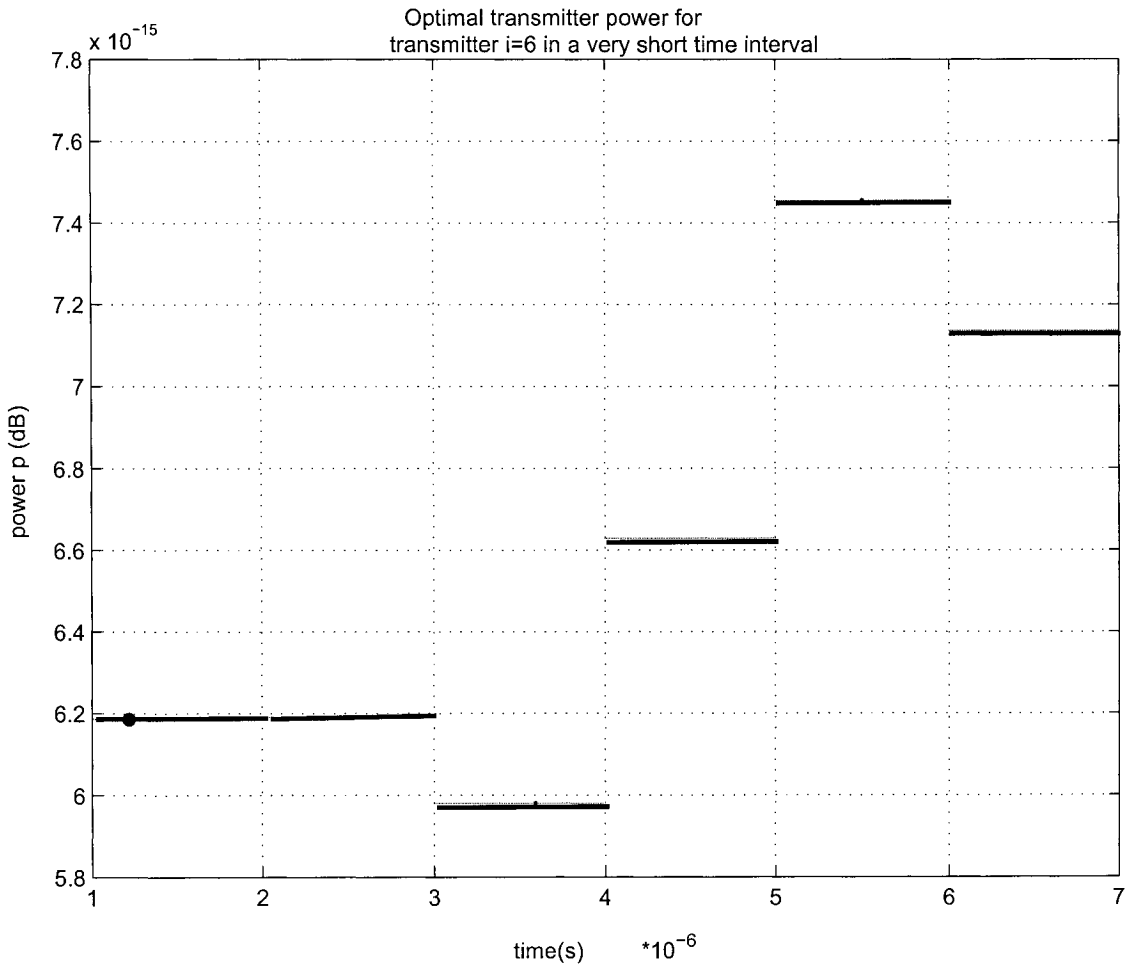

Figure 4.2.8: Power allocation for a small interval example of p_6.

Then $I(P)$ also is the standard interference function, so the power control algorithm (4.3.20) converges to an optimal solution $P^* = T(P^*)$, which is the minimum power vector required to meet the outage probability constraints in (4.2.15).

After we computed the signal attenuation as the channel gains, for a selected outage probability O_i^{max}, we consider the channel gains G_{ij} and the SIR threshold $\bar{\gamma}_i$ as parameters. Then we have the following iterative algorithm for the outage probability constrains optimization

problem.

$$P_i(n+1) = \frac{\frac{\bar{\gamma}_i \eta_i}{G_{ii}} + P_i(n) \sum_{j \neq i}^{M} \log(1 + \bar{\gamma}_i \frac{G_{ij} P_j(n)}{G_{ii} P_i(n)})}{\log \frac{1}{(1 - O_i^{max})}}. \tag{4.3.21}$$

We set the initial power to the noise level as $P_i(0) = \sigma^2, \forall i$.

In section 4.2, we computed the optimal power allocation by the linear programming problem using the software Matlab, the solution occurs when all the users meet the constraints with equality. Comparing to the linear programming solution, for the above iterative algorithm (4.3.21), we can see that for each transmitter power, the iterative algorithm can reach the optimal solution that is the minimum value for the outage probability constraints. Figure 4.3.9 illustrates that the above iterative power control algorithm can converge to the optimal power summation only after few iteration steps.

In the simulation, the dash-dot line indicates all the noise level is the same as $\eta_i = 10^{-13}$; for the solid line, we set the noise level as different, they vary from 1 to 3 times of η. Also, we give the maximum outage probability varying from 5% to 10% for different SIR as we used before from 3 to 12. The channel gains are computed by using stochastic differential equations(SDE) in Chapter 3.

In next chapter, for each transmitter-receiver pair, we can use these optimal power vectors as constant parameters and consider the channel gains as random variables to determine the properties of the outage probability.

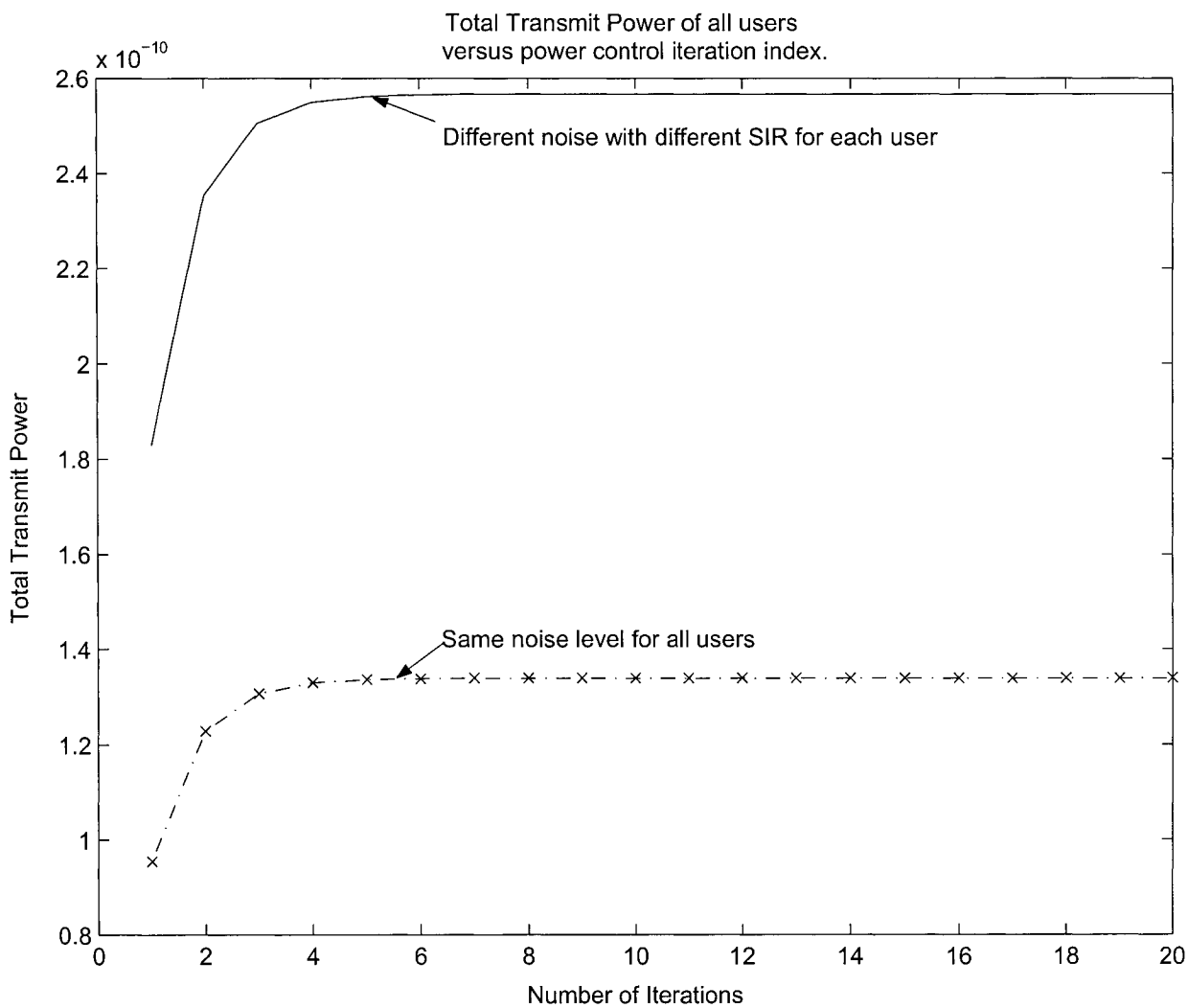

Figure 4.3.9: Total transmit power of all users versus power control iteration index.

Chapter 5

Probabilistic QoS Measures

With the rapidly increasing demand for mobile communications and the need to support the diversified requirements of users in communication systems, QoS resource management becomes more and more important. Recent research in CDMA communication systems shows that the channel capacity varies dynamically due to the variant interference levels. QoS satisfaction and the system capacity are very difficult to optimize while considering large CDMA systems. In order to provide appropriate quality of service guarantees for mobile communication systems, we need to adapt various parameters, for example, transmission power and channel coding to the wireless channel and QoS requirements. The most common performance constraints include the desired SIR and the outage probability [1], [2], [5], [15].

In this chapter, we focus on computing the outage probability by allocating optimal transmission powers when each mobile has an enlarged margin of SIR. By introducing a probability QoS measure scheme, we derive the Moment Generating Function (MGF) expressions for different fading channels such as Rayleigh channels, Rice channels, and Nakagami-m channels [1], [11], [14], [15], [26], [27], [28]. After the numerical experiments, we will provide the outage probability analysis for transmitter power and SIR for satisfying the QoS requirements.

5.1 The Static Deterministic Case

Consider a wireless network with M transmitters and M receivers. A measure of QoS for each user is defined through the SIR as [4], [5], [15], [18, [19]:

$$\begin{aligned} &\min \sum_{n=1}^{M} p_n, \\ &\text{s. t. } \Gamma_n \equiv \frac{p_n g_{nn}}{\sum_{j\neq n}^{M} p_j g_{nj} + \eta_n} \geq \bar{\gamma}_n, \end{aligned} \tag{5.1.1}$$

where $p_n \geq 0$ is the transmitter power of the nth mobile station; g_{nj} is the channel gain of the transmitter j to the receiver assigned to transmitter n; $\eta_n \geq 0$ is the noise power level at the nth receiver; Γ_n is the SIR at the nth receiver; and $\bar{\gamma}_n > 0$ is the required SIR for base station n (receiver n).

We define:

$$\gamma_n = \frac{\bar{\gamma}_n}{1 + \bar{\gamma}_n}, \tag{5.1.2}$$

then $0 < \gamma_n < 1$.

Equation (5.1.1) is equivalent to:

$$\begin{aligned} &\min \sum_{n=1}^{M} p_n, \\ &\text{s. t. } \Gamma_n \equiv \frac{p_n g_{nn}}{\sum_{j=1}^{M} p_j g_{nj} + \eta_n} \geq \gamma_n. \end{aligned} \tag{5.1.3}$$

In this problem, the variables are the powers p_1, ..., p_M. The constants γ_n, η_n, and g_{nj} are problem parameters. We can compute the channel gains g_{nj} according to the signal attenuation discussed in Chapter 3. After using the linear programming method, we can optimize these transmitter powers p_n for the above constraints,which was done in Chapter 4.

Now we define:

$$\begin{aligned} I^n(p) &= \sum_{j=1}^{M} p_j g_{nj} + \eta_n - \frac{1}{\gamma_n} p_n g_{nn} \\ &= \sum_{j\neq n}^{M} p_j g_{nj} + \eta_n + (1 - \frac{1}{\gamma_n}) p_n g_{nn}. \end{aligned} \tag{5.1.4}$$

The constraints in (5.1.1) and (5.1.3) are the same as $I^n(p) \leq 0$, $\forall n = 1, ..., M$.

On the other hand, the failure in achieving the nth QoS requirement is $I^n(p) \geq 0$,$\forall n$.

The probability of the failure is $P(I^n(p) \geq 0)$, which is called outage probability of the nth transmitter-receiver pair [1], [5], [14], [15]. In the channel fading environment, $I^n(p)$ is a random variable with what would appear to be a very complex distribution, since there is the sum of random variables with different means and a normal distributed random variable white noise.

Theorem 5.1.1 Chebyshev Inequality

Suppose that X is an arbitrary random variable with a finite mean m and a finite variance σ^2. Then for any positive number α,

$$P(|X - m| \geq \alpha) \leq \frac{\sigma^2}{\alpha^2}. \tag{5.1.5}$$

This is called the Chebyshev Inequality [1].

The Chebyshev inequality gives a loose bound. It also has two tails of the PDF (Probability Distribution Function) as we can see from Figure 5.1.1. In practice, we just want to consider the area under one tail, either in the interval (α, ∞) or $(-\infty, -\alpha)$, so we can have a bound as extremely tight as possible. For example, we compute the tail probability in the interval (α, ∞). Now, let $Y = X - m$, and we define a function $g(Y)$ as $g(Y) = 1$, for $|Y| \geq \alpha$; $g(Y) = 0$, for $|Y| < \alpha$ with probability $P(|Y| \geq \alpha)$ and $P(|Y| < \alpha)$ respectively. Its mean value is:

$$E[g(Y)] = P(|Y| \geq \alpha). \tag{5.1.6}$$

Suppose we give the upper bound of $g(Y)$ the value $g(Y) \leq (\frac{Y}{\alpha})^2$. The graph of $g(Y)$ and its upper bound are shown in Figure 5.1.1. Then we can have:

$$E[g(Y)] \leq E\Big(\frac{Y}{\alpha}\Big)^2 = \frac{\sigma^2}{\alpha^2}.$$

That is to say, for random variable Y with $N(0, \sigma^2)$, it has the Chebyshev bound:

$$P(|Y| \geq \alpha) \leq \frac{\sigma^2}{\alpha^2}. \tag{5.1.7}$$

In practice, this bound is extremely loose because we give a large upper bound $\frac{Y}{\alpha}$. There are certainly other functions that can be used to overbound $g(Y)$ in order to reach a relatively tight bound for $P(|Y| \geq \alpha)$. By using an exponential function as a bound for $g(Y)$, we can derive the following tight bound. We consider the tail probability in the interval (α, ∞), where $\alpha \geq 0$. The function $g(Y)$ is overbound as:

$$g(Y) \leq e^{s(Y-\alpha)}, \tag{5.1.8}$$

where $g(Y)$ is the same as above and $s \geq 0$ is the parameter to be optimized. The graph of $g(Y)$ and the exponential upper bound are shown in Figure 5.1.2.

Theorem 5.1.2 Chernoff Bound Theorem

The expected value of function $g(Y)$ for $Y \in (\alpha, \infty)$, $\alpha \geq 0$ is:

$$E[g(Y)] = P(|Y| \geq \alpha) \leq E(e^{s(Y-\alpha)}). \tag{5.1.9}$$

It is valid for any real value $s \geq 0$. The tightest upper bound is obtained by selecting the value of s that minimizes $E(e^{s(Y-\alpha)})$. A necessary condition for a minimum is:

$$\frac{d}{ds} E(e^{s(Y-\alpha)}) = 0. \tag{5.1.10}$$

The solution of (5.1.10) is s^*, then we have:

$$P(|Y| \geq \alpha) \leq e^{-s^*\alpha} E(e^{s^*Y}). \tag{5.1.11}$$

This bound is called the Chernoff bound [1], [2], [5], [12], [26], [27], [28].

In our study, the definition of $I^n(p)$ in formula (5.1.4) is a function of γ_n, p_n, g_{nj}, and η_n. Because we consider the channel gain g_{nj} as a sequence of random variables, it is not easy

to get the distribution of $I^n(p)$. But by using the Moment Generating Function (MGF) and the Chernoff bound theorem, we can reach a rather tight upper bound on the tail probability $P(I^n(p) \geq \alpha)$, where α is another prescribed value. For more on MGF, see section 5.2.1. In our study, we will let $\alpha = 0$.

As introduced in [12] on Chernoff bound formulas, for the $I^n(p)$, in order to get $E(e^{s_n I^n(p)})$, we need to derive the MGF of $I^n(p)$. Firstly, assuming we have a MGF of $I^n(p)$ as $\Phi(s_n) = E(e^{s_n I^n(p)})$ [31], using Cramer's theorem, we can derive the general theory formulas of the Chernoff bound for our study.

$I^n(p)$ is defined in (5.1.4) as a sequence of random variables related to g_{ij} with the MGF $\Phi(s_n)$, $s_n \in \Re$, we define the cumulant generating function for the random variable as [12], [28], [31]:

$$\Psi(s_n) \triangleq \log \Phi(s_n). \tag{5.1.12}$$

Also, we let $\psi^*(\alpha)$ be the Legendre transfer function of $\Psi(s_n)$, also known as the rate function:

$$\psi^*(\alpha) \triangleq \sup_{s_n \in \Re} \{s_n \alpha - \Psi(s_n)\}. \tag{5.1.13}$$

Then we have the following theorem.

Theorem 5.1.3 Cramer's Theorem

1. $\psi^*(\alpha) = \sup_{s_n \in \Re}\{s_n \alpha - \log \Phi(s_n)\} \geq 0, \quad \alpha \in \Re.$

2. *If* $E[I^n(p)] = m_I < \infty$, *then*

$$\psi^*(m_I) = \sup_{s_n \in \Re} \{s_n m_I - \log \Phi(s_n)\} = 0. \tag{5.1.14}$$

3. *(a) If* $\alpha > m_I$, *then*

$$P(I^n(p) \geq \alpha) \leq e^{-\psi^*(\alpha)}, \quad s_n > 0. \tag{5.1.15}$$

(b) If $\alpha < m_I$, *then*

$$P(I^n(p) \leq \alpha) \leq e^{-\psi^*(\alpha)}, \quad s_n < 0. \tag{5.1.16}$$

Applying this theorem to our study, the Chernoff bounds can be minimized with respect to $s_n \in \Re$ to yield tighter bounds [31]. Next, we introduce two kinds of probabilistic QoS measures.

5.1.1 Decentralized Probabilistic QoS Measures

Adapting Theorem 5.1.3, we introduce the following QoS measures.

Definition 5.1.4 Decentralized Probabilistic QoS Measures

For a given number of transmitters M and $-\delta_n \equiv \log \alpha_n, \alpha_n \in (0,1), \delta_n > 0, 1 \leq n \leq M$, the nth transmitter's decentralized QoS requirement is defined by:

$$\log P(I^n(p) \geq 0) \leq \log E(e^{s_n I^n(p)}) \leq -\delta_n, \quad s_n > 0. \tag{5.1.17}$$

The goal of the above definition is that for a given sequence $\alpha_n \in (0,1)$ and a given number M for all $1 \leq n \leq M$, the nth mobile user's probabilistic QoS requirement is satisfied if there exists a set of power sequences $\{p_n\}_{n=1}^{M}$ in some admissible control set U_{ad}, such that:

$$A(s_n) \equiv \{p \in U_{ad}, \min \log E(e^{s_n I^n(p)}) \leq -\delta_n\}, \quad s_n > 0. \tag{5.1.18}$$

For any positive value s_n, the set $A(s_n)$ is non-empty for $1 \leq n \leq M$.

5.1.2 Centralized Probabilistic QoS Measures

Similarly, the joint probability of failing to achieve the QoS of all transmitters is defined as follows.

Definition 5.1.5 Centralized Probabilistic QoS Measures

For a given number of transmitters M and $-\delta \equiv \log \alpha, \alpha \in (0,1), \delta > 0$, the centralized almost sure QoS requirement is defined by:

$$\log P\Big(I^1(p) \geq 0, ..., I^M(p) \geq 0\Big) \leq \log E[exp(\sum_{n=1}^{M} s_n I^n(p))] \leq -\delta, \quad s_n > 0. \tag{5.1.19}$$

Then the centralized probabilistic QoS requirement is satisfied if there exists a set of power sequences $\{p_n\}_{n=1}^{M}$ in some admissible control set U_{ad}, such that:

$$A(s_n) \equiv \Big\{p \in U_{ad}, \min \log E[exp(\sum_{n=1}^{M} s_n I^n(p))] \leq -\delta\Big\}. \tag{5.1.20}$$

For any positive value s_n, there exists an optimal $s^* > 0$, such as $s^* = \arg\min\{s_1, ..., s_M\}$ and the set $\{A(s_n)\}$ is non-empty for $1 \leq n \leq M$.

These centralized probabilistic QoS requirements enable us to optimize the power with respect to the number of transmitters M, thus linking the power control and admission control problems [5].

5.2 Application of the Theorems

5.2.1 Moment Generating Function

Next, we introduce several MGFs, which are used in subsequent sections to compute the outage probability.

Definition 5.2.1 Moment Generating Function

The Moment Generating Function (MGF) of random variable X is defined by [12], [27], [28], [31]:

$$\Phi(\theta) = E[e^{\theta X}] = \int_{-\infty}^{\infty} e^{\theta x} f(x) dx, \quad if\ E|e^{\theta X}| < \infty, \tag{5.2.21}$$

where $f(x)$ is the density function of X.

Corollary 5.2.2 *If X is a normal random variable with $N(\mu, \sigma^2)$ and has $f(x) = \frac{1}{\sigma\sqrt{2\pi}} e^{-\frac{(x-\mu)^2}{2\sigma^2}}$, then it has a moment generating function $\Phi(\theta) = e^{\mu\theta + \frac{\sigma^2\theta^2}{2}}$.*

Corollary 5.2.3 *If $S = X + Y$, where X and Y are independent random variables, then S has a moment generating function $\Phi_S(\theta) = \Phi_X(\theta)\Phi_Y(\theta)$. A similar formula holds true for sums of more than two independent random variables.*

Similarly, we consider $I^n(p)$ in (5.1.4), which is a summation of independent random variables. In order to find the excepted value of (5.2.17), we consider $\{g_{nj}\}$ as a sequence of random variables, then we can use the MGF to find the expected value of $I^n(p)$. Now we discuss some different propagation environments according to $s_{nj} = \{\sqrt{g_{nj}}\}$ which can be considered as Rayleigh distribution random variables, Rice distribution random variables, or Nakagami-m distribution random variables.

5.2.2 Chi-Square Distribution

Suppose X is a Gaussian-distributed random variable with $N(0, \sigma^2)$,

$$p_X(x) = \frac{1}{\sqrt{2\pi}\sigma} e^{-x^2/2\sigma^2}. \tag{5.2.22}$$

If the new random variable $Y = X^2$, then Y has a central Chi-square distribution with PDF in the form [1], [2], [26], [27], [28]:

$$p_Y(y) = \frac{1}{\sqrt{2\pi y}\sigma} e^{-y/2\sigma^2}, \quad y \geq 0. \tag{5.2.23}$$

The Cumulative Distribution Function (CFD) of Y is:

$$F_Y(y) = \int_0^y p_Y(u)du = \frac{1}{\sqrt{2\pi}\sigma} \int_0^y \frac{1}{\sqrt{u}} e^{-u/2\sigma^2} du. \tag{5.2.24}$$

The characteristic function of Y has the closed form:

$$\psi(j\upsilon) = \frac{1}{(1 - j2\upsilon\sigma^2)^{1/2}}. \tag{5.2.25}$$

For the sum of random variables, $Y = \sum_{i=1}^{n} X_i^2$, where X_i, i=1,2,...,n, are statistically independent and identically distributed Gaussian random variables with a mean of zero and a variance of σ^2, the characteristic function of Y is:

$$\psi(j\upsilon) = \frac{1}{(1 - j2\upsilon\sigma^2)^{n/2}}. \tag{5.2.26}$$

The MGF of Y is:

$$\Phi(\upsilon) = \frac{1}{(1-2\upsilon\sigma^2)^{n/2}}. \tag{5.2.27}$$

For n=2, $Y = X_1^2 + X_2^2$, the MGF of Y is: [32]

$$\Phi(\upsilon) = \frac{1}{1-2\upsilon\sigma^2}. \tag{5.2.28}$$

The inverse transform of this characteristic function yields the PDF:

$$p_Y(y) = \frac{1}{\sigma^n 2^{n/2}\Gamma(n/2)} y^{n/2-1} e^{-y/2\sigma^2}, \quad y \geq 0, \tag{5.2.29}$$

where $\Gamma(.)$ is the gamma function.

The CDF of Y is:

$$F_Y(y) = \int_0^y \frac{1}{\sigma^n 2^{n/2}\Gamma(n/2)} u^{n/2-1} e^{-u/2\sigma^2} du, \quad y \geq 0. \tag{5.2.30}$$

If X is a Gaussian-distributed random variable with a mean of m_x and a variance of σ^2, the random variable $Y = X^2$ is said to have a noncentral Chi-square distribution with its PDF in the form [1]:

$$p_Y(y) = \frac{1}{\sqrt{2\pi y}\sigma} e^{-(y+m_x^2)/2\sigma^2} cosh(\frac{\sqrt{y}m_x}{\sigma^2}), \quad y \geq 0. \tag{5.2.31}$$

Similarly, let $Y = \sum_{i=1}^n X_i^2$, where X_i, i=1,2,...,n, are statistically independent and identically distributed Gaussian random variables with means of m_i and the same variance of σ^2.

The PDF of Y is:

$$p_Y(y) = \frac{1}{2\sigma^2}(\frac{y}{s^2})^{(n-2)/4} e^{-(s^2+y)/2\sigma^2} I_{n/2-1}(\sqrt{y}\frac{s}{\sigma^2}), \quad y \geq 0, \tag{5.2.32}$$

where $s^2 = \sum_{i=1}^n m_i^2$.

The CDF of Y is:

$$F_Y(y) = \int_0^y \frac{1}{2\sigma^2}(\frac{u}{s^2})^{(n-2)/4} e^{-(s^2+u)/2\sigma^2} I_{n/2-1}(\sqrt{u}\frac{s}{\sigma^2}) du. \tag{5.2.33}$$

For n=2, $Y = X_1^2 + X_2^2$, the PDF of Y is:

$$p_Y(y) = \frac{1}{2\sigma^2} e^{-(s^2+y)/2\sigma^2} I_0(\frac{\sqrt{y}s}{\sigma^2}), \quad y \geq 0, \tag{5.2.34}$$

where $s^2 = m_1^2 + m_2^2$.

The characteristic function of Y is:

$$\psi(j\upsilon) = \frac{1}{1 - j2\upsilon\sigma^2} e^{\frac{sj\upsilon}{1-j2\upsilon\sigma^2}}. \tag{5.2.35}$$

Similarly, we have the MGF of $Y = X_1^2 + X_2^2$ as [1]:

$$\Phi(\upsilon) = \frac{1}{1 - 2\upsilon\sigma^2} e^{\frac{s\upsilon}{1-2\upsilon\sigma^2}}. \tag{5.2.36}$$

5.2.3 Cramer's Theorem for Outage Probability

In Section 5.1.1, we state the definition of $I^n(p)$ in formula (5.1.4). Using Subsections 5.2.1 and 5.2.2, the MGF and the Chi-square distribution, combined with the Chernoff bound theorem using (5.1.11), we have:

$$P\Big(I^n(p) \geq \alpha\Big) \leq e^{-s_n\alpha} E[e^{s_n I^n(p)}] = e^{-s_n\alpha}\Phi(s_n) = e^{-s_n\alpha + \log\Phi(s_n)}, \tag{5.2.37}$$

where we have:

$$\Phi(s_n) = E[e^{s_n I^n(p)}] = E[e^{(s_n\eta_n)}] * E[e^{(s_n(1-\frac{1}{\gamma_n})p_n g_{nn})}] * E[e^{(\sum_{j\neq n}^{M} s_n p_j g_{nj})}]. \tag{5.2.38}$$

In our study, we focus on large CDMA systems with different transmitter-receiver pairs M. In the following sections of this chapter, we propose our own contributions to derive outage probability expressions by using the MGF of $I^n(p)$ for three different cases when $M \to \infty$. In a large CDMA system, we want to know how the above probabilistic estimation affects the outage probability when $M \to \infty$. Firstly, we introduce the general concepts of the Large Deviation Theorem.

Theorem 5.2.4 Large Deviation Theorem

Let $\{X_i\}_{i=1}^{M}$ *be iid random variables with common mean* m *and the MGF* $\Phi(s)$*, cumulant generating function* $\Psi_{P_X}(s)$*, and Legendre transfer function* $\psi^*_{P_X}(\alpha)$ *associated with* X_1 *defined in (5.2.21), (5.1.12), and (5.1.13), respectively. Then the large deviation principle with rate function* $\psi^*_{P_X}(\alpha)$ *is:*

for all closed sets F*,*

$$\lim \sup_{M\to\infty} \frac{1}{M} \log P(\frac{1}{M}\sum_{k=1}^{M} X_k \in F) \leq -\inf_{F} \psi^*_{P_X}, \tag{5.2.39}$$

and for all open sets G*,*

$$\lim \inf_{M\to\infty} \frac{1}{M} \log P(\frac{1}{M}\sum_{k=1}^{M} X_k \in G) \geq -\inf_{G} \psi^*_{P_X}. \tag{5.2.40}$$

5.2.4 Rayleigh Distribution

In mobile radio channels, the Rayleigh distribution is commonly used to describe the statistical time-varying nature of the received envelope of a flat fading signal, or the envelope of an individual multipath component. It is well known that the envelope of the sum of two quadrature Gaussian noise signals obeys the Rayleigh distribution [1], [2], [5], [15].

The Rayleigh distribution is frequently used to model the statistics of signals transmitted through radio channels. Suppose a random variable R is a Rayleigh distribution defined as:

$$R = \sqrt{Y} = \sqrt{X_1^2 + X_2^2}. \tag{5.2.41}$$

We can see $Y = X_1^2 + X_2^2$, where X_1 and X_2 are zero-mean statistically independent Gaussian random variables, each having a variance σ^2. So the PDF of Y is:

$$p_Y(y) = \frac{1}{2\sigma^2} e^{-y/2\sigma^2}, \quad y \geq 0. \tag{5.2.42}$$

Also we get the PDF of R in the form:

$$p_R(r) = \frac{r}{\sigma^2} e^{-r^2/2\sigma^2}, \quad r \geq 0. \tag{5.2.43}$$

For the equation (5.1.4), let

$$Y_n = \sum_{j \neq n}^{M} p_j g_{nj} + (1 - \frac{1}{\gamma_n}) p_n g_{nn}, \tag{5.2.44}$$

then $I^n(p) = Y_n + \eta_n$. Let $g_{nj} = {s_{nj}}^2$ or $s_{nj} = \sqrt{g_{nj}}$. Since the attenuation s_{nj} is a Rayleigh distribution, then g_{nj} is a central Chi-square distribution and its MGF has the form as in (5.2.28).

Hence we have the following result:

$$\begin{aligned}
\Phi(s_n) &= E[e^{s_n \sum_{j \neq n}^{M} p_j g_{nj}} * e^{s_n \eta_n} * e^{s_n (1 - \frac{1}{\gamma_n}) p_n g_{nn}}] \\
&= e^{\frac{s_n^2 {\sigma_n}^2}{2}} * \frac{1}{1 - 2p_n(1 - \frac{1}{\gamma_n}) s_n \sigma_{nn}^2} * \prod_{j \neq n}^{M} \left(\frac{1}{1 - 2p_j s_n \sigma_{nj}^2} \right) \\
&= e^{\frac{s_n^2 {\sigma_n}^2}{2}} * \frac{1 - 2p_n s_n \sigma_{nn}^2}{1 - 2p_n(1 - \frac{1}{\gamma_n}) s_n \sigma_{nn}^2} * \prod_{j=1}^{M} \left(\frac{1}{1 - 2p_j s_n \sigma_{nj}^2} \right).
\end{aligned} \tag{5.2.45}$$

From (5.1.2), we know $0 < \gamma_n < 1$. Also we have $p_j > 0$, $s_j > 0$, and $\sigma_{nj}^2 > 0$, so $1 - 2p_n(1 - \frac{1}{\gamma_n}) s_n \sigma_{nn}^2 > 0$. Now we assume that $1 - 2p_j s_n \sigma_{nj}^2 > 0$, that is $2p_j s_n \sigma_{nj}^2 < 1$ for all n, j. Then taking the logarithm of it, we have:

$$\begin{aligned}
\log \Phi(s_n) &= \frac{s_n^2 \sigma_n^2}{2} + \log (1 - 2p_n s_n \sigma_{nn}^2) - \log (1 - 2p_n(1 - \frac{1}{\gamma_n}) s_n \sigma_{nn}^2) \\
&\quad - \sum_{j=1}^{M} \log (1 - 2p_j s_n \sigma_{nj}^2).
\end{aligned} \tag{5.2.46}$$

Let $p^* = \max\{p_j\}$ and ${\sigma_n^*}^2 = \max\{{\sigma_{nj}}^2\}$ for $1 \leq j \leq M$. Then we have $\log (1 - 2p_j s_n \sigma_{nj}^2) > \log (1 - 2p^* s_n {\sigma_n^*}^2)$.

As a result, we have:

$$\begin{aligned}
\log \Phi(s_n) &\leq \frac{s_n^2 \sigma_n^2}{2} + \log (1 - 2p_n s_n \sigma_{nn}^2) - \log (1 - 2p_n(1 - \frac{1}{\gamma_n}) s_n \sigma_{nn}^2) \\
&\quad - \sum_{j=1}^{M} \log (1 - 2p^* s_n {\sigma_n^*}^2) \\
&= \frac{s_n^2 \sigma_n^2}{2} + \log (1 - 2p_n s_n \sigma_{nn}^2) - \log (1 - 2p_n(1 - \frac{1}{\gamma_n}) s_n \sigma_{nn}^2) \\
&\quad - M \log (1 - 2p^* s_n {\sigma_n^*}^2).
\end{aligned} \tag{5.2.47}$$

Now, we apply the Large Deviation Limit Theorem to get:

$$\begin{aligned}\lim_{M\to\infty}\frac{1}{M}\log\Phi(s_n) &\leq \lim_{M\to\infty}\frac{1}{M}\Big(\frac{s_n^2\sigma_n^2}{2}+\log\left(1-2p_n s_n\sigma_{nn}^2\right)-\log\left(1-2p_n(1-\frac{1}{\gamma_n})s_n\sigma_{nn}^2\right)\Big)\\ &\quad -\log\left(1-2p^* s_n\sigma_n^{*2}\right)\\ &= \log\frac{1}{(1-2p^* s_n\sigma_n^{*2})}. \qquad (5.2.48)\end{aligned}$$

5.2.5 Rice Distribution

When there is a nonfading signal component present, such as a Line-of-Sight (LOS) propagation path, the small-scale fading envelope distribution is the Rice distribution. The Rice distribution is related to the noncentral Chi-square distribution, which has the form $R=\sqrt{Y}=\sqrt{X_1^2+X_2^2}$, where X_1 and X_2 are statistically independent Gaussian random variables with means m_1 and m_2, and the common variance σ^2. Then Y is the noncentral Chi-square distribution with the noncentrality parameter $m^2=m_1^2+m_2^2$. So, the PDF of Y is:

$$p_Y(y)=\frac{1}{2\sigma^2}e^{-(m^2+y)/2\sigma^2}I_0(\sqrt{y}\frac{m}{\sigma^2}),\quad y\geq 0. \qquad (5.2.49)$$

Also we state the PDF of R in the form:

$$p_R(r)=\frac{r}{\sigma^2}e^{-(r^2+m^2)/2\sigma^2}I_0(\frac{rm}{\sigma^2}),\quad r\geq 0,\quad m\geq 0. \qquad (5.2.50)$$

The parameter m denotes the peak amplitude of the dominant signal and $I_0(.)$ is the modified Bessel function of the first kind and zero-order. The Rice distribution is often described in terms of a parameter K, which is defined as the ratio between the deterministic signal power and the variance of the multipath. It is given as $K=\frac{m^2}{2\sigma^2}$, or in terms of dB $K(dB)=10\log\frac{m^2}{2\sigma^2}$. The parameter K is known as the Rice factor and completely specifies the Rice distribution. As $m\to 0, K\to -\infty dB$, and as the dominant path decreases in amplitude, the Rice distribution degenerates to a Rayleigh distribution [1], [2], [19], [20].

In our study, we consider the attenuation $S(t,\tau)$ as a Rice distribution corresponding to the

above R, so that $R = \sqrt{X_1^2 + X_2^2} = \sqrt{Y}$. Because in Chapters 3 and 4, we defined $S = \sqrt{G}$, now we have:

$$p_G(g) = \frac{1}{2\sigma^2} e^{-(g+m^2)/2\sigma^2} I_0(\frac{\sqrt{g}m}{\sigma^2}), \quad r \geq 0, m \geq 0. \tag{5.2.51}$$

So the channel gain G has the characteristic function:

$$\psi_G(j\upsilon) = \frac{1}{1 - j2\upsilon\sigma^2} exp\Big(\frac{j\upsilon m}{1 - j2\upsilon\sigma^2}\Big). \tag{5.2.52}$$

The MGF of $I^n(p)$ is:

$$\begin{aligned}
\Phi(s_n) &= \prod_{j\neq n}^{M} \Big((\frac{1}{1 - 2s_n p_j \sigma_{nj}^2}) e^{(\frac{ms_n p_j}{1-2s_n p_j \sigma_{nj}^2})}\Big) * \frac{1}{1 - 2(1 - 1/\gamma_n) p_n s_n \sigma_{nn}^2} \\
&\quad * e^{(\frac{ms_n(1-1/\gamma_n)p_n}{1-2(1-1/\gamma_n)p_n s_n \sigma_{nn}^2})} * e^{(\frac{s_n^2\sigma_n^2}{2})} \\
&= \prod_{j=1}^{M} \Big((\frac{1}{1 - 2s_n p_j \sigma_{nj}^2}) e^{(\frac{ms_n p_j}{1-2s_n p_j \sigma_{nj}^2})}\Big) * \frac{1 - 2p_n s_n \sigma_{nn}^2}{1 - 2(1 - 1/\gamma_n) p_n s_n \sigma_{nn}^2} \\
&\quad * e^{(\frac{ms_n(1-1/\gamma_n)p_n}{1-2(1-1/\gamma_n)p_n s_n \sigma_{nn}^2})} * e^{-\frac{ms_n p_n}{1-2p_n s_n \sigma_{nn}^2}} * e^{(\frac{s_n^2\sigma_n^2}{2})}.
\end{aligned} \tag{5.2.53}$$

Similar to the Rayleigh case, we also assume that $2p_j s_n \sigma_{nj}^2 < 1$ for both n and j. Then taking the logarithm of it, we have:

$$\begin{aligned}
\log \Phi(s_n) = &- \sum_{j=1}^{M} \log(1 - 2p_j s_n \sigma_{nj}^2) + \sum_{j=1}^{M} \frac{ms_n p_j}{1 - 2p_j s_n \sigma_{nj}^2} \\
&+ \log(1 - 2p_n s_n \sigma_{nn}^2) - \log(1 - 2(1 - \frac{1}{\gamma_n}) p_n s_n \sigma_{nn}^2) \\
&+ \frac{ms_n(1 - 1/\gamma_n)p_n}{1 - 2(1 - 1/\gamma_n)p_n s_n \sigma_{nn}^2} - \frac{ms_n p_n}{1 - 2p_n s_n \sigma_{nn}^2} + \frac{s_n^2\sigma_n^2}{2}.
\end{aligned} \tag{5.2.54}$$

As we had $\log(1 - 2p_j s_n \sigma_{nj}^2) > \log(1 - 2p^* s_n \sigma_n^{*2})$ before, now we can reach:

$$\frac{p_j}{1 - 2p_j s_n \sigma_{nj}^2} \leq \frac{p^*}{1 - 2p^* s_n \sigma_n^{*2}}. \tag{5.2.55}$$

Then (5.2.54) becomes:

$$\begin{aligned}
\log \Phi(s_n) \leq &- \sum_{j=1}^{M} \log(1 - 2p^* s_n \sigma_n^{*2}) + \sum_{j=1}^{M} \frac{ms_n p^*}{1 - 2p^* s_n \sigma_n^{*2}} \\
&+ \log(1 - 2p_n s_n \sigma_{nn}^2) - \log(1 - 2(1 - \frac{1}{\gamma_n}) p_n s_n \sigma_{nn}^2) \\
&+ \frac{ms_n(1 - 1/\gamma_n)p_n}{1 - 2(1 - 1/\gamma_n)p_n s_n \sigma_{nn}^2} - \frac{ms_n p_n}{1 - 2p_n s_n \sigma_{nn}^2} + \frac{s_n^2\sigma_n^2}{2}.
\end{aligned} \tag{5.2.56}$$

Similarly with (5.2.48), we have:

$$\lim_{M\to\infty}\frac{1}{M}\log\Phi(s_n)\leq\frac{ms_np^*}{1-2p^*s_n\sigma_n^{*2}}+\log\frac{1}{(1-2p^*s_n\sigma_n^{*2})}. \tag{5.2.57}$$

As we said before, when $m\to 0$ and the dominant path decreases in amplitude, the Rice distribution degenerates to a Rayleigh distribution. When $m\to 0$, the above result (5.2.57) is the same as (5.2.48) for the Rayleigh distribution.

5.2.6 Nakagami-m Distribution

The Rayleigh distribution and the Rice distribution are used to describe statistical fluctuations of signals received from a multipath-fading channel in a wireless network system. Another distribution, known as a Nakagami-m distribution, is used to characterize the statistics of signals transmitted through many multipath fading channels [1], [2]. The PDF is given as:

$$p_R(r)=\frac{2}{\Gamma(m)}\Big(\frac{m}{\Omega}\Big)^m r^{2m-1}e^{-mr^2/\Omega},\quad r\geq 0, \tag{5.2.58}$$

where Ω is defined as $\Omega=E(R^2)$, and $m=\frac{\Omega^2}{E[(R^2-\Omega)^2]}$, $m\geq\frac{1}{2}$, which is called the fading figure.

For $R=\sqrt{Y}$, where R is characterized statistically by the Nakagami-m distribution, then the random variable $Y=R^2$ has the PDF:

$$p_Y(y)=\frac{m^m}{\Gamma(m)\bar{y}^m}y^{m-1}e^{-my/\bar{y}}, \tag{5.2.59}$$

where $\bar{y}=E(R^2)$.

In our study, we consider the signal attenuation $S(t,\tau)$ as a Nakagami-m distribution corresponding to the above R for $R=\sqrt{X_1^2+X_2^2}=\sqrt{Y}$. Because in Chapters 3 and 4, we defined $s_{nj}=\sqrt{g_{nj}}$, we have:

$$p(g)=\frac{1}{\Gamma(m)}\Big(\frac{m}{\bar{g}}\Big)^m g^{m-1}e^{-mg/\bar{g}}, \tag{5.2.60}$$

where $\bar{g} = E(s^2)$.

So, the channel gain g_{nj} has the Gamma distribution and it has the characteristic function:

$$\psi(j\upsilon) = \Big(\frac{\lambda}{\lambda - j\upsilon}\Big)^m. \tag{5.2.61}$$

Then using MGF, we have:

$$\begin{aligned}
\Phi(s_n) &= E[e^{s_n \sum_{j\neq n}^{M} p_j g_{nj}} * e^{s_n \eta_n} * e^{s_n(1-\frac{1}{\gamma_n})p_n g_{nn}}] \\
&= \Big(\frac{\lambda}{\lambda - (1-\frac{1}{\gamma_n})p_n s_n}\Big)^m \prod_{j\neq n} \Big(\frac{\lambda}{\lambda - p_j s_n}\Big)^m \; e^{\frac{s_n^2\sigma_n^2}{2}} \\
&= \Big(\frac{\lambda}{\lambda - (1-\frac{1}{\gamma_n})p_n s_n}\Big)^m * \big(\frac{\lambda - p_n s_n}{\lambda}\big)^m \prod_{j=1} \Big(\frac{\lambda}{\lambda - p_j s_n}\Big)^m \; e^{\frac{s_n^2\sigma_n^2}{2}} \\
&= \Big(\frac{\lambda - p_n s_n}{\lambda - (1-\frac{1}{\gamma_n})p_n s_n}\Big)^m * \prod_{j=1} \Big(\frac{\lambda}{\lambda - p_j s_n}\Big)^m \; e^{\frac{s_n^2\sigma_n^2}{2}}.
\end{aligned} \tag{5.2.62}$$

Similar to the previous cases, we have $\lambda - (1-\frac{1}{\gamma_n})p_n s_n > 0$. Now we assume $\lambda - p_j s_n > 0$ for all n, j. Then taking the logarithm of it, we have:

$$\log\Phi(s_n) = \frac{s_n^2\sigma_n^2}{2} + m\log\frac{\lambda - p_n s_n}{\lambda - (1-\frac{1}{\gamma_n})p_n s_n} + m\sum_{j=1}^{M}\log\frac{\lambda}{\lambda - p_j s_n}. \tag{5.2.63}$$

Similar to the analysis in the Rayleigh and Rice cases, we have:

$$\begin{aligned}
\log\Phi(s_n) \leq\; & \frac{s_n^2\sigma_n^2}{2} + m\log\frac{\lambda - p_n s_n}{\lambda - (1-\frac{1}{\gamma_n})p_n s_n} \\
& + m\sum_{j=1}^{M}\log\frac{\lambda}{\lambda - p^* s_n}.
\end{aligned} \tag{5.2.64}$$

Similar to (5.2.48), we have:

$$\begin{aligned}
\lim_{M\to\infty}\frac{1}{M}\log\Phi(s_n) \leq\; & \lim_{M\to\infty}\frac{1}{M}\Big(\frac{s_n^2\sigma_n^2}{2} + m\log\frac{\lambda - p_n s_n}{\lambda - (1-\frac{1}{\gamma_n})p_n s_n} \\
& + m\sum_{j=1}^{M}\log\frac{\lambda}{\lambda - p^* s_n}\Big) \\
=\; & m\log\frac{\lambda}{\lambda - p^* s_n}.
\end{aligned} \tag{5.2.65}$$

It is evident that the above result degenerates to a Rayleigh fading case when $m = 1$. When $m = 1$, $\lambda = \frac{1}{\bar{g}} = \frac{1}{2\sigma_n^{*2}}$, the above result (5.2.65) becomes the same as (5.2.48) for the Rayleigh distribution.

5.3 Numerical Results and Evaluations

After using the MGF to compute the expected value for different random variables, we have the MGF for our definition of $I^n(p)$ in (5.1.4). When M is a given number, we can directly use the formulas (5.2.46), (5.2.54), and (5.2.63) for the above three cases to compute the outage probability. When $M \to \infty$, by applying the Large Deviation Limit Theorem, we have three formulas for the cumulant generating function $\Psi(s_n) = \lim_{M\to\infty} \frac{1}{M} \log E[e^{s_n I^n(p)}]$ for three cases in (5.2.48), (5.2.57) and (5.2.65) which are the Rayleigh distribution, Rice distribution, and Nakagami-m distribution, respectively. We will now use them to simulate the outage probability with respect to each case for various sets of parameters, such as $\{g_{nj}\}, \{p_n\}$, as well as the parameters α and s_n in two steps. First for a given M case and second for $M \to \infty$. For these two cases, we mainly discuss the Rayleigh case. Then we use the same method for the other two cases.

5.3.1 Rayleigh Distribution Case

According to the situation in the Rayleigh distribution, combining the Chernoff bounds and Cramer's theorem, we have (5.1.15) for $s_n > 0$ with $\alpha > m_I$; thus we can compute the upper bound. Let $m_I = E[I^n(p)]$ be the expected value of $I^n(p)$. According to Cramer's Theorem 5.1.3, the probabilistic distribution of $I^n(p)$ provided by the Chernoff bound theorem can be stated as:

1. when $\alpha = m_I, s_n = 0$, then $-\psi^*(m_I) = 0, P(I^n(p) \geq m_I) \leq 1$;

2. if $\alpha > m_I$, then $P(I^n(p) \geq \alpha) \leq e^{-\psi^*(\alpha)}$ is non-trivial while $s_n > 0$;

3. if $\alpha < m_I$, then $P(I^n(p) \leq \alpha) \leq e^{-\psi^*(\alpha)}$ is non-trivial while $s_n < 0$.

where $\psi^*(\alpha)$ is defined in (5.1.14).

Based on the MGF of $I^n(p)$ in (5.2.45), assuming it can be differentiated, the first moment

of $\Phi(s_n)$ is also the expected value of $I^n(p)$ when $s_n = 0$. So we have:

$$m_I = \frac{\partial}{\partial s_n}\Phi(s_n)|_{s_n=0} = \sum_{j=1}^{M} 2p_j\sigma_{nj}^2 - 2\frac{p_n}{\gamma_n}\sigma_{nn}^2. \tag{5.3.66}$$

Since $e^{-s_n\alpha}\Phi(s_n)$ in (5.2.37) is a convex function over $s_n \in \Re$, there exists an optimal $s_n^* \in \Re$ which minimizes $e^{-s_n\alpha}\Phi(s_n)$ to yield the tightest Chernoff bound [12].

From $\psi^*(\alpha) = \sup_{s_n\in\Re}\{s_n\alpha - \Psi(s_n)\}$, we know that the supermum of it attained at $\alpha = \frac{\partial}{\partial s_n}\Psi(s_n)|_{s_n=s_n^*}$ [12], [31]. Now, let $M = 3$, from (5.2.46), for n=1, we have:

$$\begin{aligned}\log\Phi(s_1) &= \frac{s_1^2\sigma_1^2}{2} - \log\left(1 - 2p_1(1-\frac{1}{\gamma_1})s_1\sigma_{11}^2\right) \\ &\quad - \log\left(1 - 2p_2s_1\sigma_{12}^2\right) - \log\left(1 - 2p_3s_1\sigma_{13}^2\right),\end{aligned}$$

and also

$$\begin{aligned}\alpha &= \frac{\partial}{\partial s_1}\Psi(s_1)|_{s_1=s_1^*} \\ &= s_1^*\sigma_1^2 + \frac{2p_1(1-\frac{1}{\gamma_1})\sigma_{11}^2}{1-2p_1(1-\frac{1}{\gamma_1})\sigma_{11}^2s_1^*} + \frac{2p_2\sigma_{12}^2}{1-2p_2\sigma_{12}^2s_1^*} + \frac{2p_3\sigma_{13}^2}{1-2p_3\sigma_{13}^2s_1^*}.\end{aligned} \tag{5.3.67}$$

Thus, by the theorems, we have:

$$P(I^n(p) \geq \alpha) \leq e^{-\psi^*(\alpha)} = e^{-\alpha s_1^* + \Psi(s_1^*)}. \tag{5.3.68}$$

From the Chernoff bound theorem, we have (5.1.9). The tightest upper bound is obtained by selecting the value of s that minimizes the expected value. The necessary condition can be found in (5.1.10). Combining the assumption in (5.2.46), we have $0 < 2p_js_n\sigma_{nj}^2 < 1$ for both n and j. For the definition of outage probability, we have $\alpha = 0$. Then we can compute each s_n and select the optimal s_n^* to meet all the requirements.

Then plugging the above results of s_1^* for different parameters, we derive the outage probability expression for the distribution of $I^n(p)$ for a given M as:

$$P(I^n(p) \geq 0) \leq e^{-\psi^*(0)} = e^{\Psi(s_1^*)}. \tag{5.3.69}$$

In our simulation, related to some given channels, the variance of channel gain σ^2 and the power p are constants. For example, in Figure 5.3.5, $M = 3$ is fixed. From this, we can see

that for a given SIR threshold, the outage probability decreases as power increases. This tells us that in order to reduce the outage probability and also meet the SIR requirements, more optimal transmission power is required to satisfy the outage probability bound.

5.3.2 Rice Distribution Case

Next we analyze the case of channel fading with a Rice distribution. Similar to the Rayleigh case in (5.3.67), where $\log \Phi(s_n)$ is the result of (5.3.57), we have:

$$\alpha = \frac{2Mp^*\sigma^{*2}}{1-2p^*\sigma^{*2}s_n^*} + \frac{Mmp^*}{(1-2p^*\sigma^{*2}s_n^*)^2}.$$

Based on the MGF of $I^n(p)$ in (5.2.53), assuming it can be differentiated, the first moment of $\Phi(s_n)$ is also the expected value of $I^n(p)$ when $s_n = 0$. So we have:

$$m_I = \frac{\partial}{\partial s_n}\Phi(s_n)|_{s_n=0} = \sum_{j=1}^{M} 2p_j\sigma_{nj}^2 - 2\frac{p_n}{\gamma_n}\sigma_{nn}^2 + m(\sum_{j=1}^{M} p_j - \frac{p_n}{\gamma_n}).$$

As a result, when $s_n^* > 0$, we have $\alpha > m_I$. So for the Rice case, we have:

$$P(I^n(p) \geq \alpha) \leq e^{-\psi^*(\alpha)} = e^{-\alpha s_n^* + \Psi(s_n^*)} = e^{-\alpha s_n^* + \frac{Mmp^*s_n^*}{1-2p^*\sigma^{*2}s_n^*} + M\log\frac{1}{1-2p^*\sigma^{*2}s_n^*}}, \quad (5.3.70)$$

where the parameter m is defined as in section 5.2.3 for the Rice distribution. When m=0, we have the same result as in the Rayleigh case.

Also, when $\alpha = 0$, the Chernoff bound is named outage probability, for our study, we have:

$$P(I^n(p) \geq 0) \leq e^{-\psi^*(0)} = e^{\Psi(s_n^*)} = e^{\frac{Mmp^*s_n^*}{1-2p^*\sigma^{*2}s_n^*} + M\log\frac{1}{1-2p^*\sigma^{*2}s_n^*}}. \quad (5.3.71)$$

Using the same simulation method as in the Rayleigh case, but changing the parameters, we can plot the Chernoff bound of outage probability. In this case, we also change parameter m. The results are very similar to the Rayleigh case. Figures 5.3.6 and 5.3.7 are plotted for the Rice case with different values of parameters. In Figure 5.3.8, we compare the Rice case for different values of m with the Rayleigh case while the other parameters are similar. When $m = 0.5$, the curve is very close to the Rayleigh case.

5.3.3 Nakagami-m Distribution Case

Similarly, for the channel gain in the Nakagami-m distribution, we can derive the result:

$$\alpha = \frac{Mmp^*}{\lambda - p^* s_n^*}.$$

Using the same method for the MGF of $I^n(p)$ in (5.2.62), assuming it can be differentiated, the first moment of $\Phi(s_n)$ is also the expected value of $I^n(p)$ when $s_n = 0$. So we have:

$$m_I = \frac{\partial}{\partial s_n}\Phi(s_n)|_{s_n=0} = \frac{m}{\lambda}(\sum_{j=1}^{M} p_j - \frac{p_n}{\gamma_n}).$$

Similar to the previous cases, when $s_n^* > 0$ and $\alpha = 0$, we have:

$$P(I^n(p) \geq 0) \leq e^{-\psi^*(0)} = e^{\Psi(s_n^*)} = e^{Mm \log \frac{\lambda}{\lambda - p^* s_n^*}}. \tag{5.3.72}$$

When $m = 1$, $\frac{1}{\lambda} = 2\sigma_n^{*2}$, the above outage probability expression becomes the same as the Rayleigh case. Figures 5.3.9 and 5.3.10 are plotted for the Nakagami-m case with different values of m. In Figure 5.3.11, we compare the Nakagami-m case with the Rayleigh case when they have the similar situations.

5.3.4 Comparisons and Discussions of the Three Cases

Using the Large Deviation Theorem, when $M \to \infty$, the above three results (5.3.69), (5.3.71) and (5.3.72) become the following formula:

$$\lim_{M\to\infty} \frac{1}{M} \log P(I^n(p) \geq 0) \leq -\psi^*(0), \tag{5.3.73}$$

where $\psi^*(0)$ is the Legendre transfer function as $\psi^*(0) = -\Psi(s_n^*)$, and s_n^* can be computed as before for the three different cases.

Probabilities in (5.3.73) decrease exponentially in M. When $\alpha = 0$, $P(I^n(p) \geq 0) \to 0$, as $M \to \infty$.

Simulation figures show that the measures of evaluating the outage probability bounds are

simple and effective. At the same time, we can conclude that for a given value SIR, the greater the value of $p^*\sigma^{*2}$, the less the value of outage probability.

In Figure 5.3.18, we can see that the curves of the probability estimation are closer to the exact curves as M is increased. So the formula (5.3.73) provides a very good measure of evaluating the outage probability. In order to maintain a desired SIR and QoS requirement at the receiver, each user only needs to know its own channel gain related to the parameter σ^{*2} and the optimal transmitter power p^*.

In Figure 5.3.8, we compare the Rayleigh case to the Rice case for different values of m. It indicates that as m approaches 0, the Rice case approaches the Rayleigh case. Similarly, in Figure 5.3.11, when m approaches 1, the Nakagami case also approaches the Raleigh case. Both cases are consistent with our discussion in the previous formulas.

5.3.5 Comparing the Upper Bound with the Exact Outage Probability for Rayleigh Case

In Chapter 4, we plotted the direct result of outage probability in (4.1.11) as a function of CEM. Because we defined the CEM as a function of SIR, now we plot the exact outage probability related to some given SIR thresholds. Comparing the exact outage probability versus SIR from Chapter 4 with the Chernoff bound related to MGF for the Rayleigh case, we can see that the Chernoff upper bound is always beyond the exact outage probability as the given parameter increases. Figures 5.3.17 and 5.3.18 correspond to them with different values of M and p. When M becomes larger, the upper bounds are close to the exact outage probability curves. At the same time, we can see that for figures with M=30 and lower SIR thresholds, the outage probabilities are very small and very close to the exact outage probability.

Generally, for the similar situation of the Rayleigh case, we also can plot some figures corresponding to M increasing from 5 to 40 by increments of 5. Figures 5.3.19 to 5.3.26 are

these eight cases. For each one, we also compute the average variation between the upper bound and the exact outage probability. They are $0.49, 0.4, 0.33, 0.28, 0.24, 0.21, 0.18, 0.15$ corresponding to $M = 5, 10, 15, 20, 25, 30, 35, 40$. So we can see that as M increases the error decreases, which means the larger the M, the less the variation. This corroborates our earlier assertion that when M is very large, the upper bound expression derived using MGF is a good approach for evaluating the outage probability.

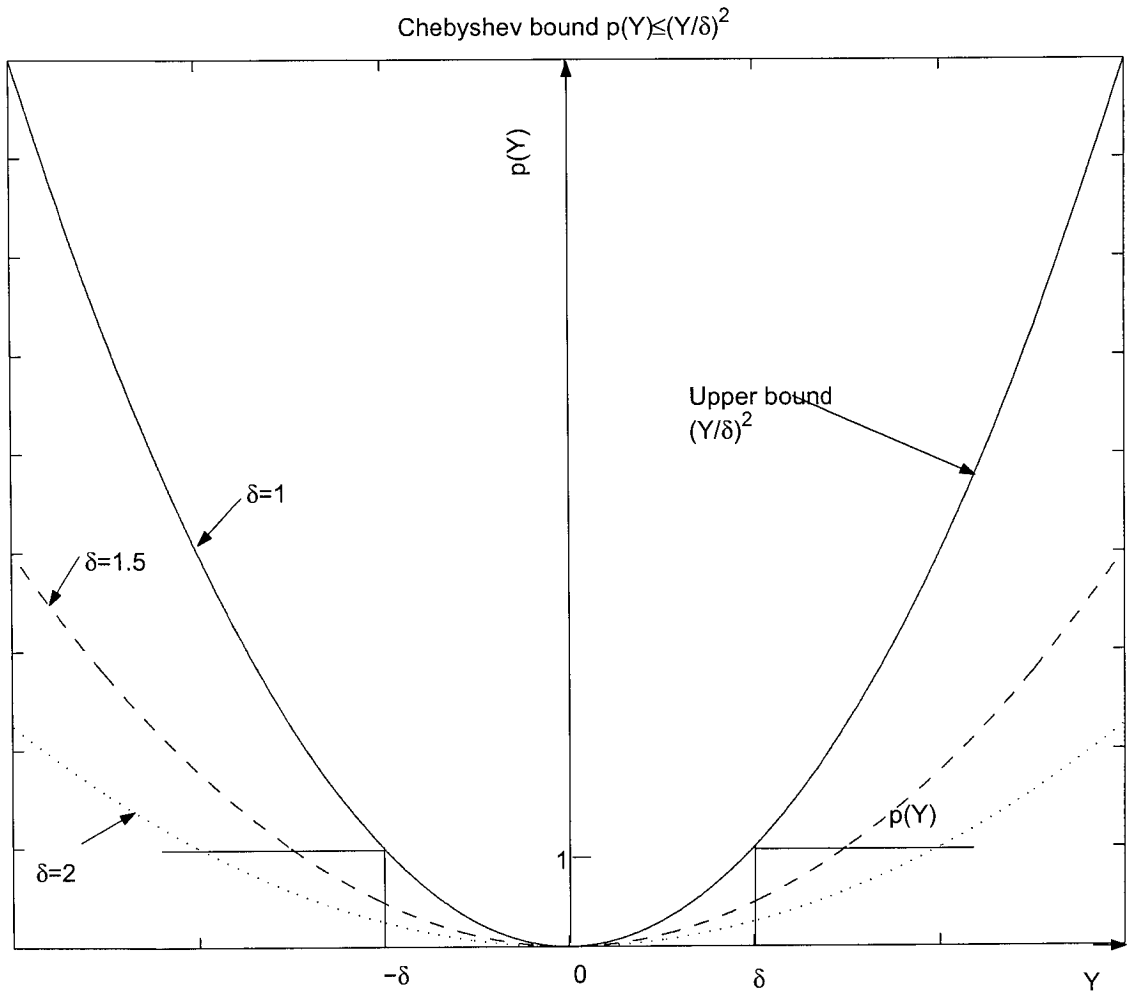

Figure 5.1.1: Chebyshev bound.

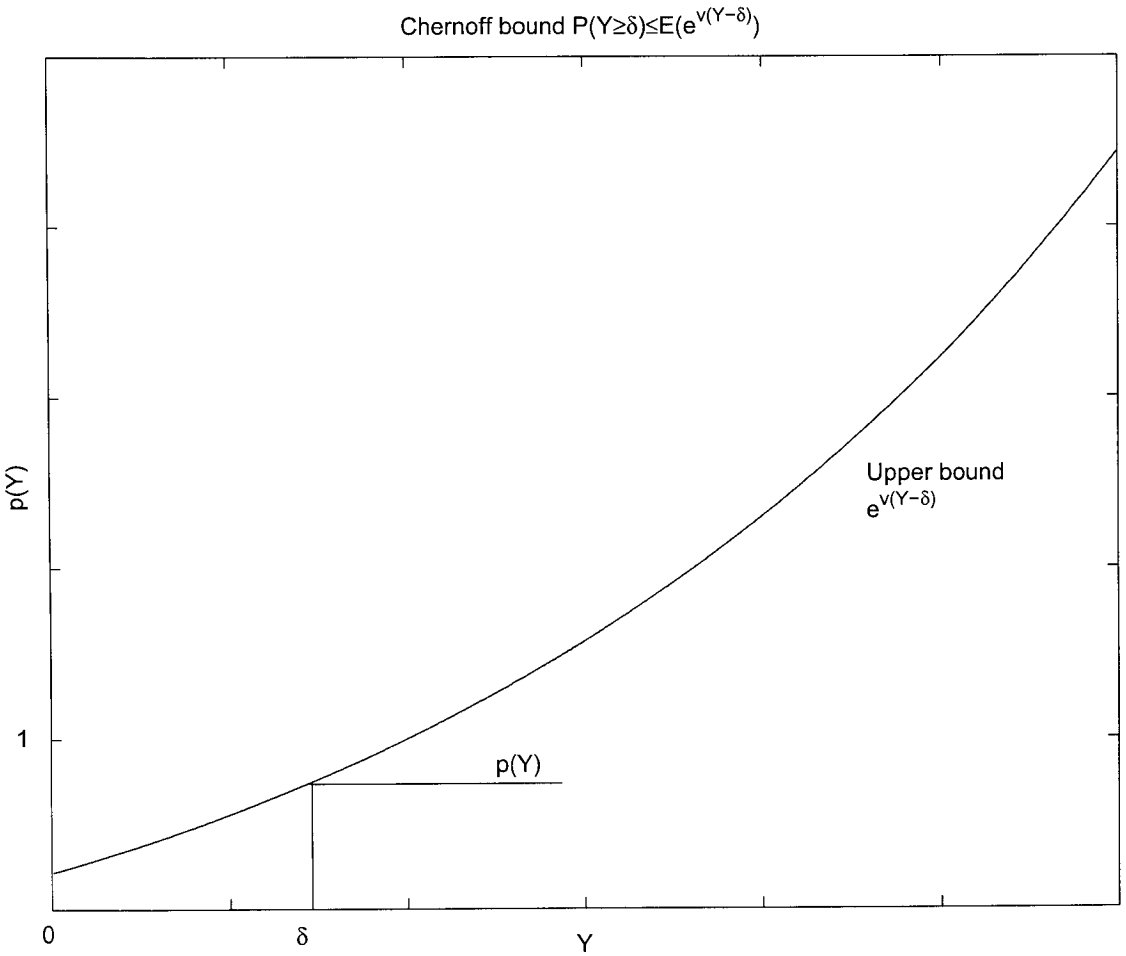

Figure 5.1.2: Chernoff bound.

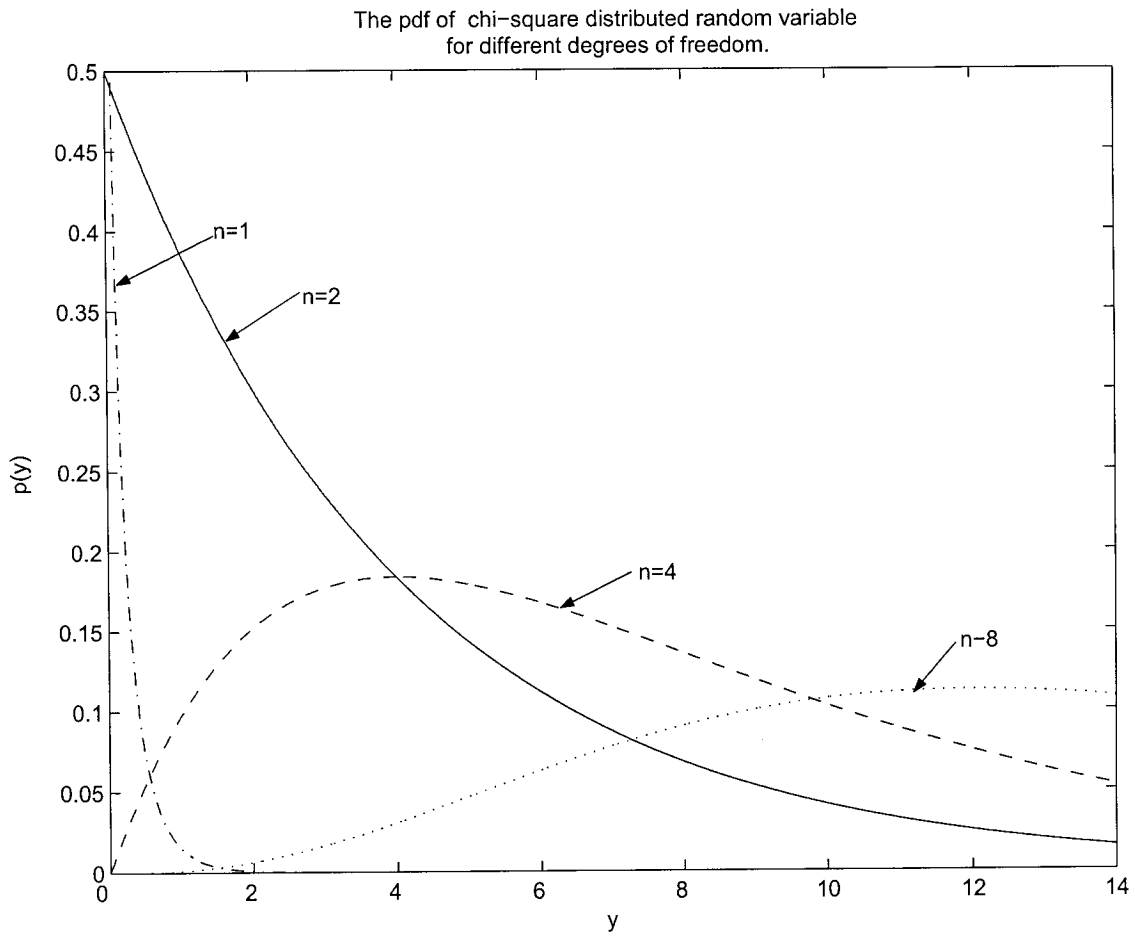

Figure 5.2.3: Chi-square distribution.

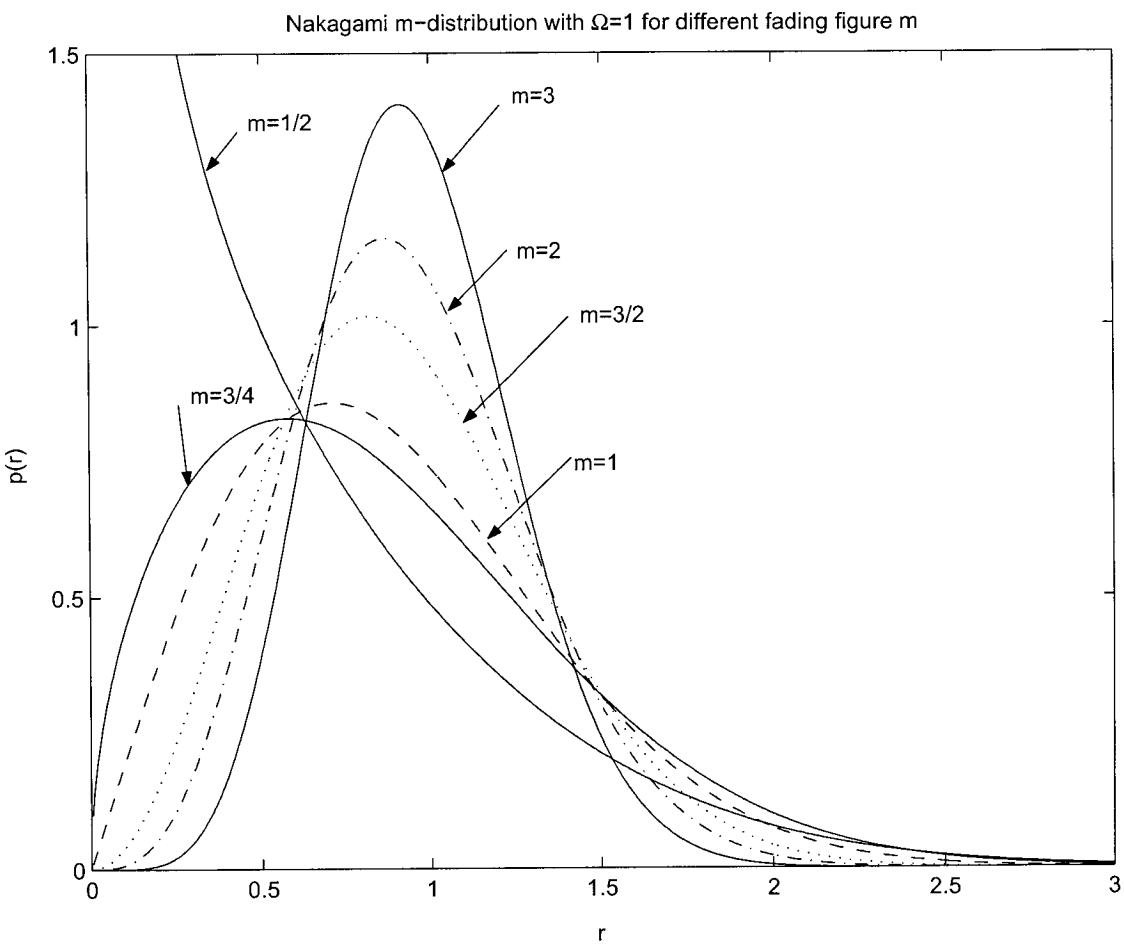

Figure 5.2.4: Gamma m-distribution.

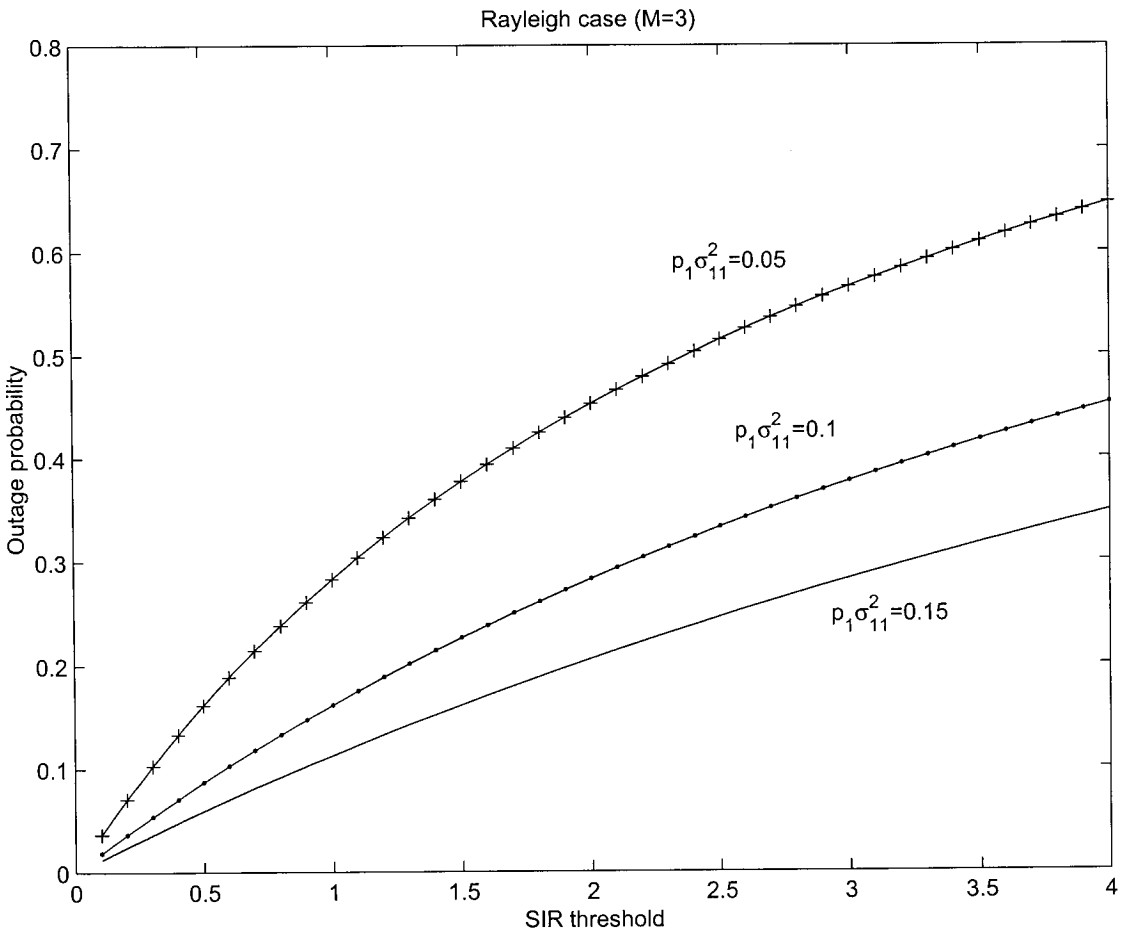

Figure 5.3.5: Outage probability with Chernoff bound versus SIR^{th} for Rayleigh case for fixed M=3. As parameter $p\sigma^2$ increases, the outage probability decreases corresponding to a given SIR^{th}.

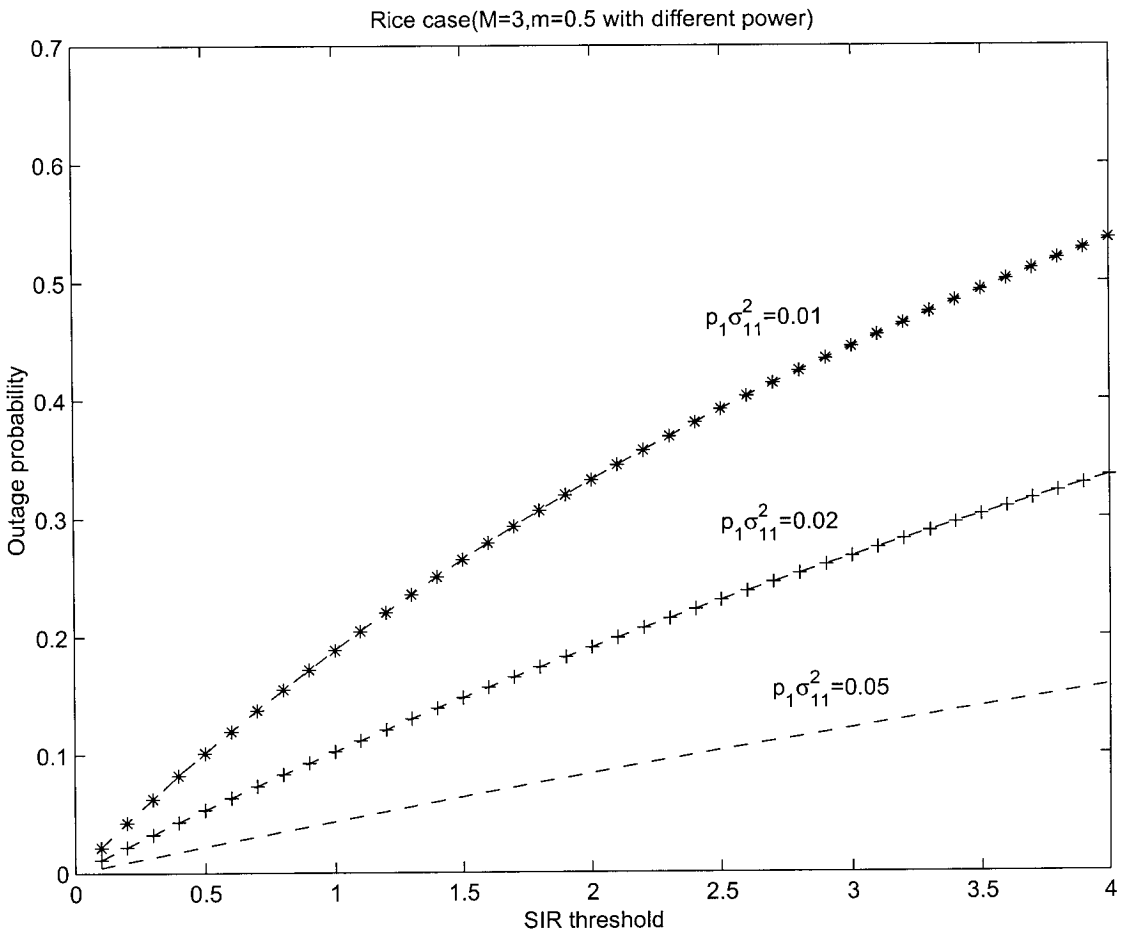

Figure 5.3.6: Rice case for M=3 and m=0.5.

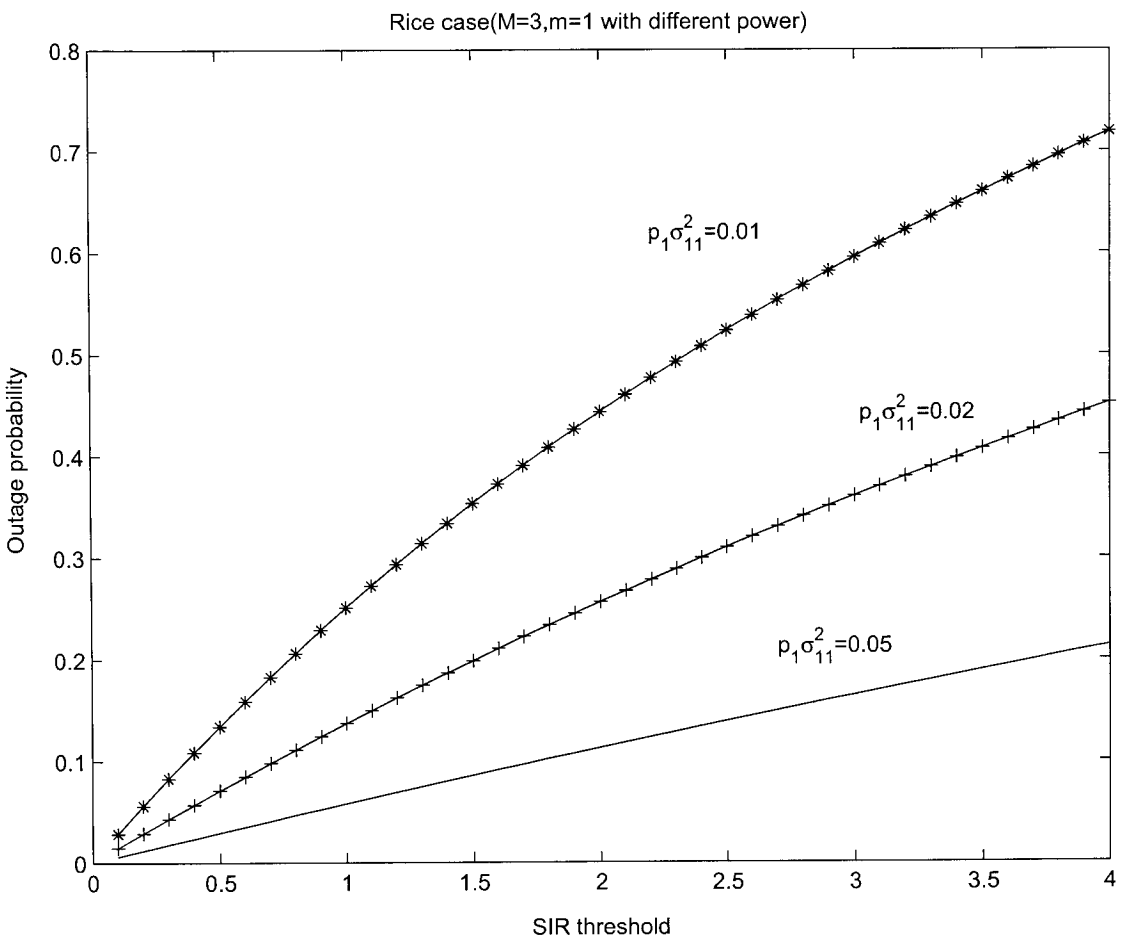

Figure 5.3.7: Rice case for M=3 and m=1.

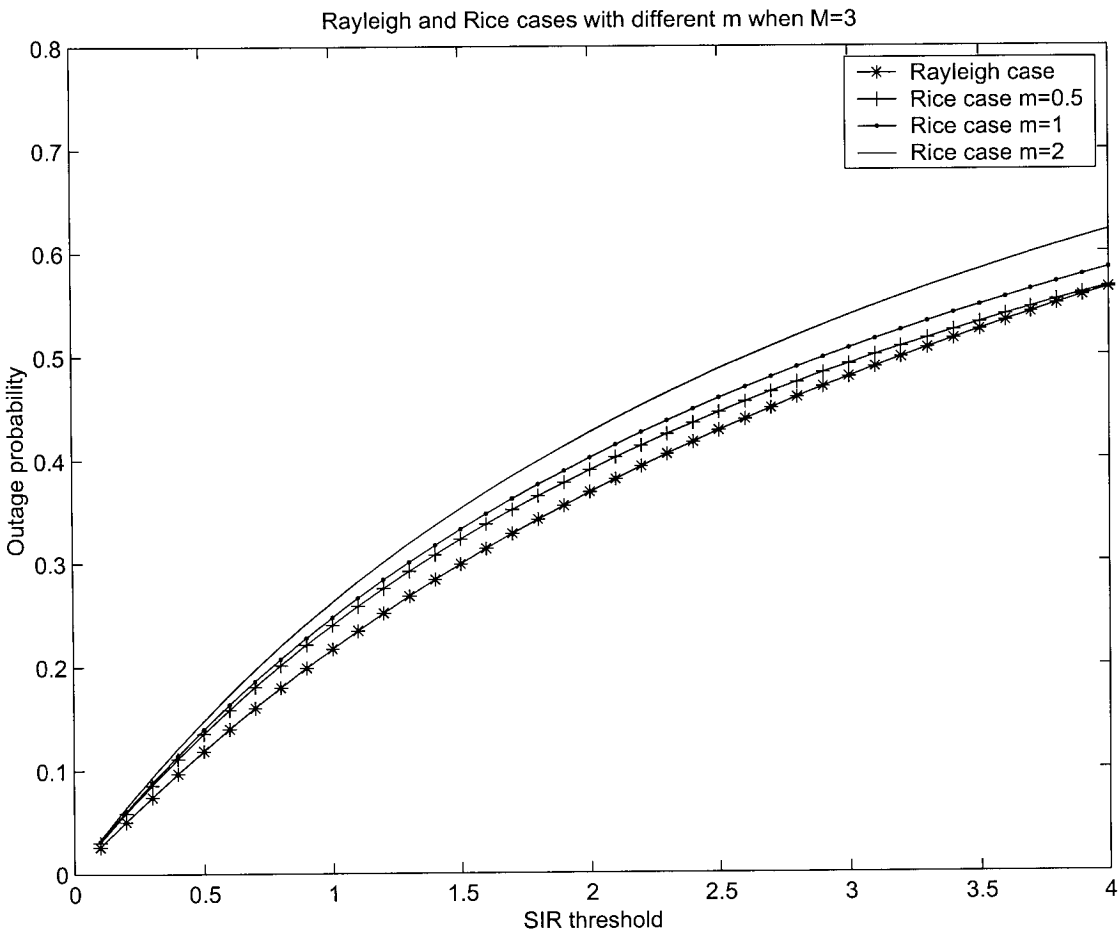

Figure 5.3.8: Rice case for different m with Rayleigh case for M=3 and similar parameters.

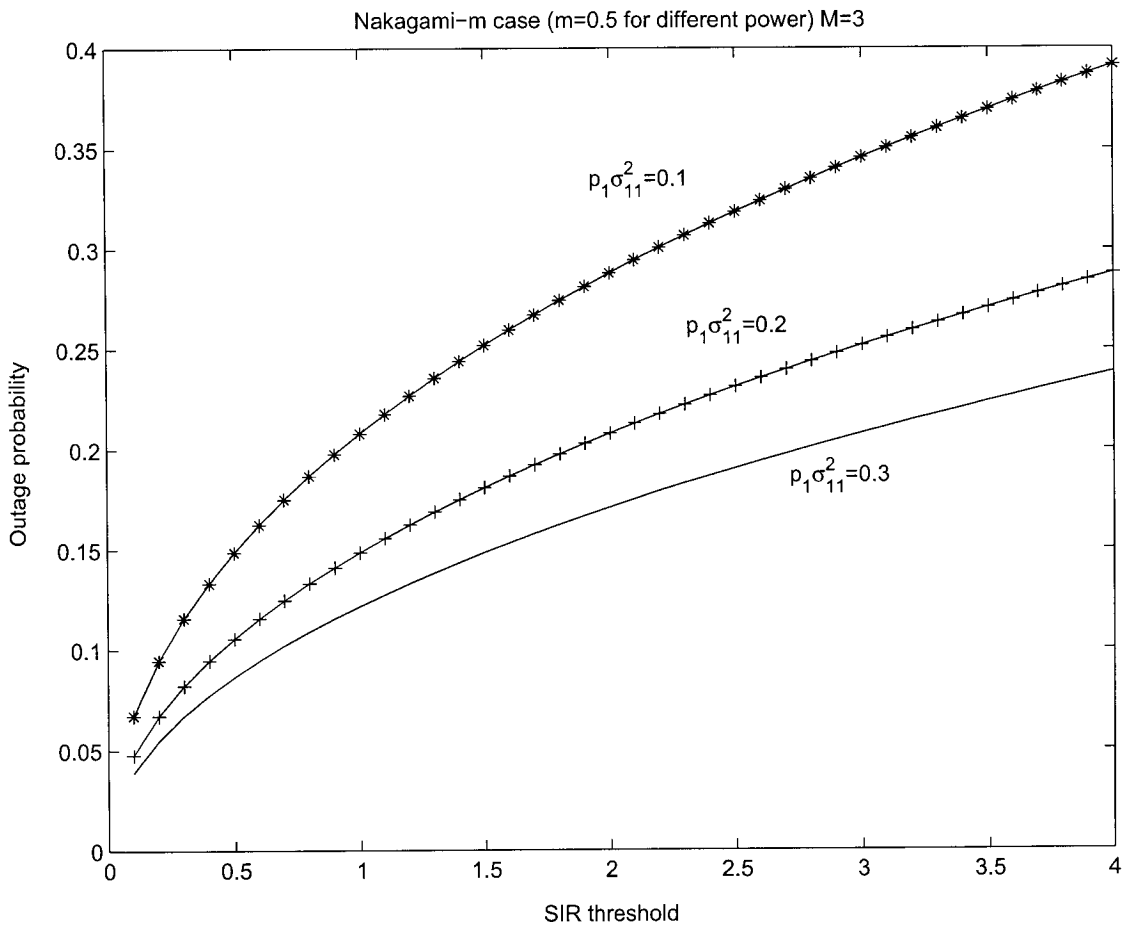

Figure 5.3.9: Nakagami-m case for M=3 and m=0.5.

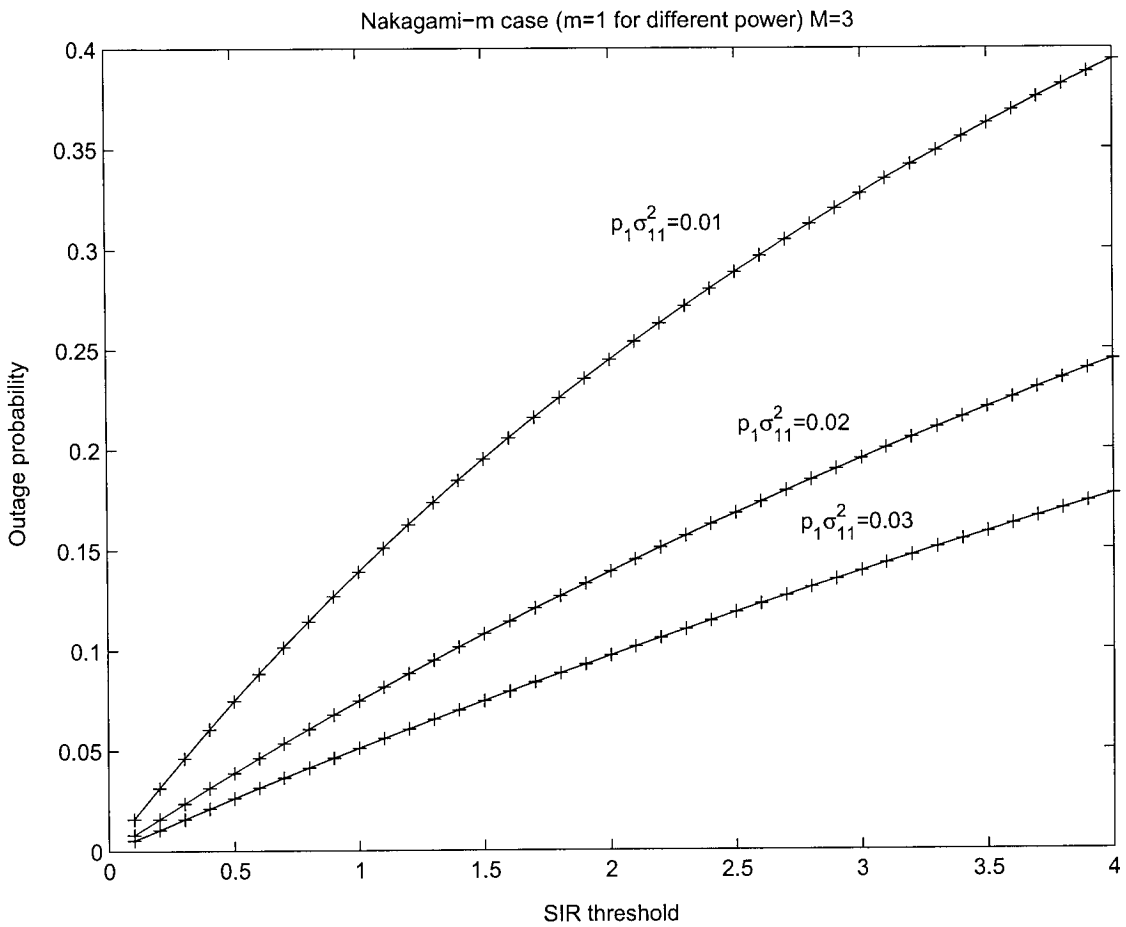

Figure 5.3.10: Nakagami-m case for M=3 and m=1.

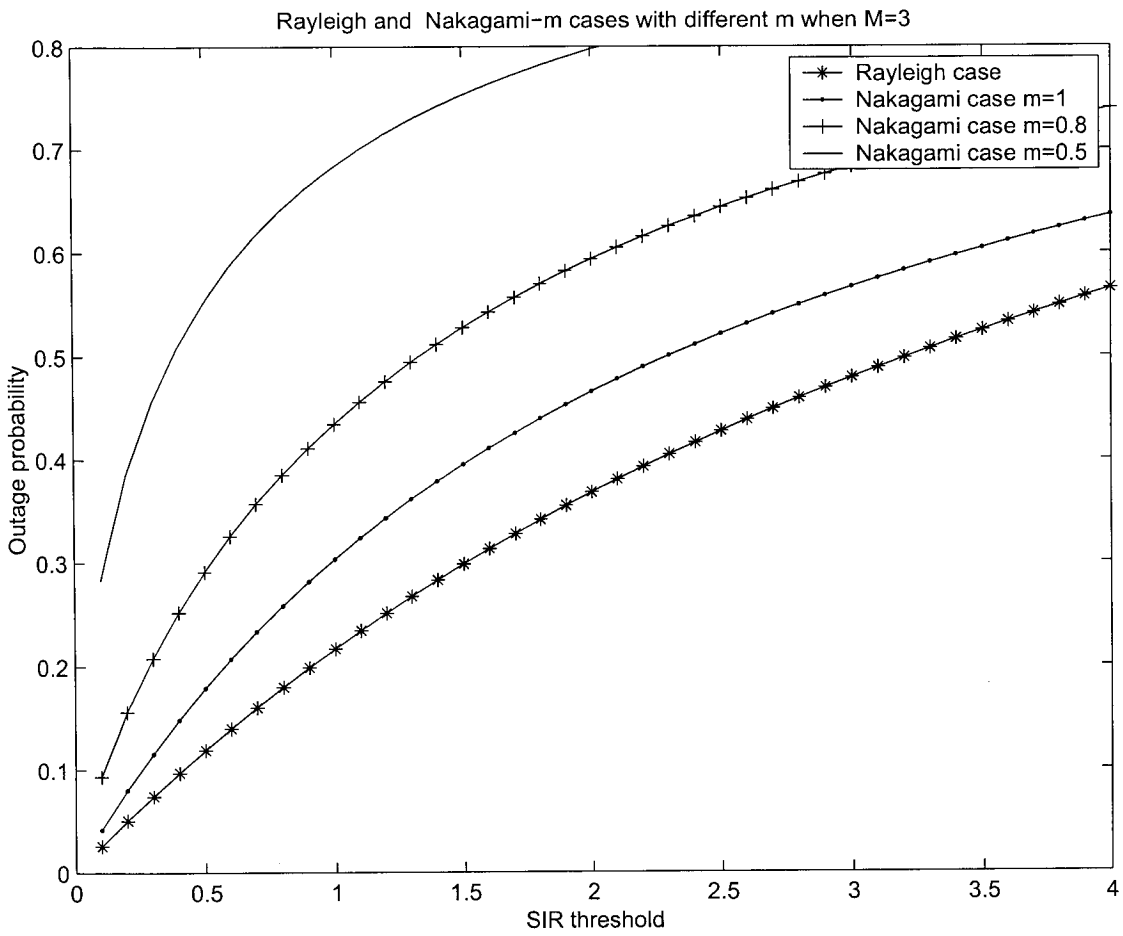

Figure 5.3.11: Comparison of Nakagami-m cases with different values of m to a Rayleigh case (M=3 for all cases).

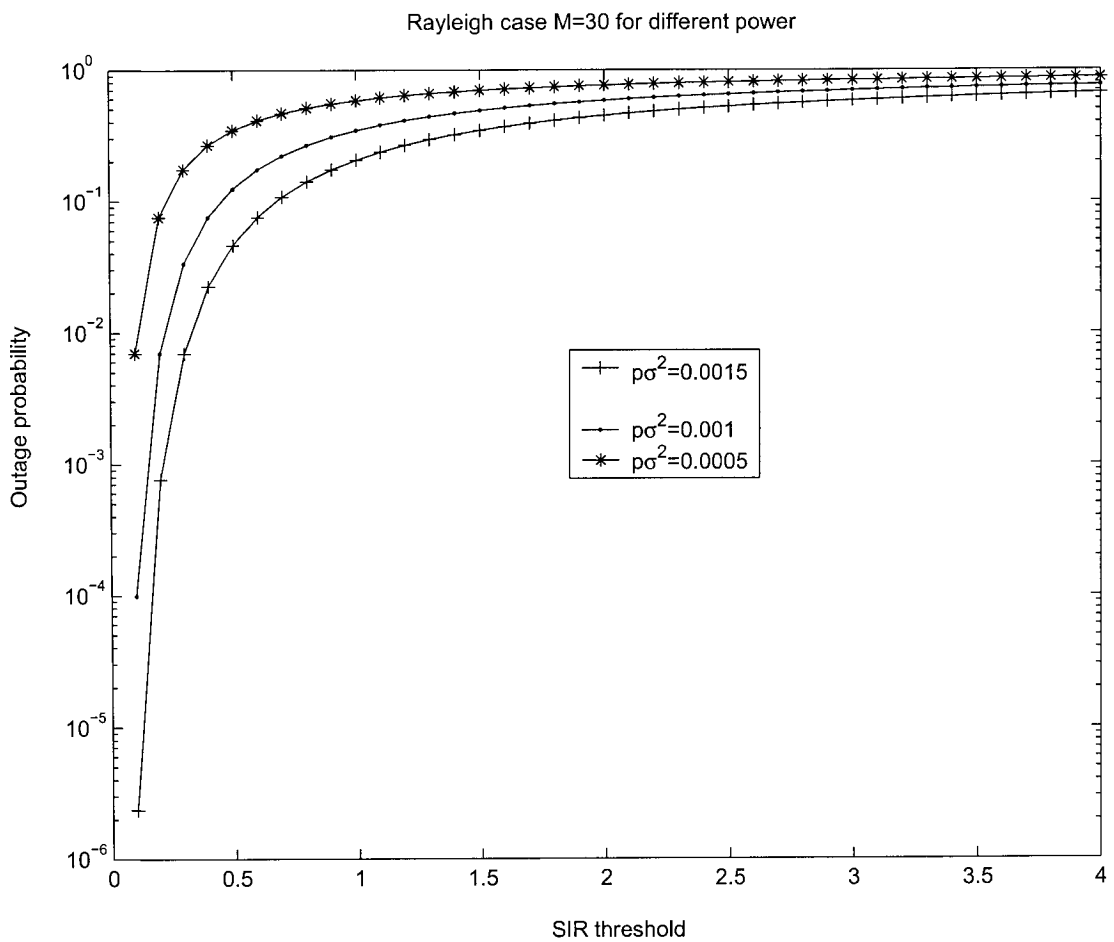

Figure 5.3.12: Rayleigh case for M=30.

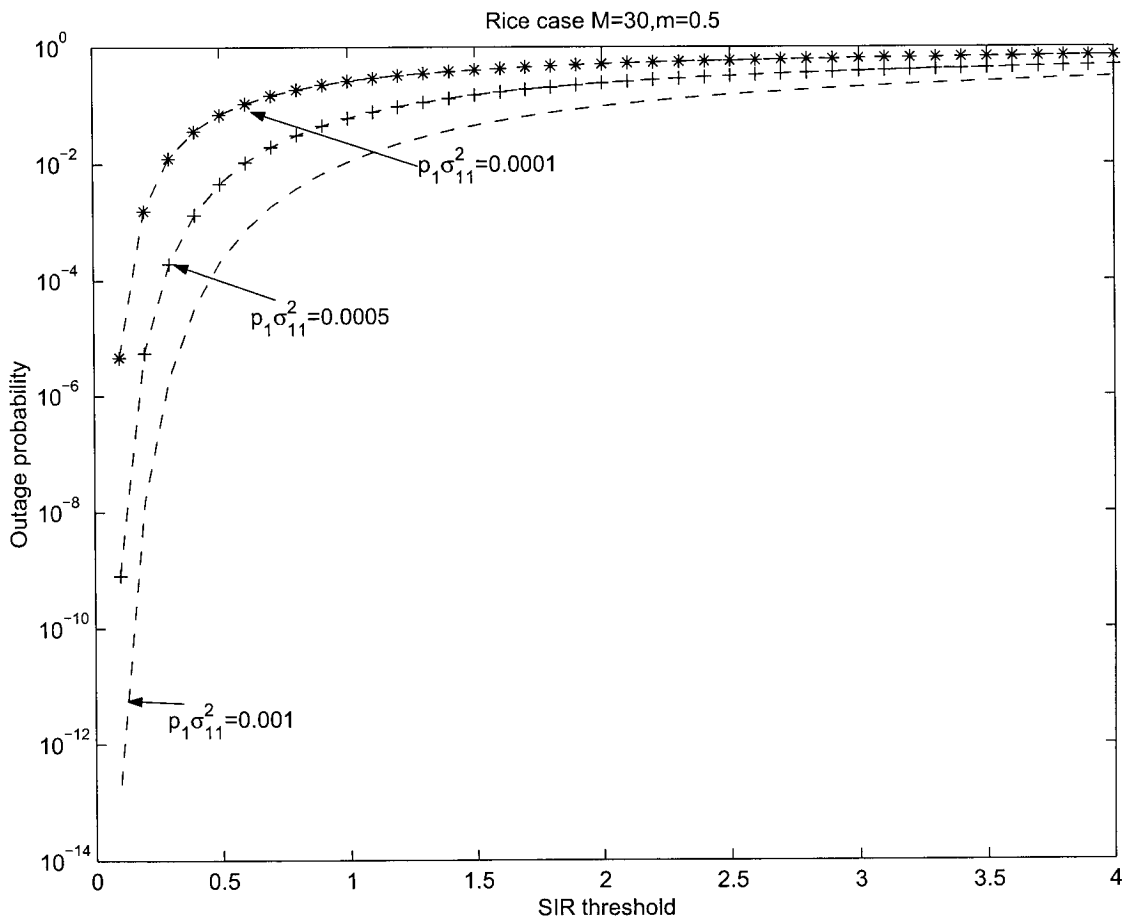

Figure 5.3.13: Rice case m=0.5 for M=30.

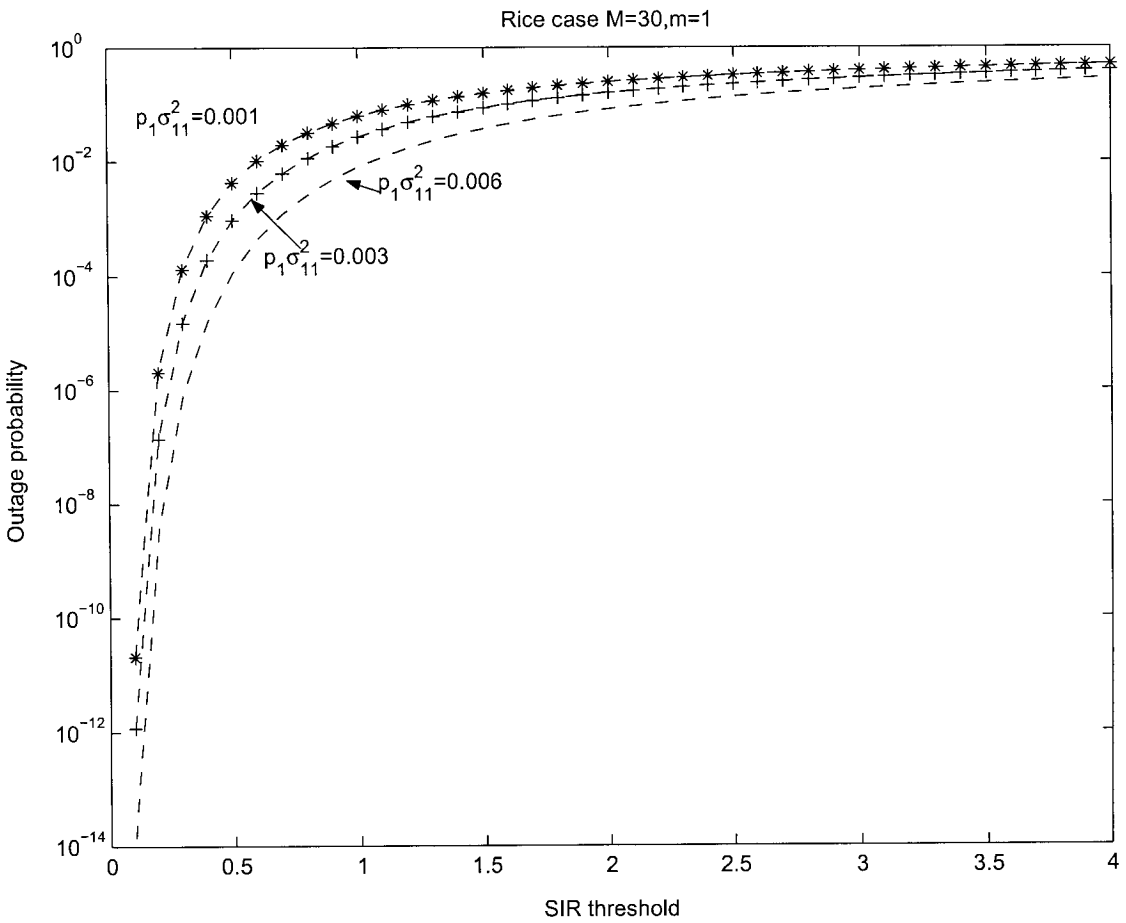

Figure 5.3.14: Rice case m=1 for M=30.

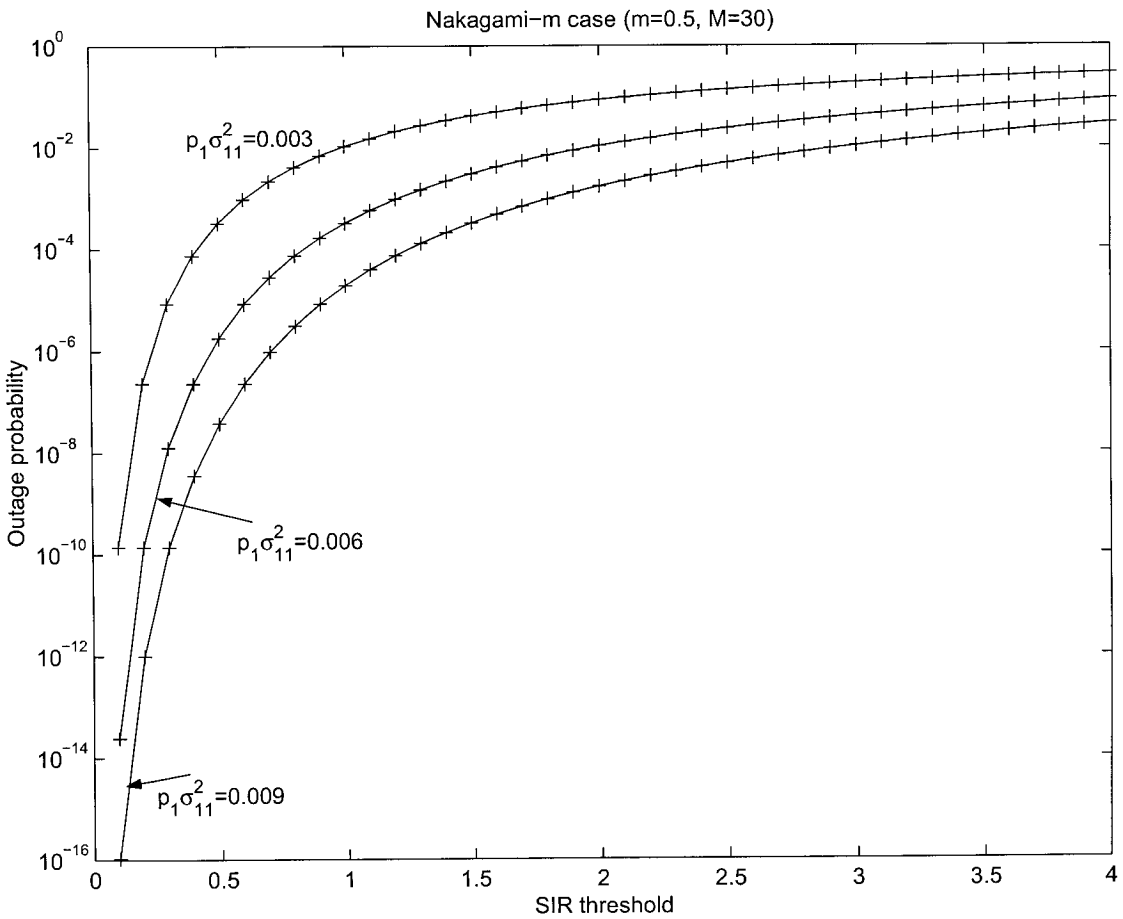

Figure 5.3.15: Nakagami-m case m=0.5 for M=30.

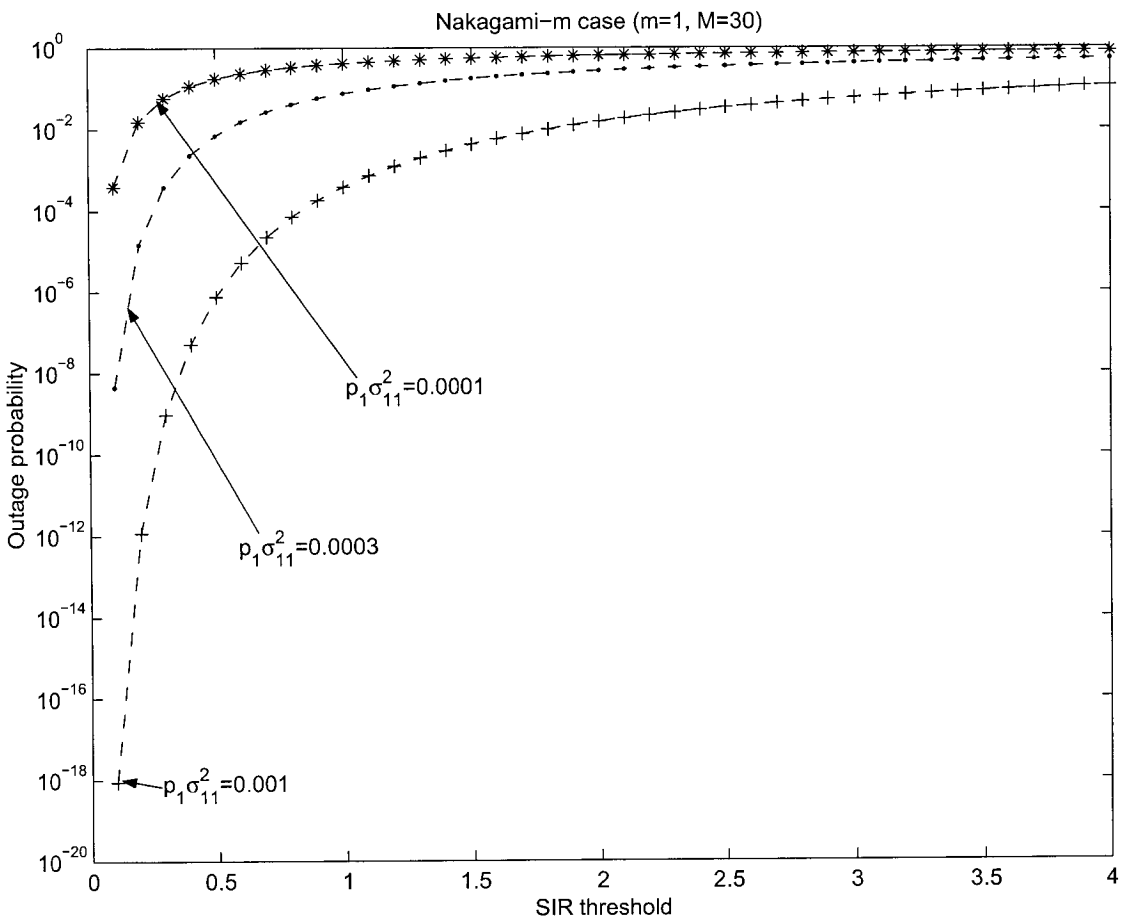

Figure 5.3.16: Nakagami-m case m=1 for M=30.

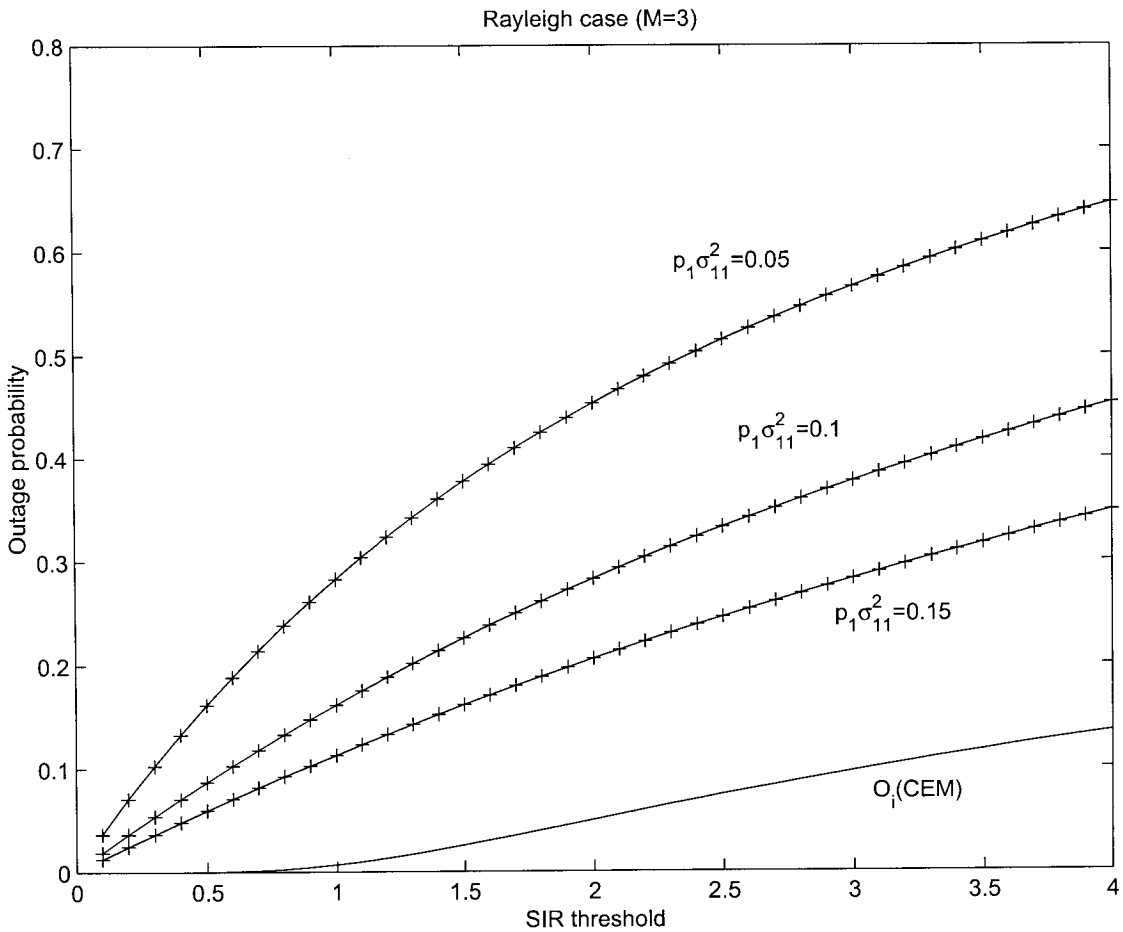

Figure 5.3.17: Comparing the upper bound with the exact outage probability related to $CEM = \Gamma/SIR^{th}$ corresponding to M=3 for Rayleigh case.

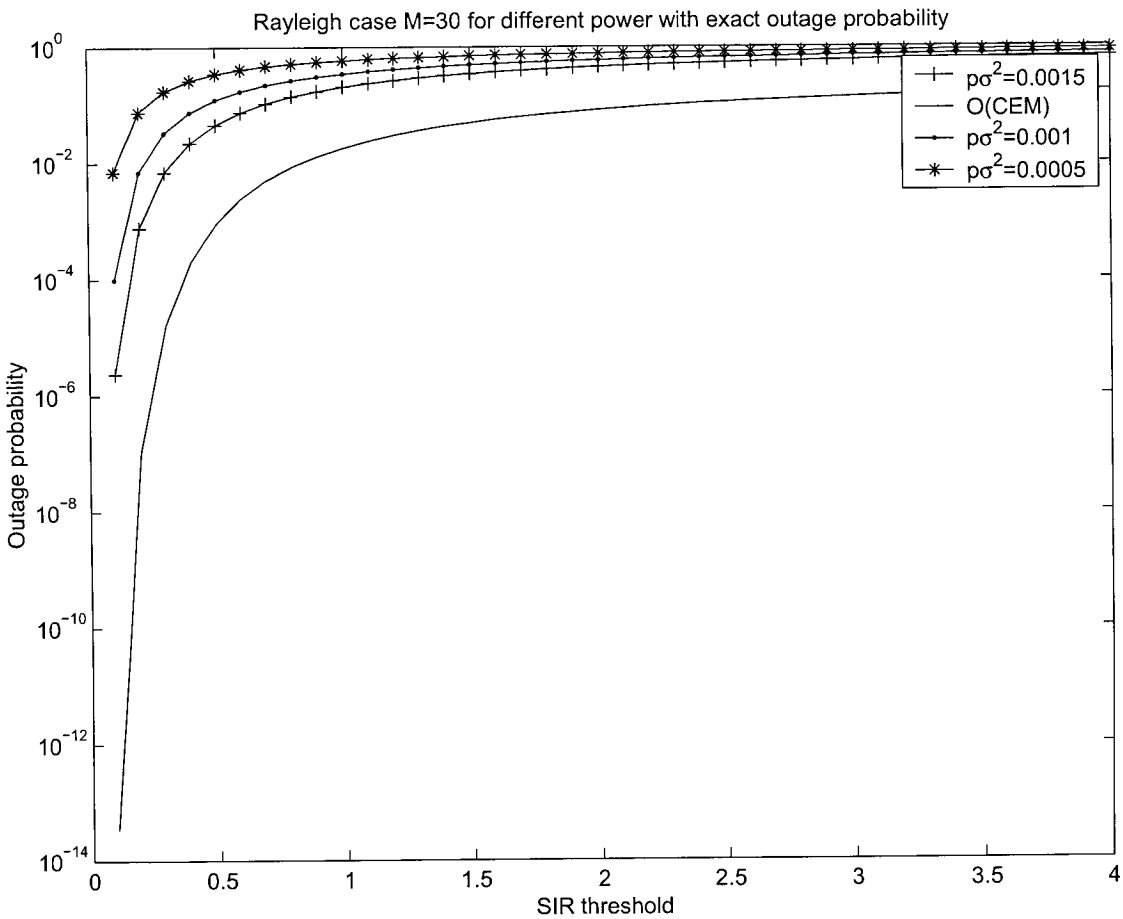

Figure 5.3.18: Comparing the upper bound with the exact outage probability related to $CEM = \Gamma/SIR^{th}$ corresponding to M=30 for Rayleigh case.

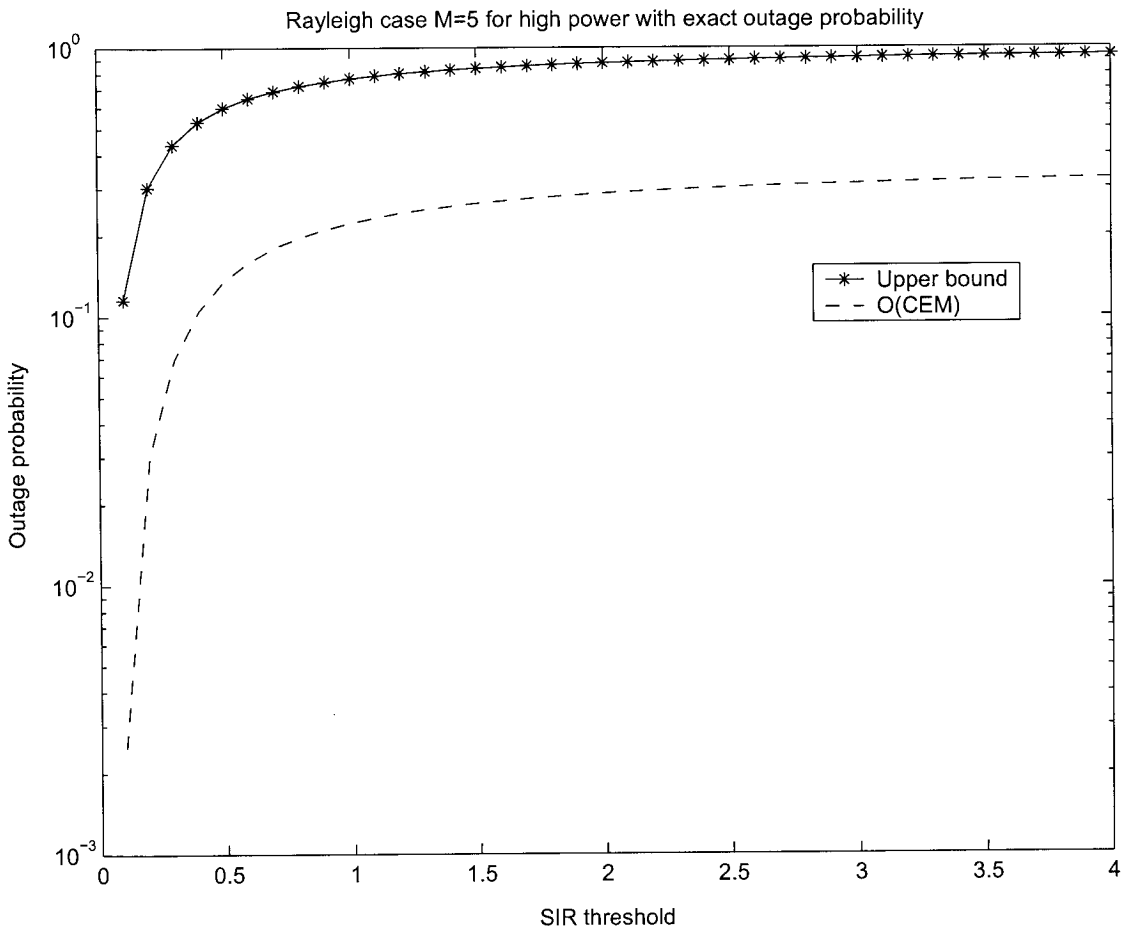

Figure 5.3.19: Comparing the upper bound with the exact outage probability related to $CEM = \Gamma/SIR^{th}$ corresponding to M=5 for Rayleigh case.

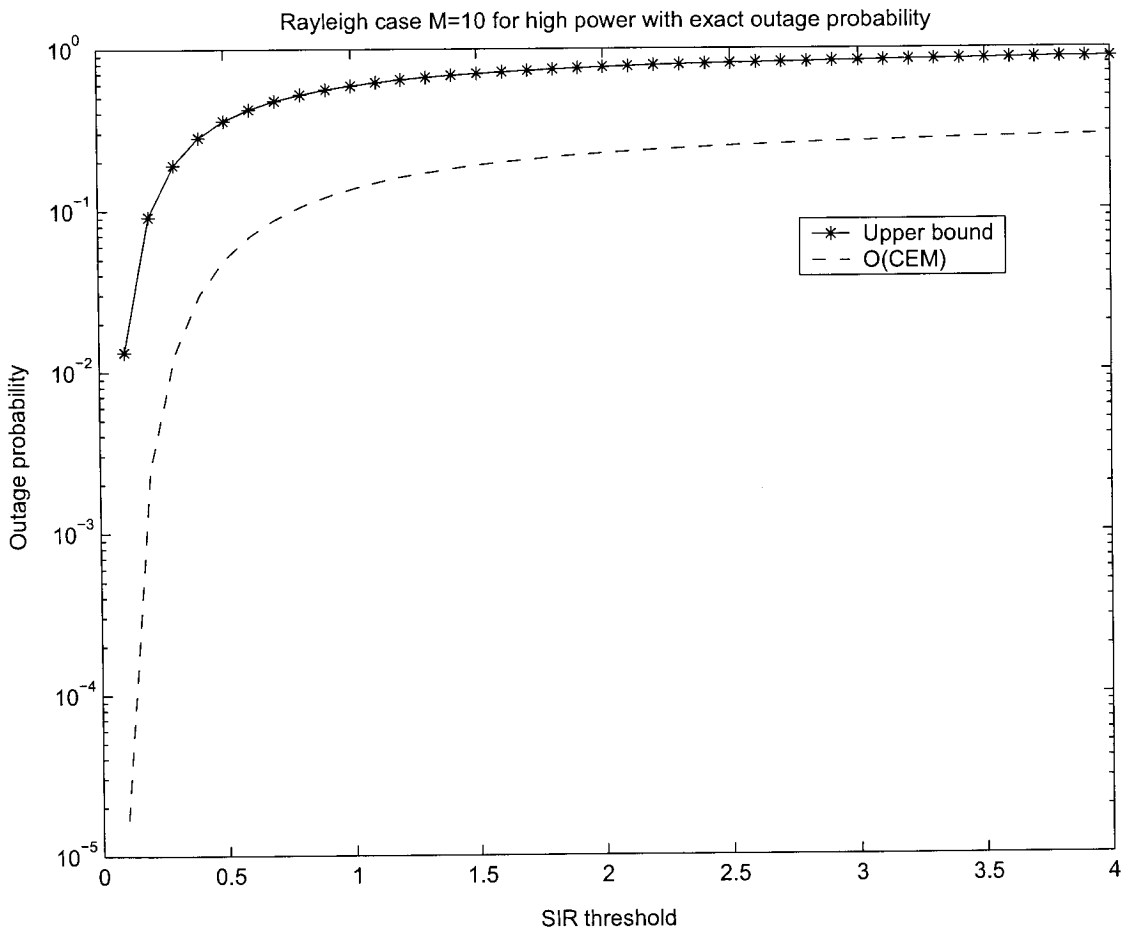

Figure 5.3.20: Comparing the upper bound with the exact outage probability related to $CEM = \Gamma/SIR^{th}$ corresponding to M=10 for Rayleigh case.

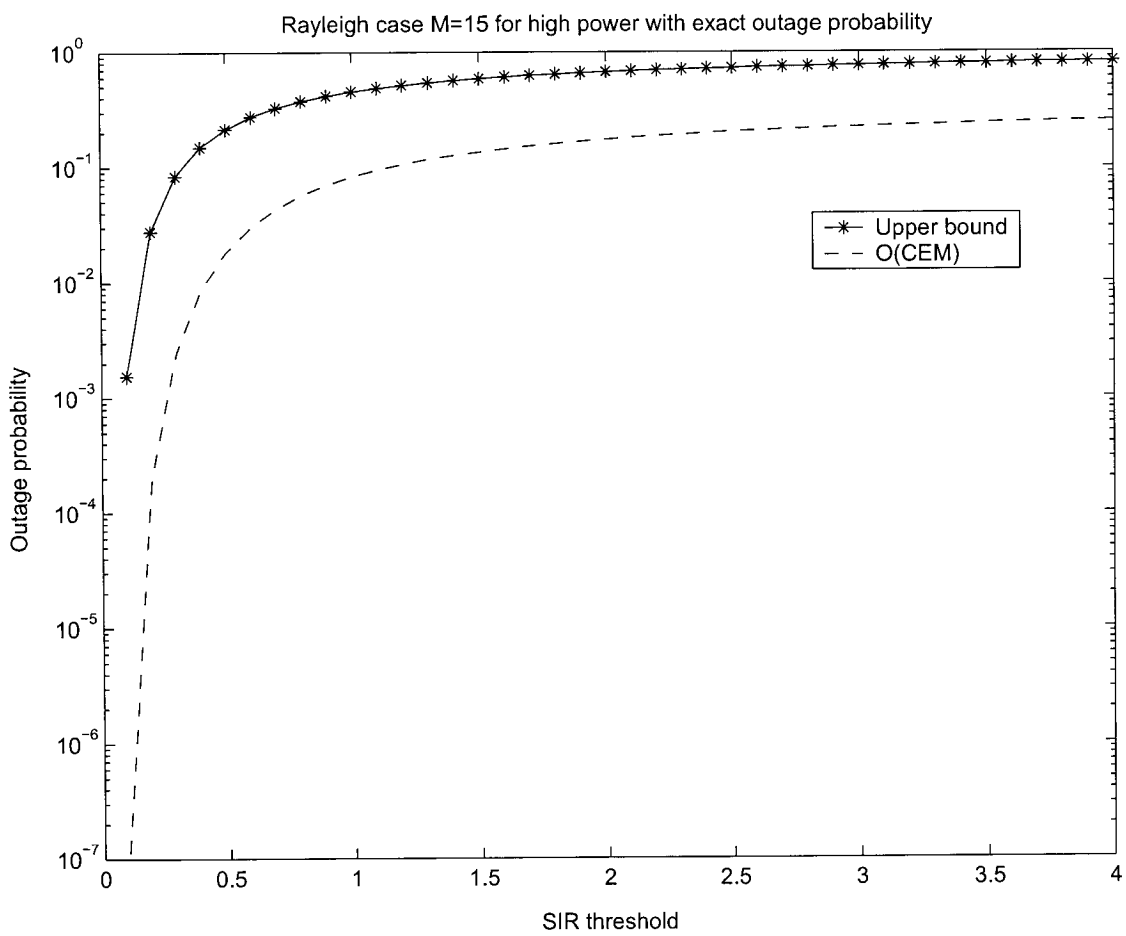

Figure 5.3.21: Comparing the upper bound with the exact outage probability related to $CEM = \Gamma/SIR^{th}$ corresponding to M=15 for Rayleigh case.

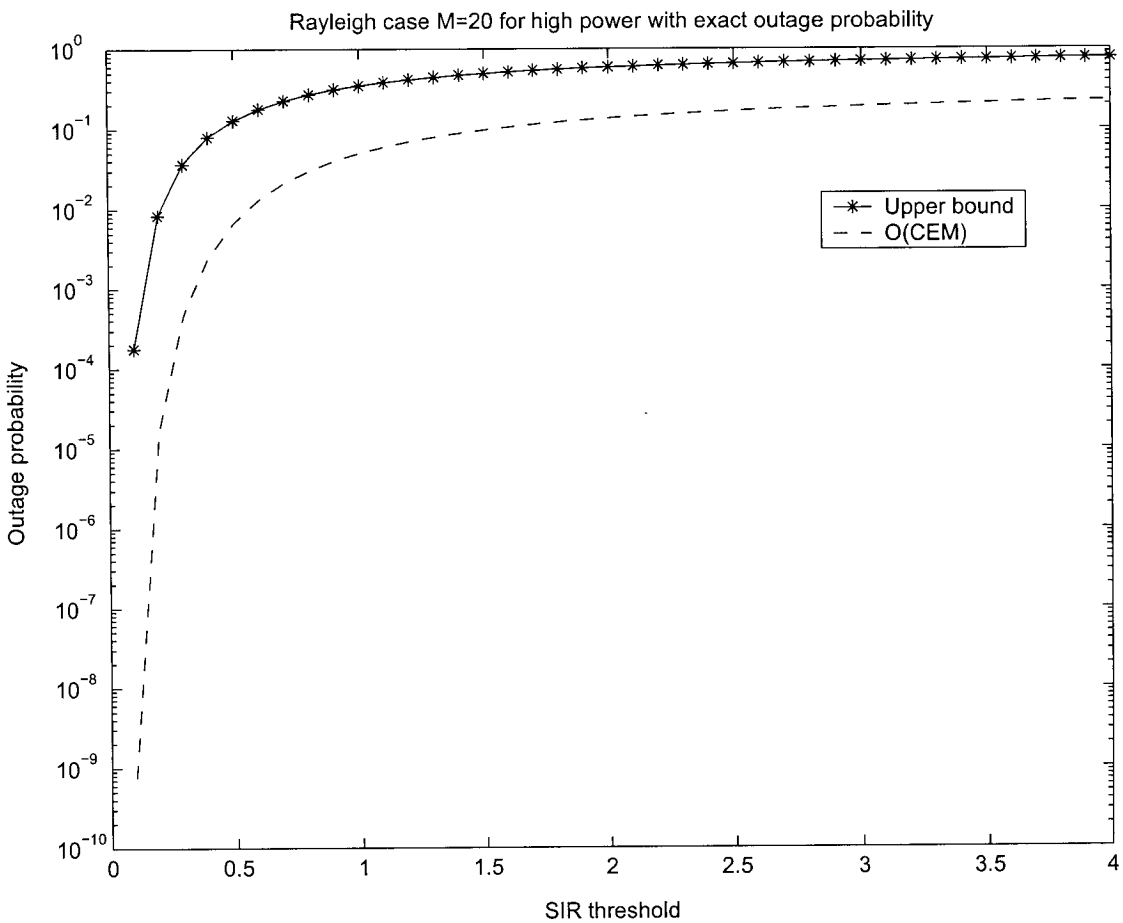

Figure 5.3.22: Comparing the upper bound with the exact outage probability related to $CEM = \Gamma/SIR^{th}$ corresponding to M=20 for Rayleigh case.

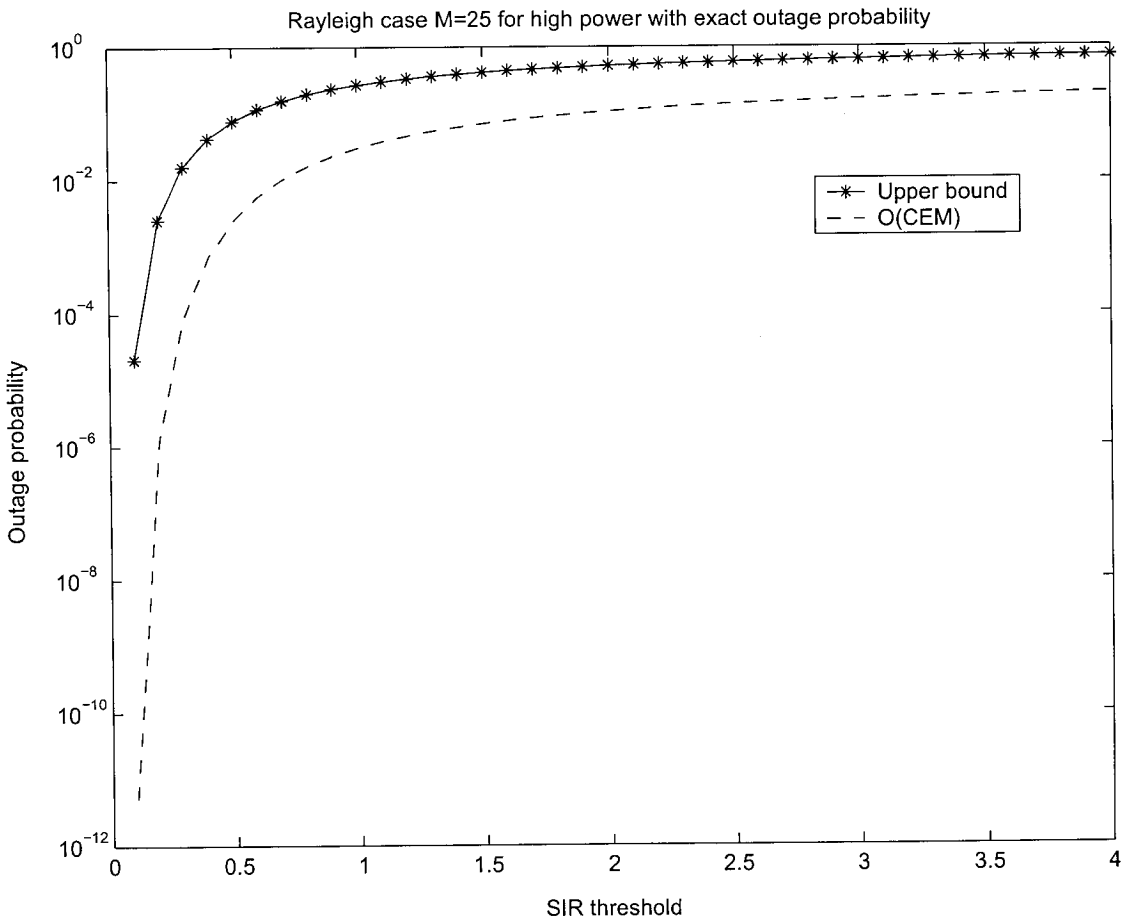

Figure 5.3.23: Comparing the upper bound with the exact outage probability related to $CEM = \Gamma/SIR^{th}$ corresponding to M=25 for Rayleigh case.

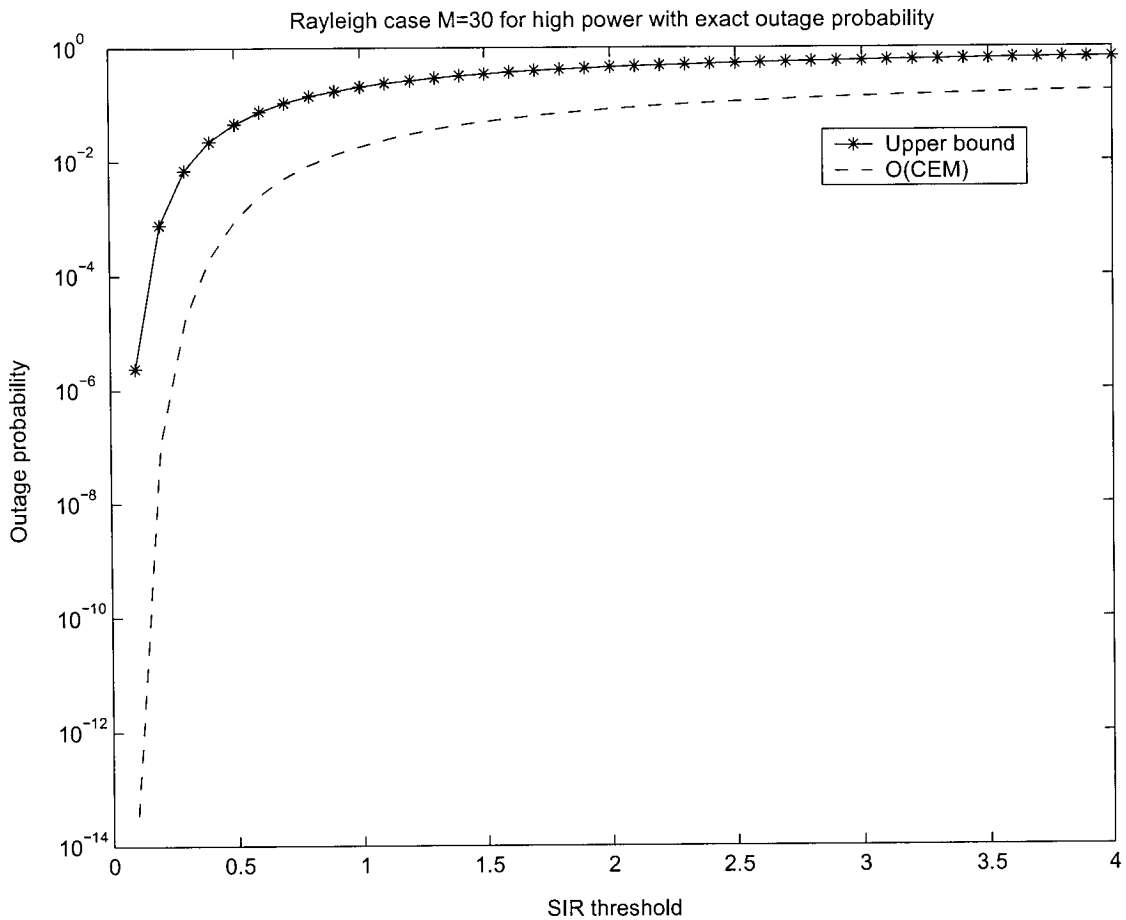

Figure 5.3.24: Comparing the upper bound with the exact outage probability related to $CEM = \Gamma/SIR^{th}$ corresponding to M=30 for Rayleigh case.

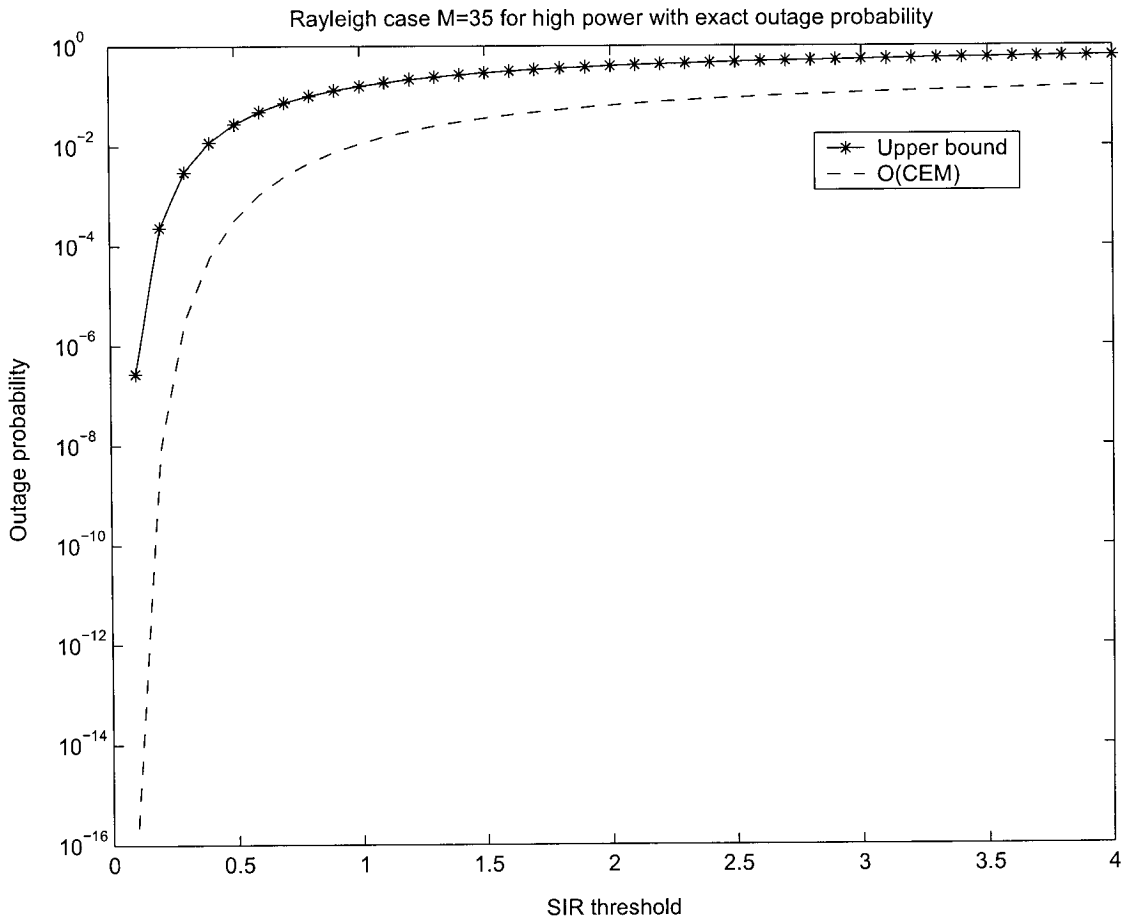

Figure 5.3.25: Comparing the upper bound with the exact outage probability related to $CEM = \Gamma/SIR^{th}$ corresponding to M=35 for Rayleigh case.

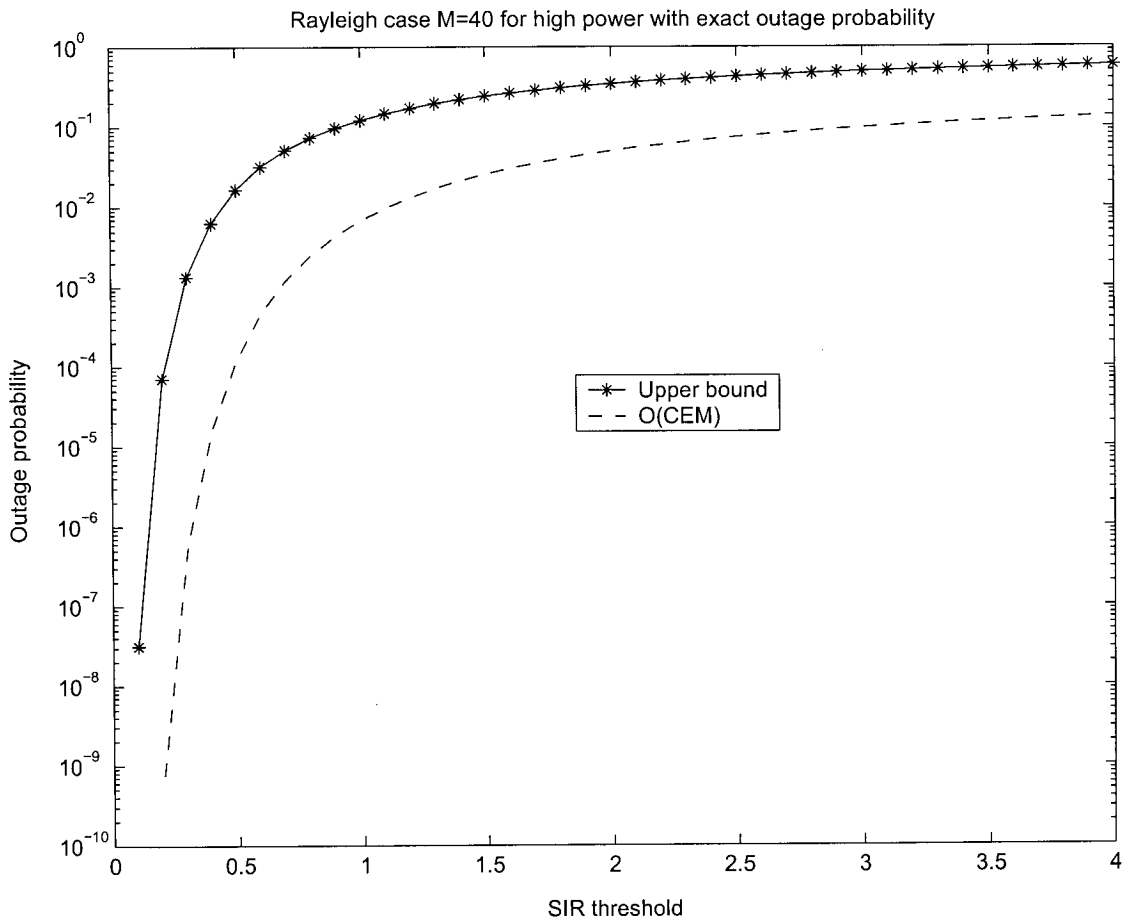

Figure 5.3.26: Comparing the upper bound with the exact outage probability related to $CEM = \Gamma/SIR^{th}$ corresponding to M=40 for Rayleigh case.

Chapter 6

Conclusion

In this thesis, we discuss the mobile systems consisting of M transmitters and M receivers, which are subject to motion and their power is described by SDE. The optimal power control problem is formulated and then the outage probability corresponding to a desired QoS requirements is computed using Moment Generating Function (MGF). Finally, we plot simulation figures with different values of parameters and compare them to give our research results.

6.1 Summary of Work

First, we introduce general concepts about wireless network systems, mainly the channel model concepts. For example, in Chapters 1 and 2, we introduce the small-scale fading and multipath propagation channels and the large-scale path-loss propagation channels. We also define some common terms, such as frequency reuse, interference, flat fading, frequency selective fading, fast fading, slow fading, reflection, diffraction, and scattering.

In Chapter 3, we focus on the power path loss and the signal attenuation varying with distance and time as random processes. There are various possible paths between transmitter and receiver. Traditional models do not take into consideration the relative motion

between the transmitter and the receiver. In reality, these properties exist and one way to model them is through stochastic processes. So we introduce the stochastic differential equations to estimate the dynamic power path loss for the space-time propagation environments. We also discuss the log-normal channel model for different situations related to varying time and changing observation locations. The models indicate that by using Stochastic Differential Equations (SDE), solutions can be retrieved and plotted.

In Chapter 4, we use iterative power control algorithms to reach an optimal power allocation. After that, using the Certainty Equivalent Margin (CEM), we calculate the exact outage probability expression for the Rayleigh case.

In Chapter 5, the probabilistic Quality of Service (QoS) measures are introduced to evaluate the performance of any control strategy. We provide tight outage probability bounds that relate to the probability of failure in achieving the desired QoS requirements by using the Moment Generating Function (MGF). We analyze three common channels, the Rayleigh channel, Rice channel, and Nakagami-m channel, respectively. We plot the figures for different parameters with different values. Simulation figures show that the measures of evaluating the outage probability bounds are simple and effective For Rayleigh case, the upper bounds are very close to the exact outage probability.

This thesis proposes that, for large scale systems such as large M transmitters and M receivers, we can determine the optimal power allocation and maximize the system capacity to reach the desired QoS requirements by using SDE and iterative power control algorithms. After the optimal transmission power is computed, the outage probability expression can be derived related to the channel gain and transmitter power by using MGF. Numerical results show that each user only needs to know its own channel gain and its own output to update

the transmitter power in order to maintain a desired Signal to Interference Ratio (SIR) and QoS requirement at the receiver.

6.2 Future Work

In future work, we will analyze the hand-off process, for example, when a mobile moves from one channel to another or from one base station to another. We will research how to transfer calls without outage between adjacent base stations.

Comparing the exact outage probability derived from Chapters 4 and the upper bound of Chernoff bound for Rayleigh case in Chapter 5, there still exists a variance. We need to evaluate how to improve the probabilistic measures.

Appendix A

A.1 Notations, Abbreviations and Acronyms

AWGN	Additive White Gaussian Noise
BS	Base Station
CCI	Co-Channel Interference
CDF	Cumulative Distribution Function
CDMA	Code Division Multiple Access
CEM	Certainty Equivalent Margin
ISI	InterSymbol Interference
LOS	Line-Of-Sight
MFC	Multipath Fading Channels
MGF	Moment Generating Function
MS	Mobile Station
MSC	Mobile Switching Center
PDF	Probability Distribution Function
PSTN	Public Switched Telephone Network
QoS	Quality of Service
Rx	Receiver
SDE	Stochastic Differential Equations
SIR	Signal to Interference Ratio

Tx	Transmitter
d	distance
t	time
τ	time delay
r	signal attenuation
PL	power path loss
Pr	received power
Pt	transmitter power
α	path loss exponent
S_{ij}	random signal attenuation
X_{ij}	random power path loss
p_i	ith transmitter power
$\bar{\gamma}_i$	ith receiver SIR
γ_i	$\gamma_i = \frac{\bar{\gamma}_i}{1+\bar{\gamma}_i}$
η_i	ith receiver noise
g_{ij}	channel gain
$I^n(p)$	failure in achieving QoS requirement
$P(.)$	probability
$E(.)$	excepted value of random variable
$f(.)$	density function of random variable
σ^2	variance of random variable
O	outage probability of Tx-Rx

$p(.)$	PDF of random variable
$F(.)$	CDF of random variable
$\psi(.)$	characteristic function of random variable
$\Phi(.)$	MGF of random variable
$\Psi(.)$	cumulant generating function of random variable
$\psi^*(.)$	Legendre transfer function of $\Psi(.)$

A.2 Derivations of Formulas

1. To show the probability expression in section 4.1.1.

Suppose $z_1, ..., z_n$ are independent exponential distributed random variables with means $E(z_i) = \frac{1}{\lambda_i}$. We know that:

$$\begin{aligned} Prob\Big(z_1 > \sum_{i=2}^{n} z_i\Big) &= \int_{t_2=0}^{\infty} ... \int_{t_n=0}^{\infty} Prob\Big(z_1 > \sum_{i=2}^{n} t_i\Big) \prod_{i=2}^{n} \lambda_i e^{-\lambda_i t_i} dt_2 ... dt_n \\ &= \int_{t_2=0}^{\infty} ... \int_{t_n=0}^{\infty} e^{-\lambda_1 (t_2 + ... + t_n)} \prod_{i=2}^{n} \lambda_i e^{-\lambda_i t_i} dt_2 ... dt_n \\ &= \prod_{i=2}^{n} \int_{t_i=0}^{\infty} \lambda_i e^{-(\lambda_1 + \lambda_i) t_i} dt_i \\ &= \prod_{i=2}^{n} \frac{\lambda_i}{\lambda_1 + \lambda_i}. \end{aligned} \tag{A.2.1}$$

Then,

$$Prob\Big(z_1 \leq \sum_{i=2}^{n} z_i\Big) = 1 - Prob\Big(z_1 > \sum_{i=2}^{n} z_i\Big) = 1 - \prod_{i=2}^{n} \frac{\lambda_i}{\lambda_1 + \lambda_i}. \tag{A.2.2}$$

2. To show $T(p)$ is standard, we need to verify the conditions in the definition.

(1) Positivity: for $I_i(p) > 0$, then it is also true for the minimizer filter. So $T_i(p) =$

$\min I_i(p) > 0$.

(2) Monotonicity: for $p > p'$, $I_i(p) > I_i(p')$, then $T_i(p) = \min I_i(p) > \min I_i(p') = T_i(p')$.

(3) Scalability: for $\alpha > 1$, we have $\alpha I_i(p) > I_i(\alpha p)$, so $\alpha T_i(p) = \min \alpha I_i(p) > \min I_i(\alpha p) = T_i(\alpha p)$.

3. To show that the standard normal density function has a moment generating function $\Phi(\theta) = e^{\frac{\theta^2}{2}}$.

Let X be the standard normal random variable with $N(0,1)$, so the density function of X is:

$$f(x) = \frac{1}{\sqrt{2\pi}} e^{-\frac{x^2}{2}}. \tag{A.2.3}$$

So we have:

$$\begin{aligned}
\Phi(\theta) = E[e^{\theta X}] &= \int_{-\infty}^{\infty} e^{\theta x} f(x) dx \\
&= \int_{-\infty}^{\infty} e^{\theta x} \frac{1}{\sqrt{2\pi}} e^{-\frac{x^2}{2}} dx \\
&= \int_{-\infty}^{\infty} \frac{1}{\sqrt{2\pi}} e^{-\frac{x^2}{2} + \theta x} dx \\
&= \int_{-\infty}^{\infty} \frac{1}{\sqrt{2\pi}} e^{-\frac{1}{2}(x-\theta)^2 + \frac{\theta^2}{2}} dx \\
&= e^{\frac{\theta^2}{2}} \int_{-\infty}^{\infty} \frac{1}{\sqrt{2\pi}} e^{-\frac{1}{2}(x-\theta)^2} dx \\
&= e^{\frac{\theta^2}{2}},
\end{aligned} \tag{A.2.4}$$

where for any density function $f(x)$, $\int_{-\infty}^{\infty} \frac{1}{\sqrt{2\pi}} e^{-\frac{1}{2}(x-\theta)^2} dx = 1$.

4. To show if $S = X + Y$, where X and Y are independent random variables, the S has the moment generating function $\Phi_S(\theta) = \Phi_X(\theta)\Phi_Y(\theta)$. By the definition of MGF,

$$\begin{aligned}
\Phi_S(\theta) = E[e^{\theta S}] &= E[e^{\theta(X+Y)}] \\
&= E[e^{\theta X} e^{\theta Y}]
\end{aligned}$$

$$= E[e^{\theta X}]E[e^{\theta Y}]$$
$$= \Phi_X(\theta)\Phi_Y(\theta). \quad \text{(A.2.5)}$$

Thus, for independent random variables, the moment generating function of the sum is simply the product of the moment generating functions of each individual term:

$$\Phi_{X+Y}(\theta) = \Phi_X(\theta)\Phi_Y(\theta). \quad \text{(A.2.6)}$$

A similar formula holds true for summation of more than two independent random variables.

5. To derive the inequality of (4.1.9).

From the right-hand inequality of (4.1.7),

$$e^{\frac{\bar{\gamma}_i\eta_i}{G_{ii}p_i}} \prod_{j\neq i}^{n} (1 + \bar{\gamma}_i \frac{G_{ij}p_j}{G_{ii}p_i}) \leq e^{\frac{\bar{\gamma}_i\eta_i}{G_{ii}p_i} + \sum_{j\neq i}^{n} \bar{\gamma}_i \frac{G_{ij}p_j}{G_{ii}p_i}}, \quad \text{(A.2.7)}$$

$$1 - e^{-\frac{\bar{\gamma}_i\eta_i}{G_{ii}p_i}} \prod_{j\neq i}^{n} \frac{1}{(1 + \bar{\gamma}_i \frac{G_{ij}p_j}{G_{ii}p_i})} \leq 1 - \frac{1}{e^{\frac{\bar{\gamma}_i\eta_i}{G_{ii}p_i} + \sum_{j\neq i}^{n} \bar{\gamma}_i \frac{G_{ij}p_j}{G_{ii}p_i}}}. \quad \text{(A.2.8)}$$

Using the definition of CEM^{η} in (4.1.6), in the right-hand of (A.2.8), we have:

$$\frac{1}{e^{\frac{\bar{\gamma}_i\eta_i}{G_{ii}p_i} + \sum_{j\neq i}^{n} \bar{\gamma}_i \frac{G_{ij}p_j}{G_{ii}p_i}}} = \frac{1}{e^{\frac{\bar{\gamma}_i}{G_{ii}p_i}(\eta_i + \sum_{j\neq i}^{n} G_{ij}p_j)}}$$
$$= \frac{1}{e^{\frac{1}{CEM^{\eta}}}} = e^{-\frac{1}{CEM^{\eta}}}. \quad \text{(A.2.9)}$$

So, the left-hand of (A.2.8) is O, the right-hand of (A.2.8) is $1 - e^{\frac{-1}{CEM^{\eta}}}$. Then (A.2.8) becomes the same as (4.1.9).

6. To derive the inequality of (4.1.10).

From the left-hand inequality of (4.1.7),

$$1 + \frac{\bar{\gamma}_i\eta_i}{G_{ii}p_i} + \sum_{j\neq i}^{n} \bar{\gamma}_i \frac{G_{ij}p_j}{G_{ii}p_i} \leq e^{\frac{\bar{\gamma}_i\eta_i}{G_{ii}p_i}} \prod_{j\neq i}^{n} (1 + \bar{\gamma}_i \frac{G_{ij}p_j}{G_{ii}p_i}). \quad \text{(A.2.10)}$$

Using the definition of CEM^{η} in (4.1.6),

$$\begin{aligned} 1-\frac{1}{1+\frac{1}{CEM^{\eta}}} &\leq 1-e^{-\frac{\bar{\gamma}_i\eta_i}{G_{ii}p_i}}\prod_{j\neq i}^{n}\frac{1}{(1+\bar{\gamma}_i\frac{G_{ij}p_j}{G_{ii}p_i})}, \\ 1+\frac{1}{CEM^{\eta}} &\leq 1-e^{-\frac{\bar{\gamma}_i\eta_i}{G_{ii}p_i}}\prod_{j\neq i}^{n}\frac{1}{(1+\bar{\gamma}_i\frac{G_{ij}p_j}{G_{ii}p_i})}. \end{aligned} \tag{A.2.11}$$

So, the right-hand of (A.2.11) is O. Then (A.2.11) becomes the same as (4.1.10).

Appendix B

Programming Code

B.1 Code 1 for the power path loss and attenuation as a function of distance.

```
%By: Shili Lu
%This program plots the power path loss and attenuation for different reference distance d0
%and varying observation location distance dn according to equation (3.2.27) on page 32.
%How to run it:
%Access MATLAB Command Window; enter "FigC3S2(2,100,47.2)",
%for example, d0=2m,dn=100m,X0=47.2dB.
%For our study, we have 6 sets; they are (2,100,47.2), (2,500,47.2), (2,1000,47.2),(10,100,64.2),
%(10,500,64.2), and (10,1000,64.2) for two initial reference d0 and X0, changing with three
%different observation distance dn, corresponding to Figures 3.2.2 to 3.2.7.
function FigC3S2(d0,dn,Xzero)
%rand('state',j);For integer j, resets the random generator to its j-th state.
randn('state',50); %best choice of random state.
alpha=2.5; %path loss exponent, varying from 2 to 5
delta=25000; %constant parameter
vc=3e+8; %the speed of light(m/s)
%Xzero=47.2; %in dB for d0=2
```

```
%Xzero=64.2; %in dB for d0=10
t0=d0/vc; %initial time point
T=dn/vc; %time interval
N=2^10;dt=(T-t0)/(N-1); %time step size.
dW=sqrt(dt)*randn(1,N);
W=cumsum(dW); %Gaussion noise
tau=t0:dt:T;dist=vc*tau;
Xtrue=Xzero-10*alpha*log10(d0)+10*alpha*log10(dist)+delta*(W-W(1));
%true power path loss X.
Xmean=Xzero-10*alpha*log10(d0)+10*alpha*log10(dist);
%the mean of the power path loss X.
c=log(10)/10;k=-c/2;
Szero=exp(k*Xzero);
Strue=exp(k*Xtrue);
Smean=exp(k*Xmean);
Struelog=10*log10(Strue);
Smeanlog=10*log10(Smean);
%plot power path loss X and attenuation S within one figure.
subplot(2,1,1); semilogx(dist,Xtrue,dist,Xmean);
ylabel('X(t,\tau) (dB)')
title('X(t,\tau) as a function of \tau = d/v_c for fixed time t')
axis on;
subplot(2,1,2); semilogx(dist,Struelog,dist,Smeanlog);
xlabel('distance (m)')
ylabel('10*logS(t,\tau) (dB)')
title('S(t,\tau) as a function of \tau = d/v_c for fixed time t')
```

%**********

B.2 Code 2 for the power path loss and attenuation as a function of time.

%This program plots the power path loss and attenuation for different

%reference distances d0 and given observation distances dn with varying times, according to equation (3.3.37) on page 38.

%How to run it:

%Access MATLAB Command Window; enter "FigC3S31(47.2,450,93.6)",

%for example, X0=47.2dB,beta=450, gamma=93.6dB.

%For our study, we have 4 sets; they are (47.2,450,93.6),(47.2,1450,93.6),(64.2,450,87.4), and

%(64.2,1450,87.4).

%for two initial reference d0,X0, and given observation distance dn, changing with time,

%corresponding to Figures 3.3.8 to 3.3.11.

function FigC3S31(Xzero,delta,gamma)

%rand('state',j);For integer j, resets the random generator to its j-th state.

randn('state',51) %best choice of state

vc=3e+8;beta=204000;

%Xzero=47.2; %d0=2m;

%Xzero=64.2; %d0=10m;

%delta=450; %or delta=1450; %parameter

%gamma=93.613; %for x0=47.2 dn=100m %mean value of Xtrue related to Code 1.

%gamma=87.402; %for x0=64.2 dn=100m

T=.0003;N=2^{10};dt=T/N;t0=dt;

dW=sqrt(dt)*randn(1,N);

```
W(1)=0; W=cumsum(dW);
time=dt:dt:T;
for i=1:N
x1(i)=exp(-beta*(i*dt-dt));
x2(i)=exp(beta*(i*dt-dt));
Xtrue=x1(i)*(Xzero+(x2(i)-1)*gamma+delta*x2(i)*(W-W(1)));
Xmean=x1(i)*(Xzero+(x2(i)-1)*gamma);
end
c=log(10)/10;k=-c/2;
St0=exp(k*Xzero);
Smean=exp(k*Xmean);
Strue=exp(k*Xtrue);
Struelog=10*log10(Strue);
Smeanlog=10*log10(Smean);
%plot power loss X and attenuation S within one figure for variable time .
subplot(2,1,1);
plot([dt:dt:T],Xtrue,[dt:dt:T],Xmean);
ylabel('X(t,τ) (dB)')
title('X(t,τ) as a function of time t for fixed distance dn=100m')
axis on;
subplot(2,1,2);
plot([dt:dt:T],Struelog,[dt:dt:T],Smeanlog);
xlabel('time (s)')
ylabel('10*logS(t,τ) (dB)')
title('S(t,τ) as a function of time t for fixed distance dn=100m')
```

%**********

B.3 Code 3 for the power path loss as a function of time and parameter β.

%This program plots the power path loss, its expected value, and parameter γ(t) with

%varying time t for lower and higher parameter β according to equation (3.3.37) on page 38.

%How to run it:

%Access MATLAB Command Window; enter "FigC3S32(47.2,1450,205000)",

%for example, X0=47.2dB,beta=450, beta=205000.

%For our study, we have 2 sets; they are (64.2, 450, 105000),(47.2, 1450, 205000),

%for two initial reference d0,X0, and given observation distance dn,

%changing with time for different parameter δ and β,

%corresponding to Figures 3.3.12 and 3.3.13.

```
function FigC3S32(Xzero,delta,beta)
%rand('state',j);For integer j, resets the random generator to its j-th state.
randn('state',50) %best choice of random state
T=.0003;N=2^10;dt=T/N;
dW=sqrt(dt)*randn(1,N);
W=cumsum(dW);
%X0=64.2;delta=450;beta=105000; %X0=47.2;delta=1450;beta=205000; for i=1:N
gamma(i)=Xzero*(1+0.15*exp(-2*i*dt/T)*sin(10*pi*i*dt/T));
EX(i)=exp(-beta*i*dt)*(Xzero+gamma(i)*(exp(beta*i*dt)-1));
Xrl(i)=exp(-beta*i*dt)*(Xzero+gamma(i)*(exp(beta*i*dt)-1)+delta*exp(beta*i*dt)*(W(i)-
W(1)));
end
```

plot([dt:dt:T],Xrl),hold on

plot([dt:dt:T],gamma,'–'),hold on

plot([dt:dt:T],EX)

xlabel('time(s)')

ylabel('X(t,τ) (dB)')

title('Power loss X(t,τ) with t-varying $\gamma(t)$ as a function of time t')

%**********

B.4 Code 4 for the power path loss as a function of time and parameter β in 3D plot.

%This program plots the power path loss, its expected value, and parameter $\gamma(t)$ with

%varying time t for lower and higher parameter β in 3D plot, according to equation (3.3.37)

on page 38.

%How to run it:

%Access MATLAB Command Window; enter "FigC3S4(47.2,1340,205000,1)",

%for example, X0=47.2dB,beta=1340, beta=205000,n=1.

%For our study, we have 5 sets; they are

%Xzero=123.5;delta=420;beta=25000;n=5;

%Xzero=103.5;delta=600;beta=35000;n=4;

%Xzero=93.5;delta=720;beta=55000;n=3;

%Xzero=63.5;delta=1080;beta=105000;n=2;

%Xzero=47.2;delta=1340;beta=205000;n=1.

%These figures are plotted together corresponding to Figure 3.4.14.

function FigC3S4(Xzero,delta,beta,n)

%rand('state',j);For integer j, resets the random generator to its j-th state.

```
randn('state',51) %best choice of random state.
T=.0003;N=2^10;dt=T/N;
dW=sqrt(dt)*randn(1,N);
W=cumsum(dW);
dd=4*ones(1,1024); %dd=4m;
for i=1:N
gamma(i)=Xzero*(1+0.15*exp(-2*i*dt/T)*sin(10*pi*i*dt/T));
EX(i)=exp(-beta*i*dt)*(Xzero+gamma(i)*(exp(beta*i*dt)-1));
Xrl(i)=exp(-beta*i*dt)*(Xzero+gamma(i)*(exp(beta*i*dt)-1)+delta*exp(beta*i*dt)*(W(i)-
W(1)));
end
plot3([dt:dt:T],n*dd,Xrl),hold on
plot3([dt:dt:T],n*dd,gamma),hold on
grid on
xlabel('time (s)')
ylabel('distance (m)')
zlabel('X(t,τ) (dB)')
title('Power path loss X(t,τ) with t-varying γ(t) as a function of time t and distance d')

%*************************************************************************
```

B.5 Code 5 for exact outage probability as a function of CEM.

```
%This program plots lower and upper bounds of exact outage probability as a function of
CEM using formula (4.1.11) corresponding to Figure 4.1.1.
for i=1:30
```

```
CEM(i)=i;
lowerb(i)=1/(1+CEM(i));
upperb(i)=1-exp(-1/CEM(i));
end
plot(CEM,lowerb),hold on
plot(CEM,upperb,'-r'),hold on
xlabel('Certainty-Equivalent Margin(CEM)')
ylabel('Outage probability')
title('Lower and upper bound of outage probability with CEM')

%*****************************************************************************
```

B.6 Code 6 for error of exact outage probability as a function of CEM.

```
%This program plots the error of lower and upper bounds of outage probability as a function
of CEM using formula (4.1.11) corresponding to Figure 4.1.2.
for i=1:30
CEM(i)=i;
lowerb(i)=1/(1+CEM(i));
upperb(i)=1-exp(-1/CEM(i));
error(i)=(upperb(i)-lowerb(i));
end
%For example when CEM=3, lowerb=25%, upperb=28.35%, error 3.35%.
plot(error*100)
xlabel('Certainty-Equivalent Margin(CEM)')
ylabel('(Upperb-Lowerb)*100 (%)')
```

```
title('Error of upper and lower bound of outage probability with CEM')

%*************************************************************************
```

B.7 Code 7 for optimal power during a very short time interval.

```
%This program plots straight lines for transmitter power during a very short time interval
%using the iteration equation (4.3.21) and corresponding to Figure 4.2.3 to Figure 4.2.8.
function FigC4S2(i)
%optimal transmitter power for each user at six time points
%time point t1 transmitter power i=1 to 6.
pt1=[1.1901e-014;1.3441e-014;1.0526e-014;7.6187e-015 ;6.1009e-015 ;6.1866e-015];
%time point t2 trans power
pt2=[1.1053e-014 ;1.2879e-014 ;1.108e-014 ;7.3566e-015 ;6.5904e-015 ;6.1918e-015];
%time point t3 trans power
pt3=[1.1206e-014 ;1.3088e-014 ;1.0526e-014 ;6.9228e-015 ;6.4914e-015 ;5.9807e-015];
%time point t4 trans power
pt4=[1.2108e-014 ;1.4849e-014 ;1.1657e-014 ;8.0665e-015 ;6.4964e-015 ;6.6298e-015];
%time point t5 trans power
pt5=[1.2566e-014 ;1.6058e-014 ;1.2611e-014 ;8e-015 ;6.9829e-015 ;7.4556e-015];
%time point t6 trans power
pt6=[1.3507e-014 ;1.7269e-014 ;1.1715e-014 ;7.613e-015 ;6.8904e-015 ;7.1361e-015];
p=[pt1,pt2,pt3,pt4,pt5,pt6];


for j=1:6
for x=j:0.01:j+1
```

```
y=p(i,j); %plot transmitter i following 6 time delay points
plot(x,y), hold on
end
end
xlabel('time(s) *10^-6')
ylabel('power p (dB)')
title('Optimal transmitter power')% for transmitter i in a very short time interval')
grid on
%*************************************************************************
```

B.8 Code 8 for the total transmission power of all users versus iteration index.

```
%This program plots the total transmission power of all users versus iteration index.
%Optimal transmitter power for each user i=1 to 6 at six time points are the same as Code 7.

sir=[3,4,5,6,7,8]; % given threshold SIR
outprob=[.1,.09,.08,.07,.06,.05]; %supposed maximum outage probability
gain=[ 1,.0010,.0005,.0008,.0010,.0009
.0010, 1,.0007,.0006,.0009,.0010
.0005,.0007, 1,.0008,.0009,.0006
.0008,.0006,.0008, 1,.0010,.0009
.0010,.0009,.0009,.0010, 1,.0009
.0009,.0010,.0006,.0009,.0009, 1]; % channel gain

eta1=ones(1,6)*1e-13; %noise power
eta2=[1,1.4,1.7,2.1,2.3,2.7]*1e-13;
```

```
powitera1=eta1;%initial power equals to noise power
powitera2=eta2;

for k=1:20
for i=1:6
for j=1:6
powlg(i,j)=log10(1+sir(i)*(gain(i,j)/gain(i,i))*(powitera(j)/powitera(i)));
end
end

notnpowlg=powlg-diag(diag(powlg));
notnpowlgSM=sum(notnpowlg,2)';

for i=1:6
pownext1(i)=[sir(i)*eta1(i)/gain(i,i)+powitera1(i)*notnpowlgSM(i)]/log10(1/(1-outprob(i)));
pownext2(i)=[sir(i)*eta2(i)/gain(i,i)+powitera2(i)*notnpowlgSM(i)]/log10(1/(1-outprob(i)));
end
powitera1=pownext1;
powsumpoint1(k)=sum(pownext1);

powitera2=pownext2;
powsumpoint2(k)=sum(pownext2);
end

plot(powsumpoint1,'r-.*'), hold on %assume the same noise.
plot(powsumpoint2), hold on %assume different noise for each receiver.
```

xlabel('Number of Iterations')

ylabel('Total Transmit Power')

title('Total Transmit Power of all users versus power control iteration index.')

%**********

B.9 Code 9 for the Chebyshev bound.

%This program plots the Chebyshev bound in Figure 5.1.1.

function FigC5S11(delta) %delta¿=3

for i=1:600

%delta=3;%=4;5;

dy=.005;

hz=dy:dy:3;

pcheb(i)=$(i * dy/delta)^2$;

end

plot(hz,pcheb), hold on

plot(-hz,pcheb), hold on

xlabel('Parameter δ')

ylabel('Probability bound')

title('Chebyshev bound $p(Y) \leq (Y/\delta)^{2}$')

%**********

B.10 Code 10 for the Chernoff bound.

%This program plots the Chernoff bound in Figure 5.1.2.

function FigC5S12(delta) %*delta* >= 3

for y=1:600

nu=0.5;

%delta=3;%=4;5;

dy=.005;

hz=dy:dy:3;

pchern(y)=exp(nu*(y*dy-delta));

end

plot(hz,pchern), hold on

xlabel('Parameter δ')

ylabel('Probability bound')

title('Chernoff bound $p(Y) \leq E(e^{\nu(Y-\delta)})$')

%**********

B.11 Code 11 for the Chi-square distribution.

%This program plots the Chi-square distribution in Figure 5.2.3.

for y=1:1400

dy=.005;

hz=dy:dy:7;

pc1(y)=exp(-y*dy/2)/sqrt(2*pi*y*dy);%n=1

pc2(y)=0.5*exp(-y*dy/2);%n=2

pc4(y)=y*dy*exp(-y*dy/2)/4;%n=4

pc8(y)=$(y * dy)^3 * exp(-y * dy/2)/(16 * 6)$;%n=8

end

plot(hz,pc1),axis([0 7 0 0.5]), hold on

plot(hz,pc2), hold on

plot(hz,pc4), hold on

plot(hz,pc8), hold on

xlabel('Random variable')

ylabel('PDF')

title('Chi-square distribution with different degrees of freedom')

%**********

B.12 Code 12 for the Gamma distribution.

%This program plots the Gamma distribution in Figure 5.2.4.

for y=1:600

dy=.005;

hz=dy:dy:3;

pg12(y)=$2 * exp(-0.5 * (y * dy)^2)/sqrt(2 * pi * y * dy)$;%m=1/2

pg34(y)=$(2/1.15) * (0.75)^0.75 * sqrt(y * dy) * exp(-0.75 * (y * dy)^2)$;%m=3/4

pg1(y)=$2 * y * dy * exp(-(y * dy)^2)$;%m=1

pg32(y)=$4 * (y * dy)^2 * exp(-1.5 * (y * dy)^2)/sqrt(8 * pi/27)$;%m=3/2

pg2(y)=$8 * (y * dy)^3 * exp(-2 * (y * dy)^2)$;%m=2

pg3(y)=$27 * (y * dy)^5 * exp(-3 * (y * dy)^2)$;%m=3

end

plot(hz,pg12),axis([0 3 0 1.5]), hold on

plot(hz,pg34), hold on

plot(hz,pg1), hold on

plot(hz,pg32), hold on

plot(hz,pg2), hold on

plot(hz,pg3), hold on

xlabel('Random variable')

ylabel('PDF')

title('Gamma distribution with different parameters m')

%**********

B.13 Code 13 for the Chernoff bound versus SIR with the Rayleigh case.

%This program plots the outage probability with the Chernoff bound versus SIR for the Rayleigh case with fixed M=3 as in Figure 5.3.5.

s=45; sgm=0.001;ps1=0.05;%0.15,0.1,0.05

ps2=0.001;ps3=0.001;sir=0.1:0.1:4;Rsir=max(sir);M=3;

for i=1:40

$r1(i) = sir(i)/(sir(i)+1);$

$alp(i) = s*sgm + 2*ps1*(1-1/r1(i))/(1-2*ps1*(1-1/r1(i))*s) + 2*ps2/(1-2*$

$ps2*s) + 2*ps3/(1-2*ps3*s);$

$prob3(i) = exp(s3^2*sgm^2/2 - log(1-2*ps1*(1-1/r1(i))*s3) - log(1-2*ps2*s3) -$

$log(1-2*ps3*s3));$

end

plot(sir,prob3,'r*-'),axis([0 4 0 0.8]); hold on

xlabel('SIR threshold')

ylabel('Outage probability')

title('Rayleigh case (M=3)')

%**********

B.14 Code 14 for the Chernoff bound versus SIR with the Rice case.

%This program plots the outage probability with the Chernoff bound versus SIR for the Rice case with fixed M=3 as in Figure 5.3.6 and 5.3.7.

s=33;sgm=0.001;p1=0.001;p2=0.001;p3=0.001;ps2=0.00001;ps3=0.00001;

s3=s;m=0.5;ps1=0.05;%0.01,0.02,0.05

sir=0.1:0.1:4;Rsir=max(sir);M=3;

for i=1:40

$r1(i) = sir(i)/(sir(i)+1);$

$alp1(i) = s*sgm + 2*ps1*(1-1/r1(i))/(1-2*ps1*(1-1/r1(i))*s) + 2*ps2/(1-2*ps2*s) + 2*ps3/(1-2*ps3*s);$

$alp2(i) = m*ps1*(1-1/r1(i))/(1-2*ps1*(1-1/r1(i))*s)^2 + m*ps2/(1-2*ps2*s)^2 + m*ps3/(1-2*ps3*s)^2;$

$alp(i) = alp1(i) + alp2(i);$

$logsum21(i) = m*s*p1*(1-1/r1(i))/(1-2*ps1*(1-1/r1(i))*s) + m*s*p2/(1-2*ps2*s) + m*s*p3/(1-2*ps3*s);$

$logsum22(i) = -log(1-2*ps1*(1-1/r1(i))*s) - log(1-2*ps2*s) - log(1-2*ps3*s);$

$prob2(i) = exp(-s*alp(i) + s^2*sgm/2 + logsum21(i) + logsum22(i));$

$logsum31(i) = m*s3*p1*(1-1/r1(i))/(1-2*ps1*(1-1/r1(i))*s3) + m*s*p2/(1-2*ps2*s3) + m*s*p3/(1-2*ps3*s3);$

$logsum32(i) = -log(1-2*ps1*(1-1/r1(i))*s3) - log(1-2*ps2*s3) - log(1-2*ps3*s3);$

$prob3(i) = exp(s3^2*sgm^2/2 + logsum31(i) + logsum32(i));$

end

plot(sir,prob3,'b-'), hold on

xlabel('SIR threshold')

ylabel('Outage probability')

title('Rice case(M=3,m=1 with different power)')

%**********

B.15 Code 15 for the Chernoff bound versus SIR with the Nakagami-m case.

%This program plots the outage probability with the Chernoff bound versus SIR for the Nakagami case with fixed M=3 as in Figure 5.3.9 and 5.3.10.

sgm=0.001;p1=0.001;p2=0.001;p3=0.001;ps2=0.00001;ps3=0.00001;

s=37;m=1.5;ps1=.003;%0.001;0.002;0.003

s=33;m=1;ps1=.03;%0.01;0.02;0.03

s=23;m=0.5;ps1=0.3;%0.1 0.2 0.3

lam=1/(2*m);sir=0.1:0.1:4;Rsir=max(sir);M=3;

for i=1:40

$r1(i) = sir(i)/(sir(i)+1);$

$alp(i) = s*sgm + m*ps1*(1-1/r1(i))/(lam - ps1*(1-1/r1(i))*s) + m*ps2/(lam - ps2*s) + m*ps3/(lam - ps3*s);$

$logsum(i) = -m*log(1-ps1*(1-1/r1(i))*s/lam) - m*log(1-ps2*s/lam) - log(1-ps3*s/lam);$

$prob2(i) = exp(-s*alp(i) + s^2*sgm1^2/2 + logsum(i));$

$prob3(i) = exp(s^2*sgm^2/2 + logsum(i));$

end

plot(sir,prob3,'r-+'), hold on

xlabel('SIR threshold')

ylabel('Outage probability')

title('Nakagami-m case (m=1 for different power) M=3')

%**********

B.16 Code 16 for comparison the exact outage probability to the Rayleigh case of different values of M.

s=18;ps1=0.0015;sir=0.1:0.1:2;

M=5;

for i=1:20

$r1(i) = sir(i)/(sir(i)+1);$

$prob(i) = exp(-M * log(1 - 2 * ps1 * (1 - 1/r1(i)) * s));$

$exactOP(i) = 1 - exp(-(sir(i) + M/10)/(sir(i)));$

$err(i) = prob(i) - exp(-(sir(i) + M/10)/(sir(i)));$

end

avgerr=mean(err);

semilogy(sir,prob,'r*-'), hold on

semilogy(sir,1-exactOP,'b–'), hold on

xlabel('SIR threshold')

ylabel('Outage probability')

title('Rayleigh case M=5 for high power with exact outage probability')

Bibliography

[1] J. G. Proakis, *Digital Communications.* NY, USA: McGraw Hill, 1989, 2001.

[2] T.S. Rappaport, *Wireless Communications Principles and Practice.* NJ, USA: Prentice Hall PTR, 1996.

[3] D. Parsons, *The Mobile Radio Propagation Channel.* NY, USA: John Wiley and Sons, 1992.

[4] J. Zander, Performance of Optimum Power Control in Cellular Radio Systems, IEEE Trans. On Vehicular Tech., vol. 41, no. 1, Feb. 1992.

[5] C. D. Charalambous, S. Z. Denic, S. M. Djouadi, and N. Menemenlis, Stochastic Power Control for Short-term Flat Fading Wireless Networks: Almost Sure QoS Measures, Decision and Control, 2001. Proceedings of the 40th IEEE Conference on, vol. 2, 4-7 Dec. 2001 pp 1049 - 1052.

[6] C. D. Charalambous and S. Denic, On the channel capacity of wireless fading channels, Decision and Control, 2002, Proceedings of the 41st IEEE Conference on, vol. 4, 10-13 Dec. 2002, pp 4036 - 4041.

[7] C. D. Charalambous and N. Menemenlis, A State Space Approach in Modeling Multipath Fading Channels: SDE and Ornstein-Uhlenbeck Processes, Proceedings of IEEE ICC 2001, Finland, Helsinski, Jun 11-15, 2001.

[8] C.D. Charalambous and N. Menemenlis, Stochastic Models for Long-Term Multipath Fading Channels, Proceedings of 38th IEEE CDC, pages 4947-4952, Phoenix, AZ, Dec. 1999.

[9] C.D. Charalambous and N. Menemenlis, Stochastic Models for Short-Term Multipath Fading Channels:Chi-Square and Ornstein-Uhlenbeck Processes, Proceedings of 38th IEEE CDC, pp 4959-4964, Phoenix, AZ, Dec. 1999.

[10] J. Yong and X.Y. Zhou, *Stochastic Controls Hamiltonian Systems and HJB Equations.* NY, USA: Springer-Verlag, 1999.

[11] Nickie Menemenlis, Ph. D Thesis, McGill University, Montreal, Quebec, Canada, May 2002. Supervised by Dr. C.D. Charalambous.

[12] Lingling Wang, Master Thesis, McGill University, Montreal, Quebec, Canada, August 2002. Supervised by Dr. C.D. Charalambous.

[13] Xin Li, Master Thesis, University of Ottawa, Ottawa, Ontario, Canada, March 2002. Supervised by Dr. C.D. Charalambous.

[14] J. Papandriopoulos, J. Evans, and S. Dey, Iterative power control and multiuser detection with outage probability constraints, Communications, 2003. ICC '03. IEEE International Conference on, vol. 4, 11-15 May 2003, pp 2509 - 2513.

[15] S. Kandukuri and S. Boyd, Optimal Power Control in Interference-Limited Fading Wireless Channels With Outage Probability Specifications, IEEE Trans. on Wireless Communications, vol. 1, no. 1, Jan 2002.

[16] Lecture notes, Perron-Frobenius Theory, http://www.stanford.edu/class/ee363, Winter 2001-02.

[17] Eitan Altman and Zwi Altman, S-modular Games and Power Control in Wireless Networks, Automatic Control, IEEE Transactions on, vol. 48, Issue:5, May 2003, pp 839 - 842

[18] Sennur Ulukus and Roy D. Yates, Stochastic Power Control for Cellular Radio Systems, IEEE Trans. on Communications, vol. 46, no. 6, June 1998.

[19] Lijun Qian and Zoran Gajic, Joint Optimization of Mobile's Transmission Power and SIR Error in CDMA Systems, Proceedings of the American Control Conference, Arington,

VA, June 25-27, 2001.

[20] Lijun Qian and Zoran Gajic, Variance Minimization Stochastic Power Control in CDMA Systems, Communications, 2002. ICC 2002. IEEE International Conference on, vol. 3, 28 April-2 May 2002, pp 1763 - 1767.

[21] Deepak Das and Mahesh K. Varansi, Stochastic Power Control with Averaging, Personal Wireless Communications, 2000 IEEE International Conference on, 17-20 Dec. 2000, pp 325 - 329.

[22] Aylin Yener, Roy D. Yates, and Sennur Ulukus, Interference management for CDMA Systems through Power Control, Multiuser Detection, and Beamforming, IEEE Trans. on Communications, vol. 49, no. 7, July 2001.

[23] Halim Yanikomeroglu, Theory of Transmit Power Control in Wireless Multiple-Access Systems, MCWS Lab, Carleton University, 1999.

[24] Desmond J. Higham, An Algorithmic Introduction to Numerical Simulation of Stochastic Differential Equations, Society for Industrial and Applied Mathematics, vol. 43, no. 3, pp 525-546, 2001.

[25] The Mathworks, Inc., *MATLAB User's Guide.* NAtick, MC, USA, 1992.

[26] I.N. Kovalenko, N.Yu. Kuznetsov, and V.M.Shurenkov, *Models of Random Processes: A Handbook for Mathematicians and Engineers.* Boca Raton, FL, USA: CRC Press, Inc., 1996.

[27] A. Bruce Clarke and Ralph L. Disney, *Probability and Random Processes: A First Course with Applications.* NY, USA: John Wiley and Sons, Second Edition, 1985.

[28] Gunnar Blom, *Probability and Statistics: Theory and Applications.* NY, USA: Springer-Verlag, 1989.

[29] Thomas C. Gard, *Introduction to Stochastic Differential Equations.* NY, USA: Marcel Dekker, Inc., 1988.

[30] Richard B. Darst, *Introduction to Linear Programming: Application and Extensions.*

NY, USA: Marcel Dekker, Inc., 1991.

[31] C.D. Charalambous, course notes, Detection and Estimation, University of Ottawa, 2002.

[32] A. Annamalai, C. Tellambura, and V. K. Bhargava, A Unified Approach to Performance Evaluation of Switched Diversity in Independent and Correlated Fading Channels, IEEE Trans. on Communications, 1999.

[33] A. A. Abu-Daya and N. C. Beaulieu, Outage Probabilities of Cellular Mobile Radio systems with Multiple Nakagami Interferers, IEEE Trans. Veh. Tech., vol. 40, Nov. 1991, pp 757-768.

[34] http://mathworld.wolfram.com/Chi-SquaredDistribution.html

[35] http://mathworld.wolfram.com/GammaDistribution.html

[36] N. O'Connell, course notes, Large Deviations with Applications to Telecommunications, Uppsala University, 1999.